NOX
N-62-3-1

UED

UNITED ELECTRODYNAMICS, INC.

Received at AFTAC
27 March 1962
Walter J. Davis
Capt USAF

FIELD STUDY OF VARIATION
IN CHARACTERISTICS OF
SEISMIC NOISE AND SIGNALS
WITH
GEOLOGIC AND GEOGRAPHIC ENVIRONMENT

SEMIANNUAL PROGRESS REPORT
NO. VT/078-16
1 JULY TO 31 DECEMBER 1961

UED REPORT NO. AAD 62-19

Prepared for
UNITED STATES AIR FORCE
TECHNICAL APPLICATIONS CENTER
WASHINGTON 25, D.C.

5 FEBRUARY 1962

Prepared by:

J. R. Woolson
Project Engineer

Approved by:

F. B. Coker
Division Manager

UNITED EARTH SCIENCES
division of

UNITED ELECTRODYNAMICS, INC.
200 ALLENDALE ROAD, PASADENA, CALIFORNIA, MURRAY 2-1134

TABLE OF CONTENTS

(continued)

TABLE OF CONTENTS (pg. 2)

(continued)

TABLE OF CONTENTS (pg. 3)

INTRODUCTION

Two profiles have been occupied in the program (Project VT/078) of relating seismic noise and signals to geology and topography. The California profile has been completed. Work on the Pacific Northwest has been started. Although both these profiles are similarly oriented relative to the Pacific Ocean, there is marked contrast in the geologic aspects. The California profile extends from the coast range across the central valley into the ridge and valley province of the Great Basin. The Pacific Northwest Profile extends from the Pacific Coast near Grays Harbor across the Puget Sound Trough, the volcanic and batholithic core of the Cascades into the thick basalts of the Columbia Basin. It terminates on granite in the Blue Mountains of northeastern Oregon.

The method of establishing noise levels and relative signal response of the various sites occupied (10 in California) consists of using two essentially identical tripartite seismic recording systems, one fixed and one which is relocated about once a month. The fixed station is the Master and the relocated station is the Slave. The triangular array of short period seismometers at the slave station is expanded at one week intervals from ¼ mile from a central point by ¼ mile intervals to a total central distance of one mile. The results are simultaneously recorded on film and magnetic tape and brought to an analysis office for processing.

Because of the large amount of data obtained and the relative rapidity of machine methods, it was early decided that machine methods be used. This results in establishing an average noise level of a site, rather than the peak level of noise as is commonly obtained by visual methods. The machine output is average peak squared of the noise. One of the reasons for using this function of the noise is the large body of statistical communication theory literature which is developed in this format.

The wave analyzer used is essentially a device which looks at a noise sample with a very narrow (nominally 2 cps wide) filter which is swept across the sample. The values obtained from the system are the coefficients of the Fourier expansion of the sample, defining the amplitude of each component part of the complex wave form.

Analysis work is continuing on the data from the California profile. A station factor has been defined which represents the ratio of the average signal to noise ratios of the sites. This factor varies from 0.37 to 1.4 and can be thought of as a measure of the relative capability of a station to detect seismic signals relative to the Master Station on granite in the Sierra Nevada. The stations in the Sierra Nevada and east had a factor between 1.0 and 1.4, those in the San Joaquin Valley and west were less than 1.0. One example of this data is the station in Death Valley, where although the noise level was high the signal level was also high and the station factor was 1.3.

Data from the Washington profile is limited since work began in Washington in November. Preliminary indications are that the noise level is the same order of magnitude as in California.

Work is continuing along the profile in the Pacific Northwest. The analysis group is presently located in Pasadena. The work in the Pacific Northwest is scheduled for completion in June, prior to which time a third profile will be selected.

AFTAC Project No. VT/078

Field Study of Variation of Seismic Noise and Signals with Geologic and Geographic Environment

ARPA Order No. 104-60
ARPA Code No. 8100

Contractor: United Earth Sciences Division of United ElectroDynamics, Inc.

UED Report No. AAD 62-19

Date of Contract: 2 September 1960

Amount of Contract: $503,731 (partial funding)

Contract No.: AF 33(600)-42048

Contract Expiration Date: September 1962

Project Engineer: John R. Woolson
SYcamore 9-9575
Pasadena, California

1. California Profile

Field work was completed on the California profile on 10 November 1961. At that time the Master and Slave field recording systems were moved to the Pacific Northwest. They were back in operation south of Yakima, Washington on 27 November 1961.

1.1 Geology and Topography of the California Profile

Figure 1.1 is a regional tectonic map of the western United States adapted from P. B. King[1]. The California Profile is located a short distance (about 50 kilometers) north of the east-west interruption of the trend of acidic-plutonic rocks which appears to be associated with the Murray fracture zone, which extends at least 1500 kilometers across the Pacific. The general trend of tectonic belts in far western North America, is parallel to the Pacific shoreline; the California profile is located far enough north of the Murray fracture zone to cross the tectonic belts where they are essentially parallel to the Pacific shoreline.

There are from west to east, the coast range province of complexly folded and faulted Cretaceous and Tertiary rocks, the deep asymmetric Tertiary basin of the San Joaquin Valley, the Sierra Nevada intrusive, the complex horst and graben structural and topographic province which includes Owens, Panamint and Death Valleys. The eastern part of the profile includes the western part of the Great Basin area, which lies mainly in Nevada. Slave Station locations were selected to occupy at least one location in each of those tectonic belts.

Figures 1.2 and 1.3 illustrate in the form of a map and geologic cross section the location, topography and geologic environment of each of the Slave Station sites along the California profile.

1.2 Geology and Topography of the Huasna River and Carrizo Slave Station Sites

These two Slave Station sites are located in the Coast Range province of California and north of the transverse range province. The Garlock and Big Pine Fault (see Figure 2.2), mark the northern boundary of the transverse range province.

The Coast Range province may be subdivided into the Salinas-Cuyama Basin, the portion west of the Naciemiento Fault, and the portions of the Temblor range east of the San Andreas

1. King, P. B. - The Evolution of North America, Princeton University Press, 1959

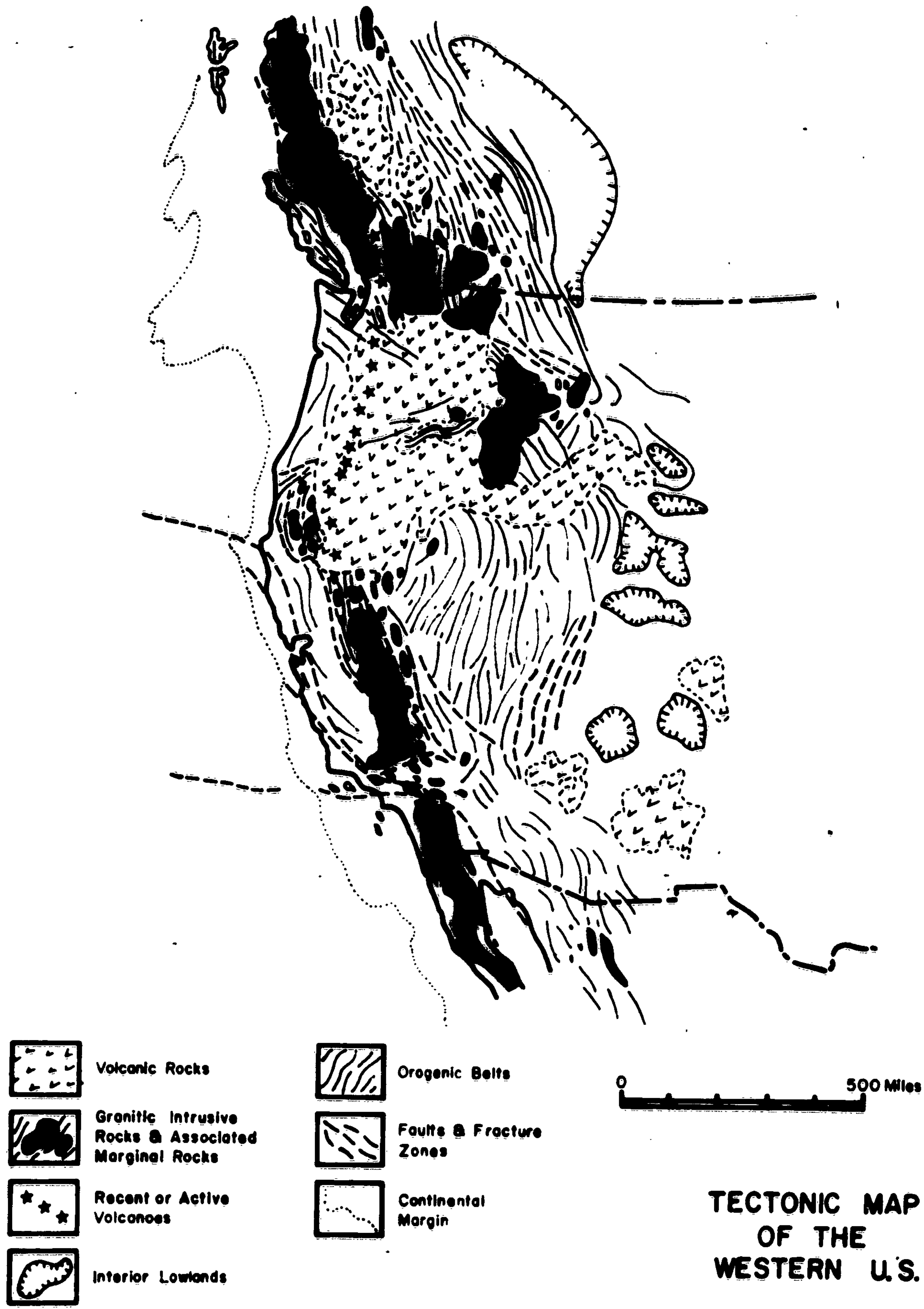

TECTONIC MAP
OF THE
WESTERN U.S.

FIGURE 1.1

H-10,962 Date 1-15-62
UNITED ELECTRODYNAMICS INC
PASADENA CALIFORNIA

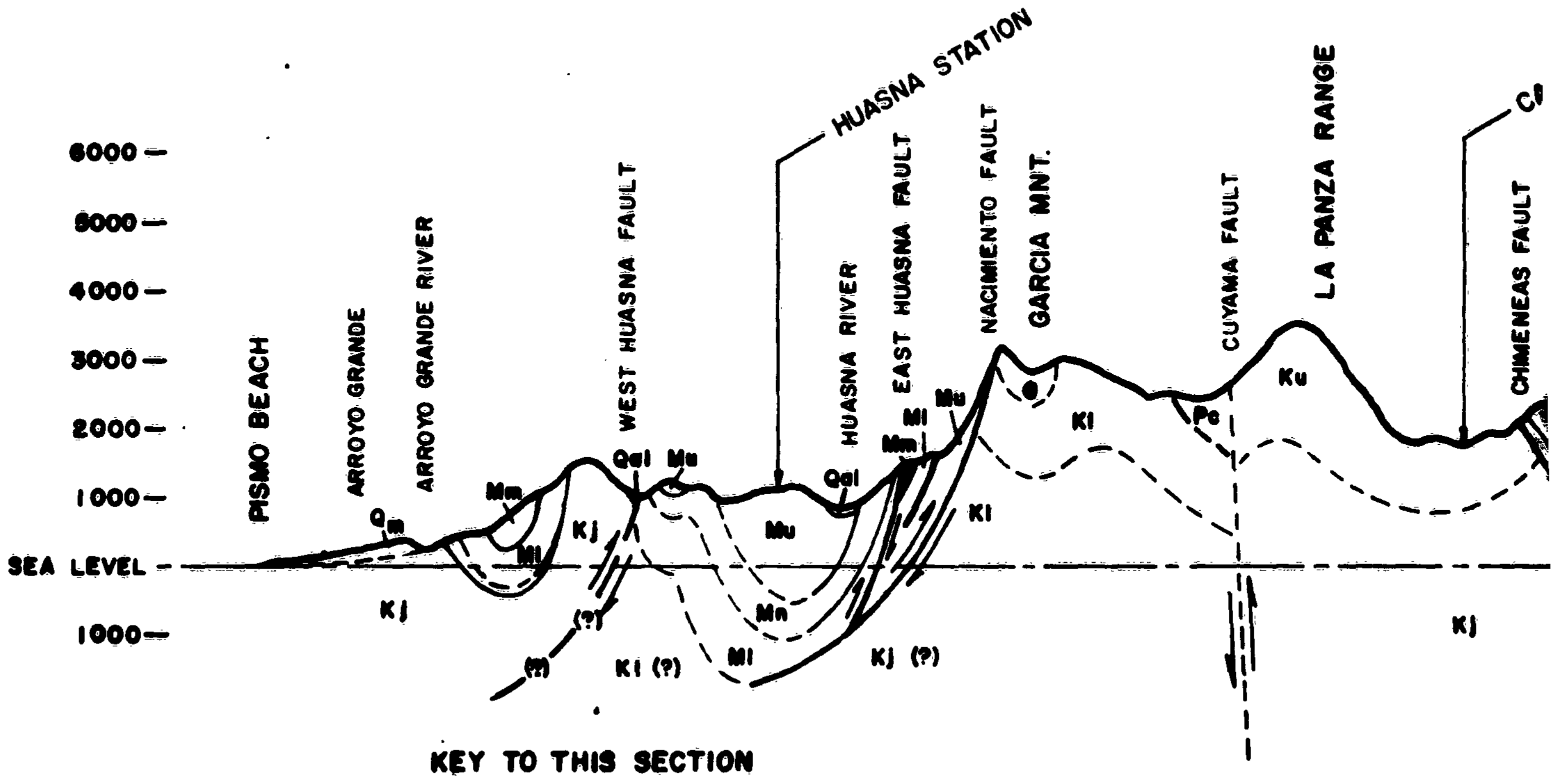

KEY TO THIS SECTION

Qal	Quaternary Alluvium
Qm	Quaternary Beach Terraces
Pc	Pliocene Non-Marine
Mu	Upper Miocene Marine
Mm	Middle Miocene Marine
Ml	Lower Miocene Marine
O	Oligocene Non-Marine
Ku	Upper Cretaceous Marine
Kl	Lower Cretaceous Marine
Kj	Cretaceous-Jurassic Franciscan Fm (Meta-Sediments)

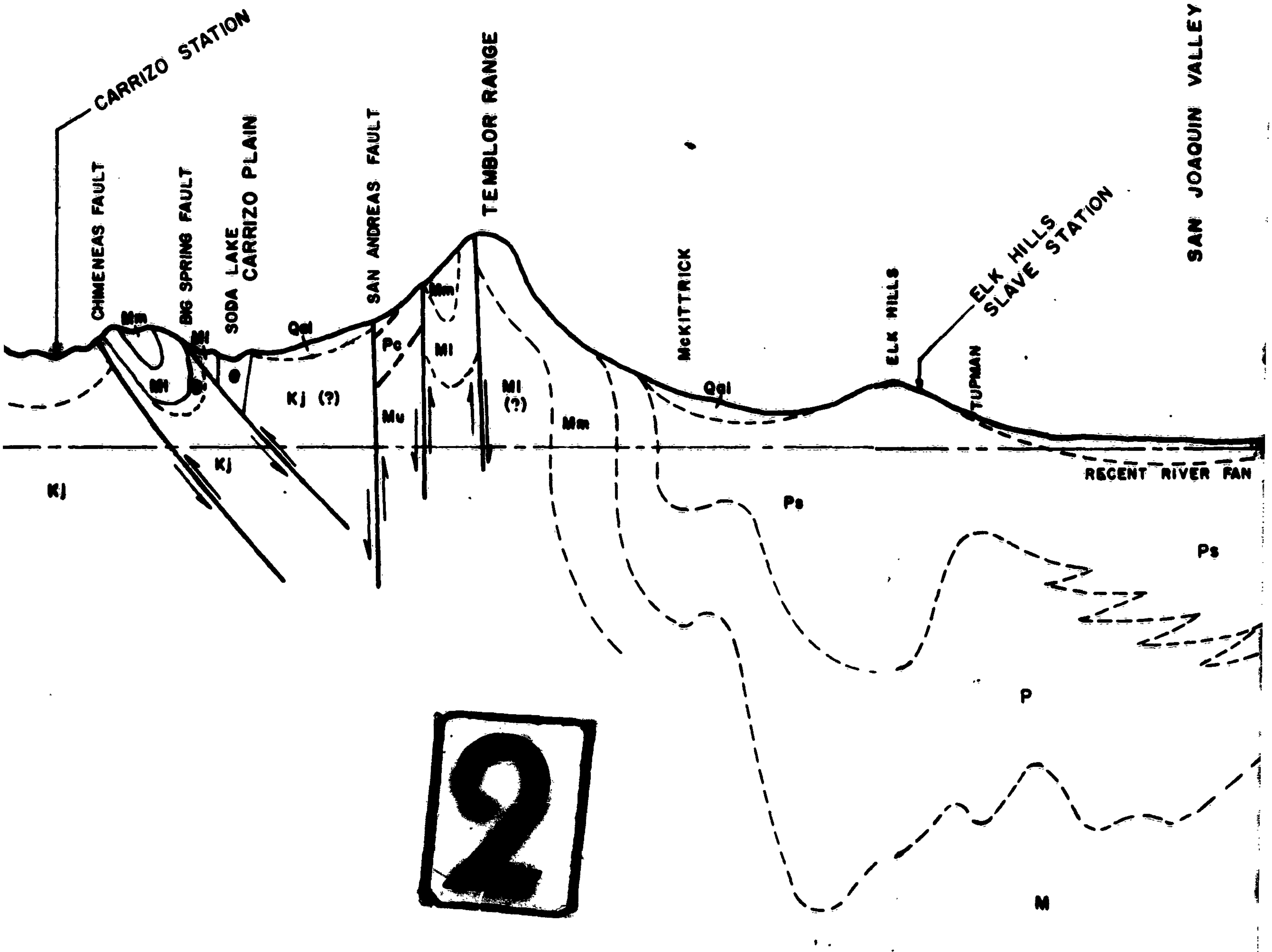

CARRIZO STATION
CHIMENEAS FAULT
BIG SPRING FAULT
SODA LAKE
CARRIZO PLAIN
SAN ANDREAS FAULT
TEMBLOR RANGE
McKITTRICK
ELK HILLS
ELK HILLS SLAVE STATION
TUPMAN
SAN JOAQUIN VALLEY
RECENT RIVER FAN
Mm
Ml
Qal
Kj (?)
Kj
Pc
Mu
Ml (?)
Ps
P
M
2

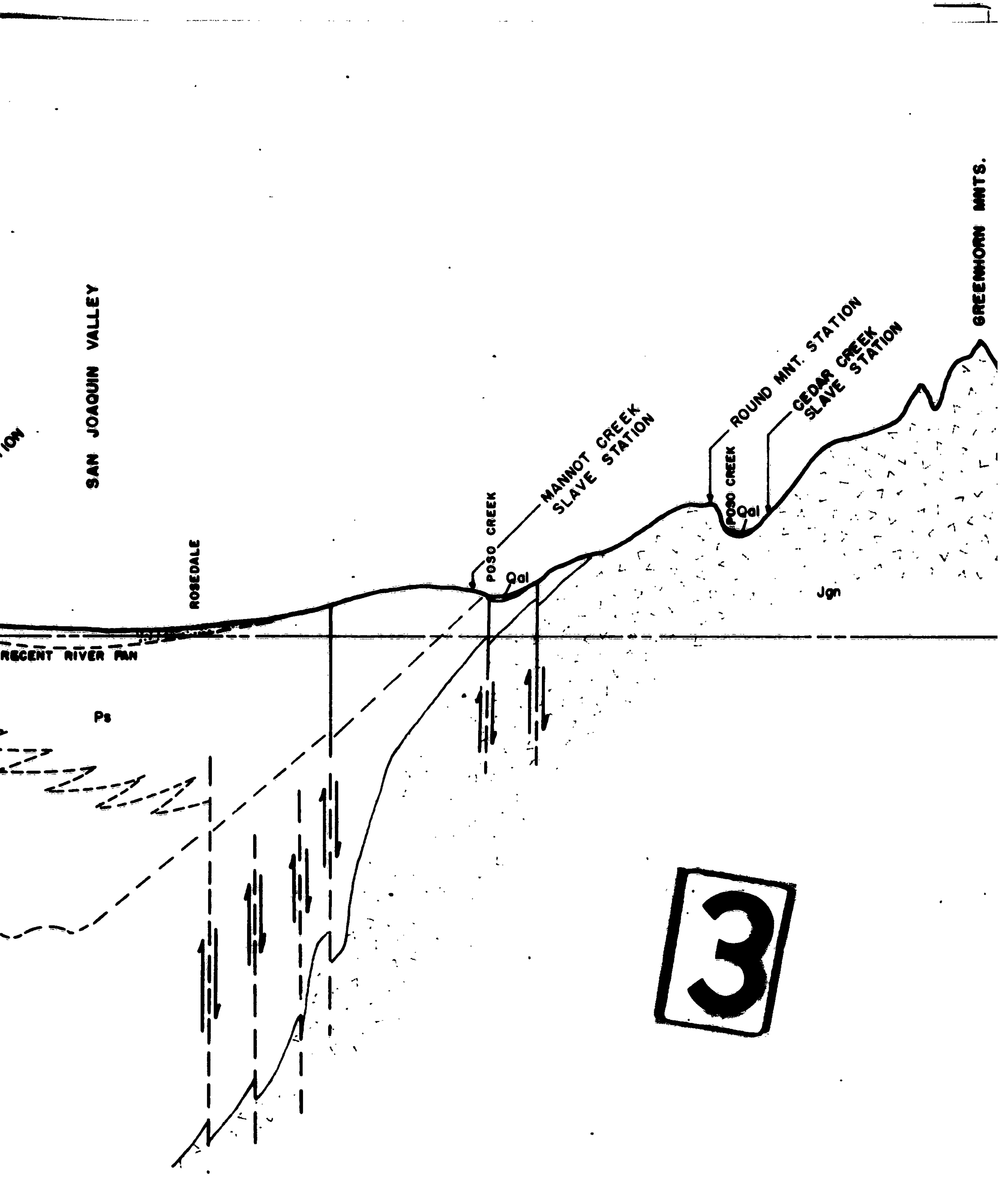

SAN JOAQUIN VALLEY
ROSEDALE
POSO CREEK
MANNOT CREEK SLAVE STATION
POSO CREEK
ROUND MNT. STATION
CEDAR CREEK SLAVE STATION
GREENHORN MNTS.
Qal
Qal
Jgn
RECENT RIVER FAN
Ps
3

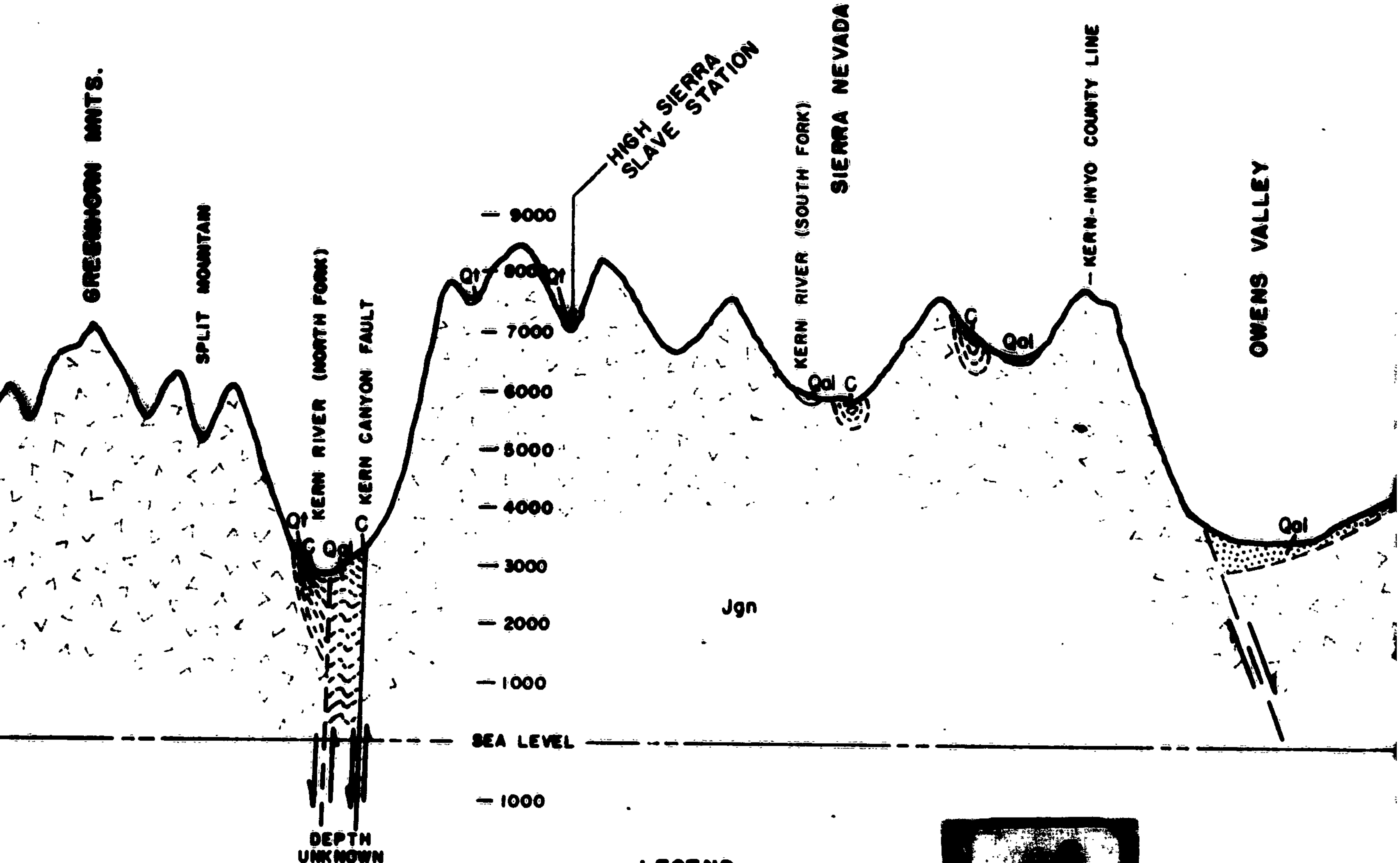

LEGEND

M - MIOCENE MARINE
Mv - MIOCENE VOLCANIC
Kl & Kf = K - CRETACEOUS MARINE
P - PLIOCENE MARINE
Bc - BASEMENT CRYSTALLINE
O - OLIGOCENE MARINE & NON-MARINE
Ps - PLEISTOCENE NON-MARINE
Jgn - JURASSIC GRANITE
C - CARBONIFEROUS META-SEDIMENTS (MARINE) FOUND AS ROOT PENDENTS
Cm - CARBONIFEROUS MARINE
Qp - PLIO-PLEISTOCENE NON-MARINE
Є - CAMBRIAN MARINE
Pre Є - PRE-CAMBRIAN MARINE
Qb - QUATERNARY BASALT
Qt - QUATERNARY TERRACES
Qal - QUATERNARY ALLUVIAL FILL

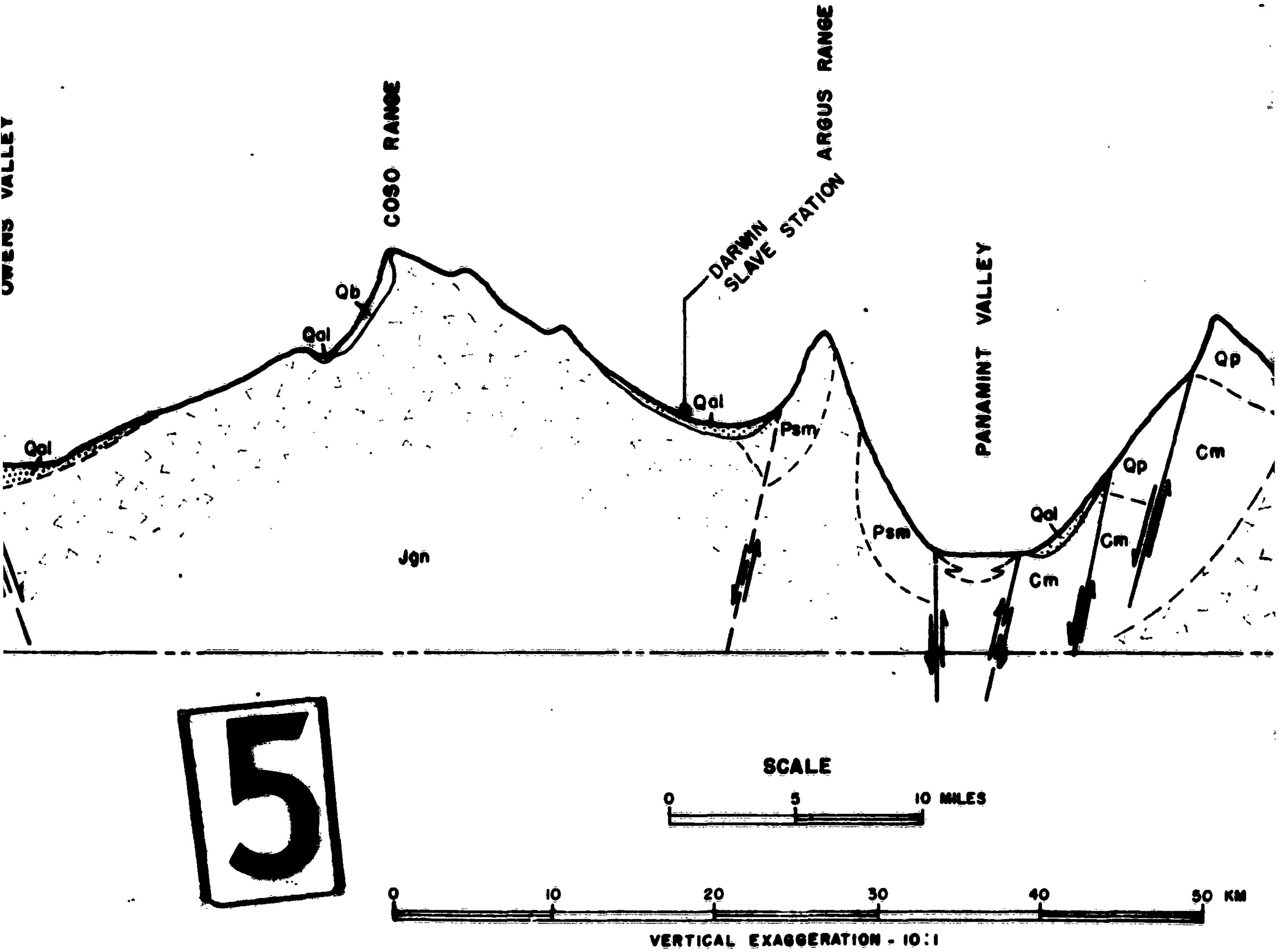

VALLEY
COSO RANGE
ARGUS RANGE
DARWIN
SLAVE STATION
PANAMINT VALLEY
Qal
Qb
Qal
Qal
Psm
Psm
Qal
Qp
Qp
Cm
Cm
Cm
Jgn
5
SCALE
0 5 10 MILES
0 10 20 30 40 50 KM
VERTICAL EXAGGERATION - 10:1

ENTS

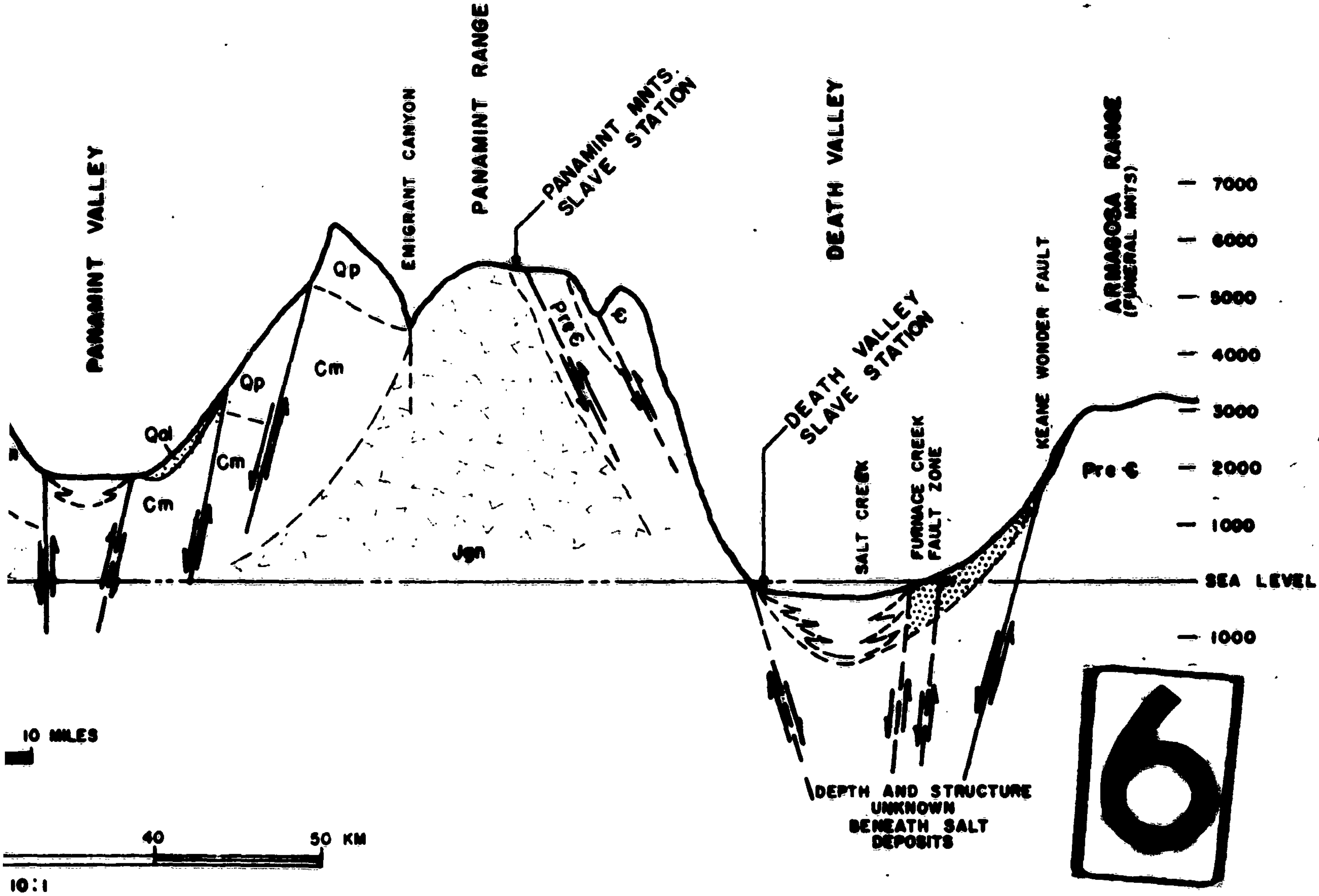

6

GEOLOGICAL CROSS SECTION
PISMO BEACH TO DEATH VALLEY,
CALIFORNIA

FIGURE 1.2

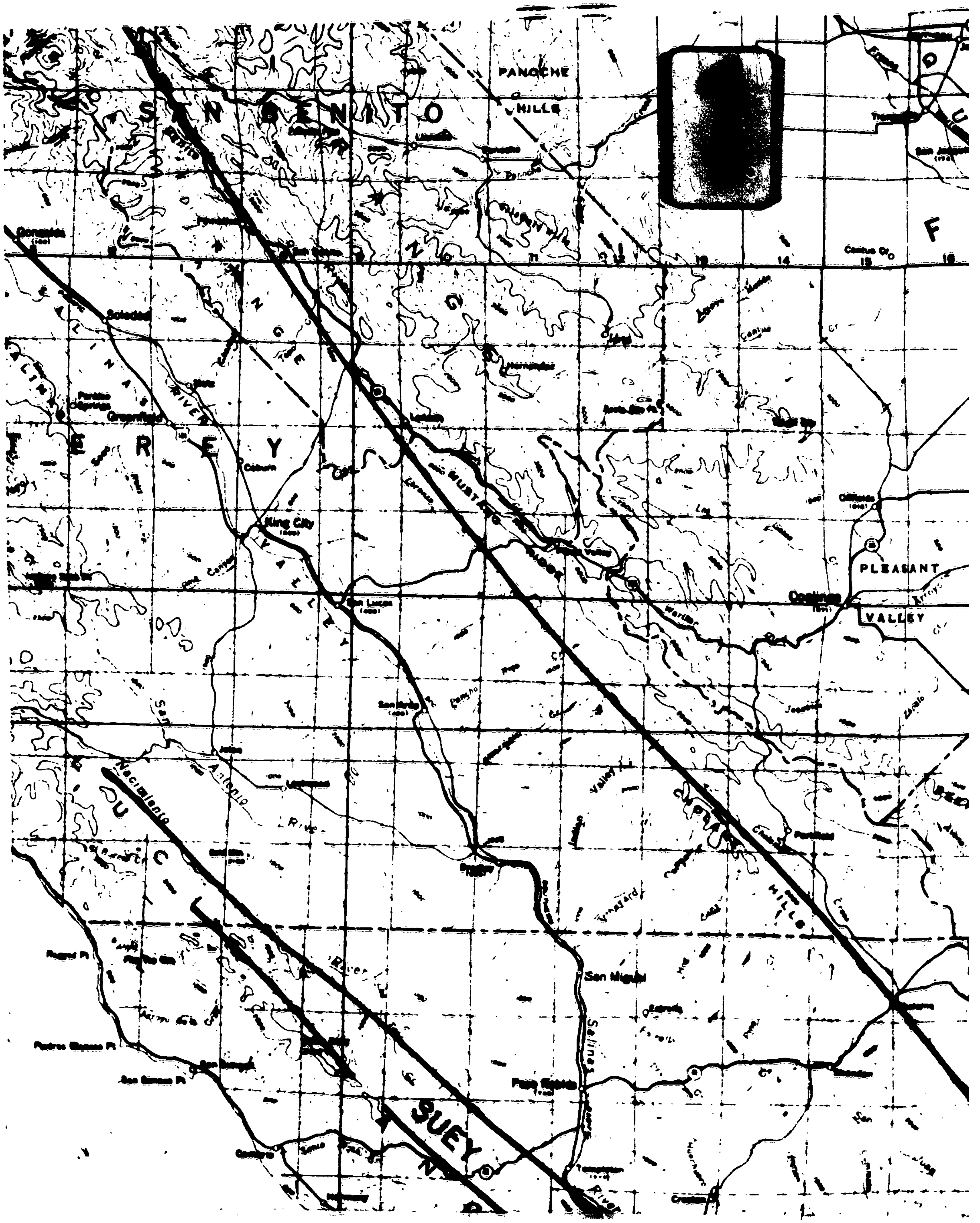

PANOCHE
HILLS
SAN BENITO
Gonzales
Soledad
Greenfield
T E R E Y
King City
San Lucas
San Ardo
San Antonio River
Nacimiento
San Miguel
Salinas
Paso Robles
SUEY
Coalinga
PLEASANT
VALLEY
HILLS
F

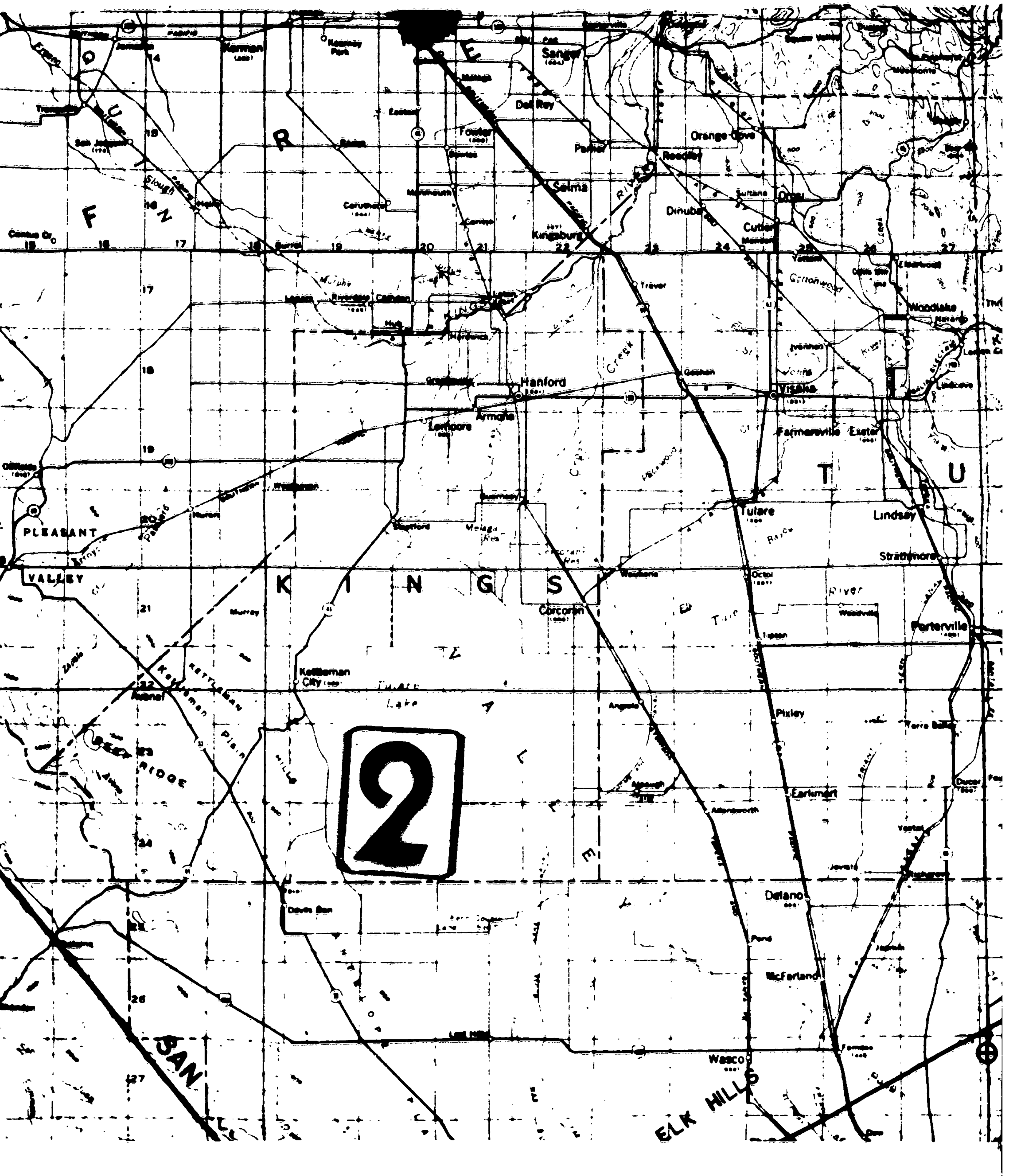

2
F
R
E
S
N
O
K
I
N
G
S
T
U
L
A
R
E
Sanger
Del Rey
Fowler
Parlier
Reedley
Orange Cove
Selma
Kingsburg
Dinuba
Cutler
Orosi
Caruthers
Traver
Woodlake
Hanford
Goshen
Visalia
Armona
Lemoore
Farmersville
Exeter
Tulare
Lindsay
Strathmore
PLEASANT
VALLEY
Corcoran
Porterville
Kettleman City
Tulare
Lake
Avenal
Kettleman
Plain
Allensworth
Pixley
Earlimart
Delano
McFarland
Wasco
ELK HILLS
SAN
River
Tule
Slough
Creek

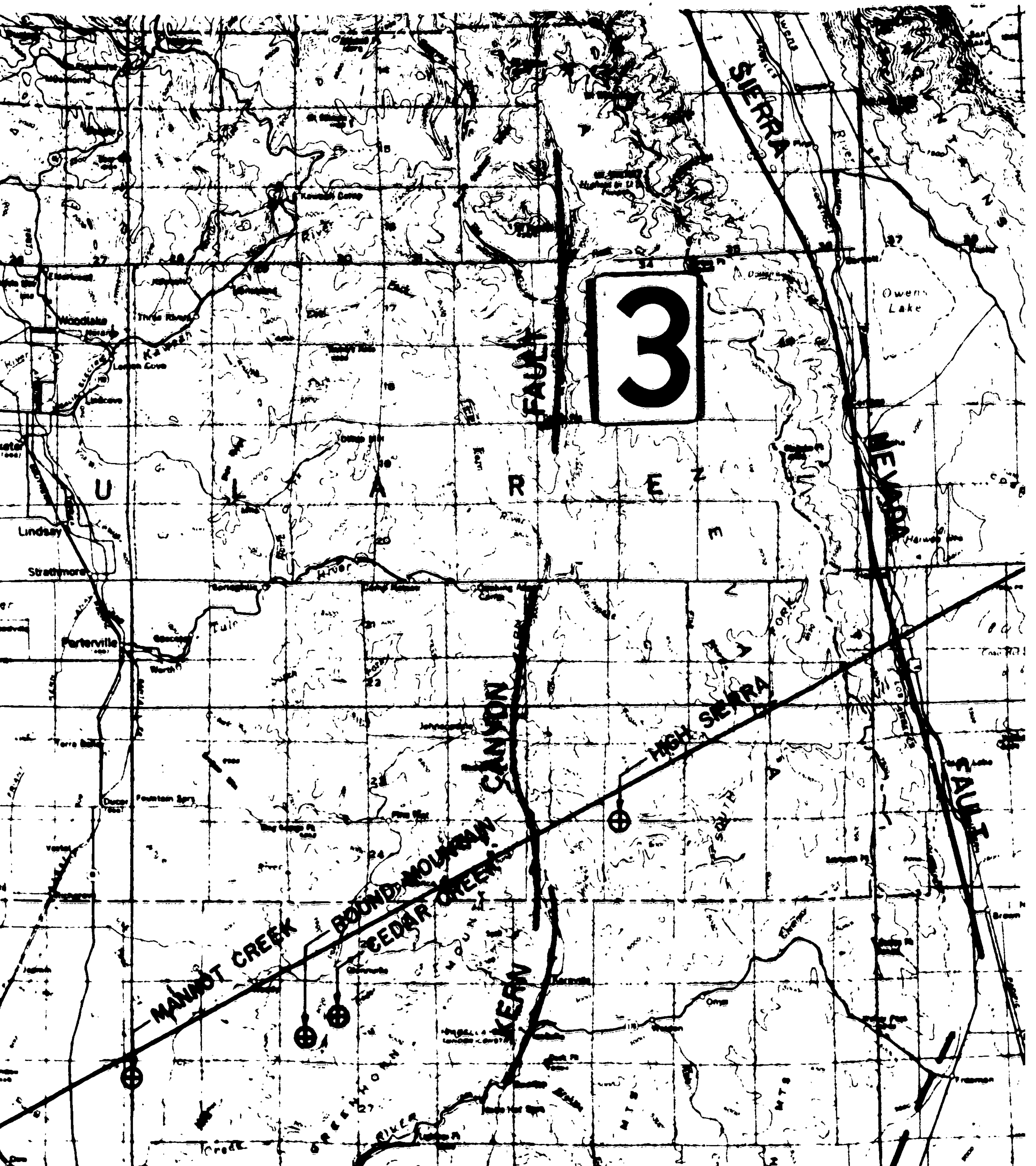

3
SIERRA
NEVADA
FAULT
FAULT
KERN
CANYON
HIGH SIERRA
CEDAR CREEK
Owens Lake
Woodlake
Three Rivers
Lemon Cove
Lindsay
Strathmore
Porterville
Tule

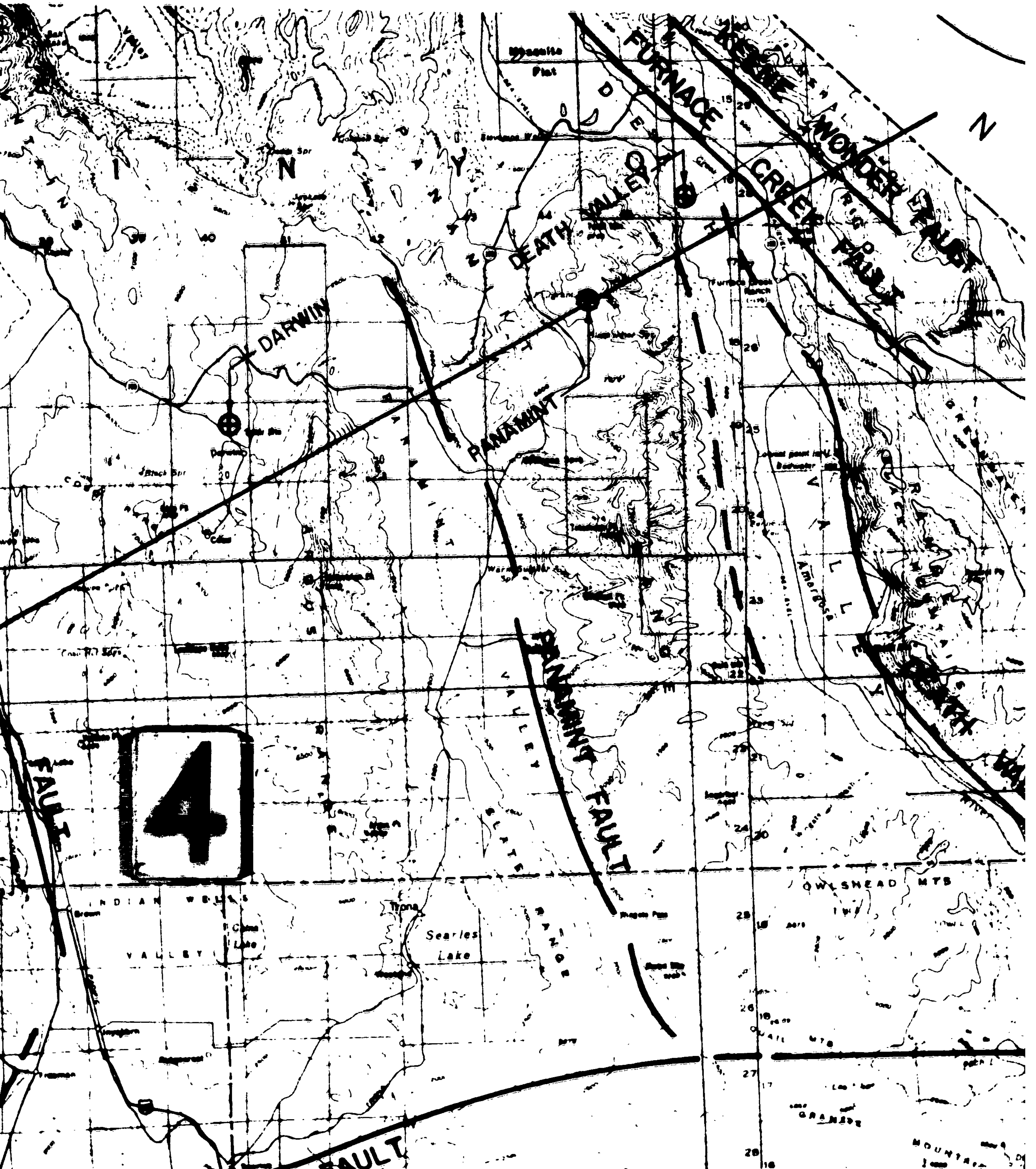

FURNACE CREEK FAULT
WONDER FAULT
DEATH VALLEY
DARWIN
PANAMINT
PANAMINT FAULT
N
4
FAULT
FAULT
Searles Lake
Trona
OWLSHEAD MTS
INDIAN WELLS
VALLEY
Amargosa
Mesquite Flat

5

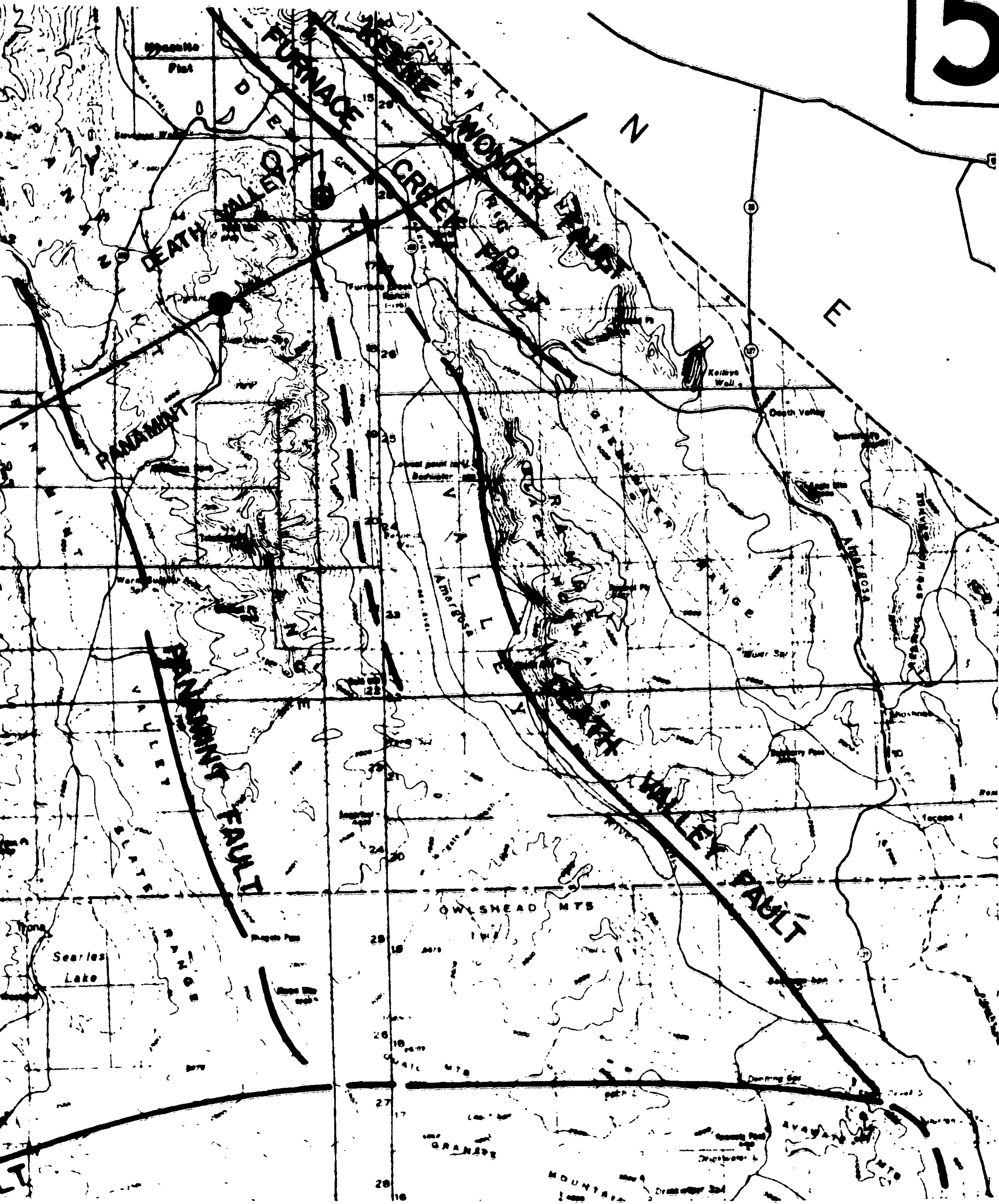
FURNACE CREEK FAULT
KEANE WONDER FAULT
DEATH VALLEY FAULT
PANAMINT FAULT
DEATH VALLEY
PANAMINT
N E
OWLSHEAD MTS
Searles Lake
Amargosa
Kelleys Well
Death Valley
Furnace Creek Ranch
Mesquite Flat

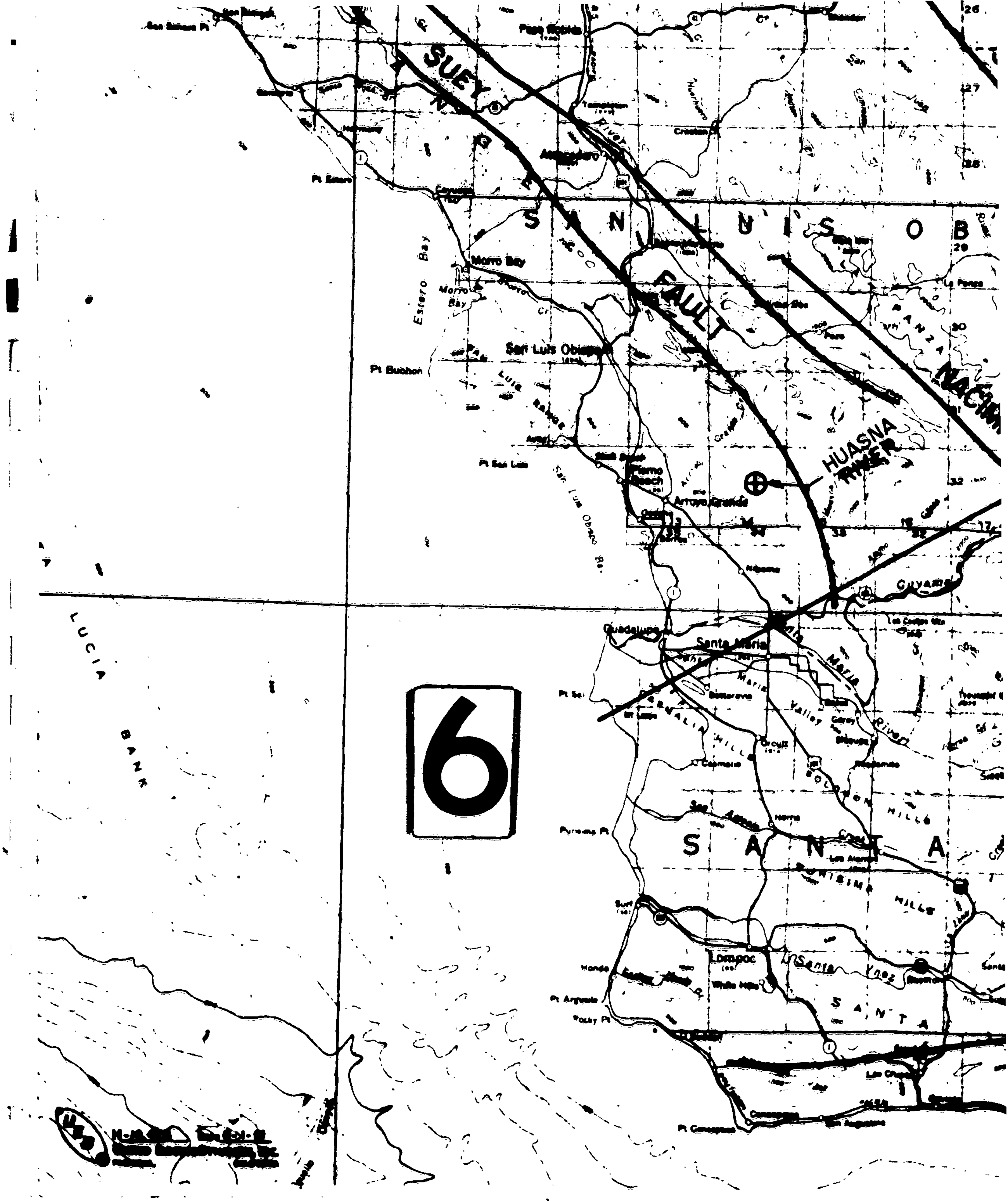

Paso Robles
Templeton
Creston
Atascadero
SUEY
S A N L U I S O B
Morro Bay
Estero Bay
San Luis Obispo
Pt Buchon
FAULT
HUASNA
RIVER
Pismo Beach
Arroyo Grande
Pt San Luis
San Luis Obispo Bay
Nipomo
Cuyama
Guadalupe
Santa Maria
Betteravia
Orcutt
Casmalia
Pt Sal
Garey
Sisquoc
Purisima Pt
S A N T A
Surf
Lompoc
Honda
Pt Arguello
Pt Conception
LUCIA
BANK
6

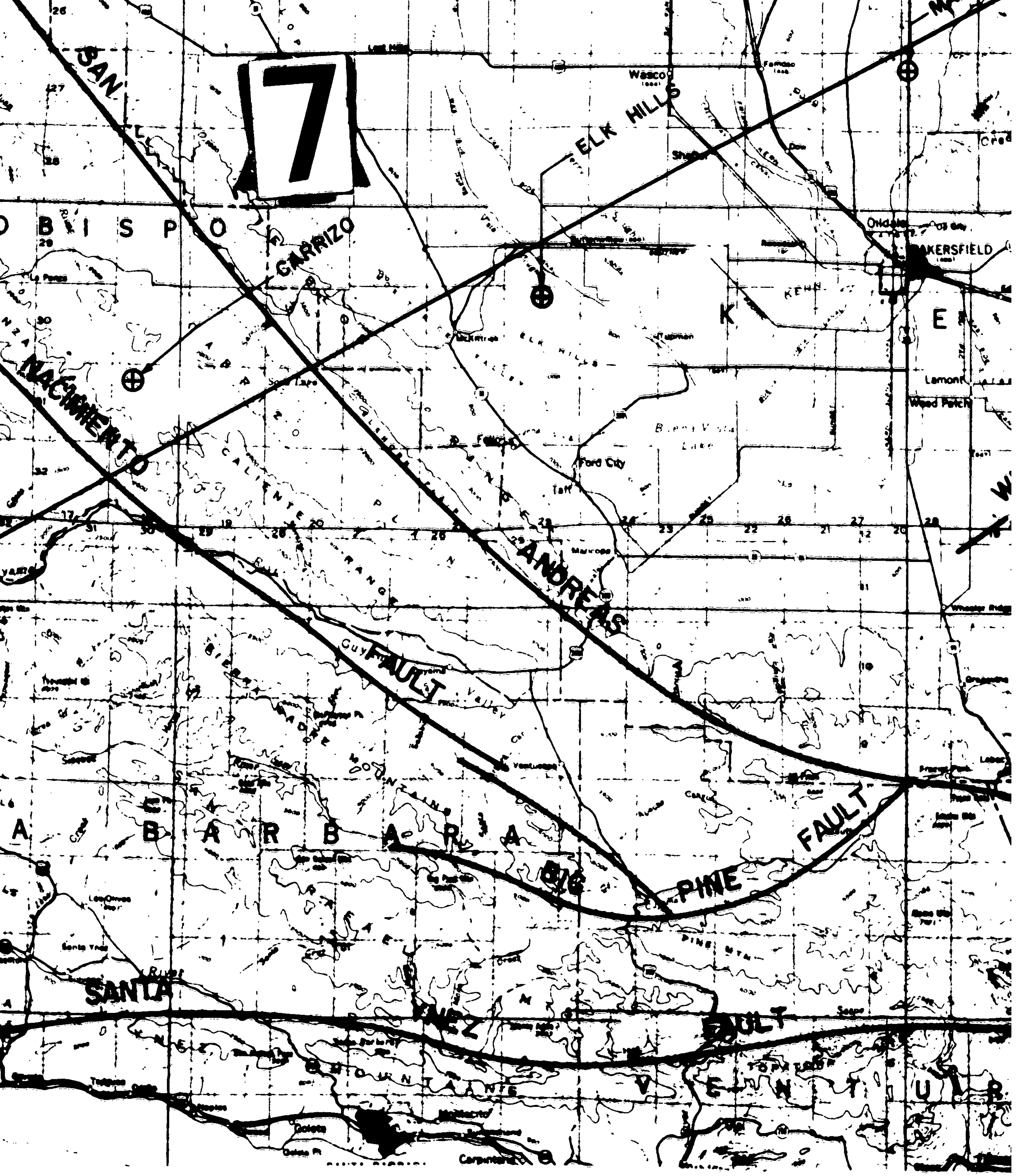

7
SAN
ANDREAS
FAULT
NACIMIENTO
FAULT
BIG PINE FAULT
SANTA YNEZ FAULT
CARRIZO
ELK HILLS
O B I S P O
B A R B A R A
V E N T U R
K E
Lost Hills
Wasco
Shafter
Oildale
BAKERSFIELD
KERN
Lamont
Weed Patch
McKittrick
ELK HILLS
Soda Lake
Fellows
Ford City
Taft
Buena Vista Lake
Maricopa
Wheeler Ridge
Guy
Valley
Ventucopa
PINE MTN
Los Olivos
Santa Ynez
Goleta
Carpinteria
Montecito

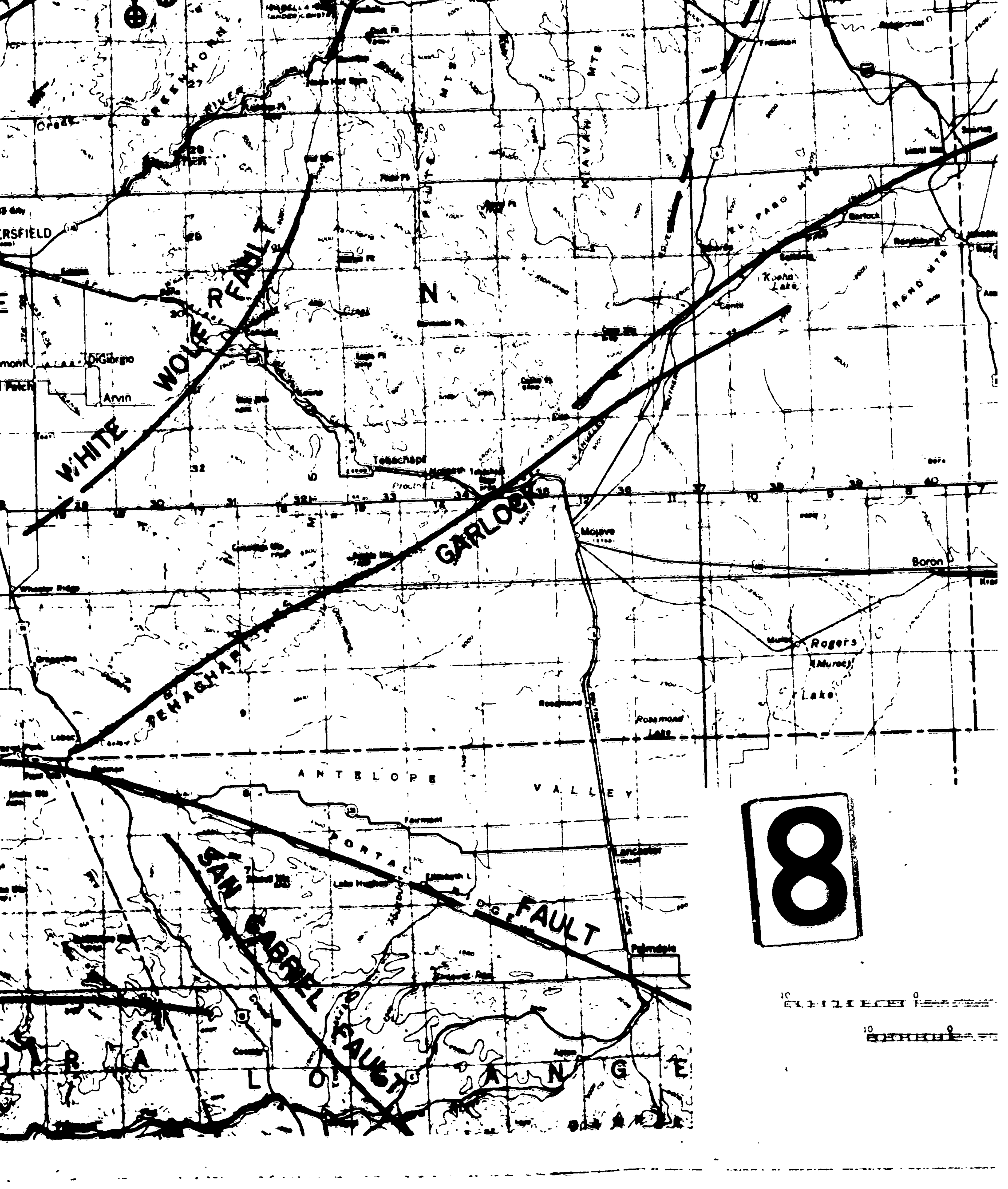

WHITE WOLF FAULT
GARLOCK
SAN GABRIEL FAULT
FAULT
ANTELOPE
VALLEY
EL PASO MTS
RAND MTS
Koehn Lake
Garlock
Randsburg
Cantil
Arvin
DiGiorgio
Tehachapi
Mojave
Boron
Rogers
(Muroc)
Lake
Rosamond
Rosamond Lake
Lancaster
Palmdale
Fairmont
Lake Hughes
Elizabeth L
8

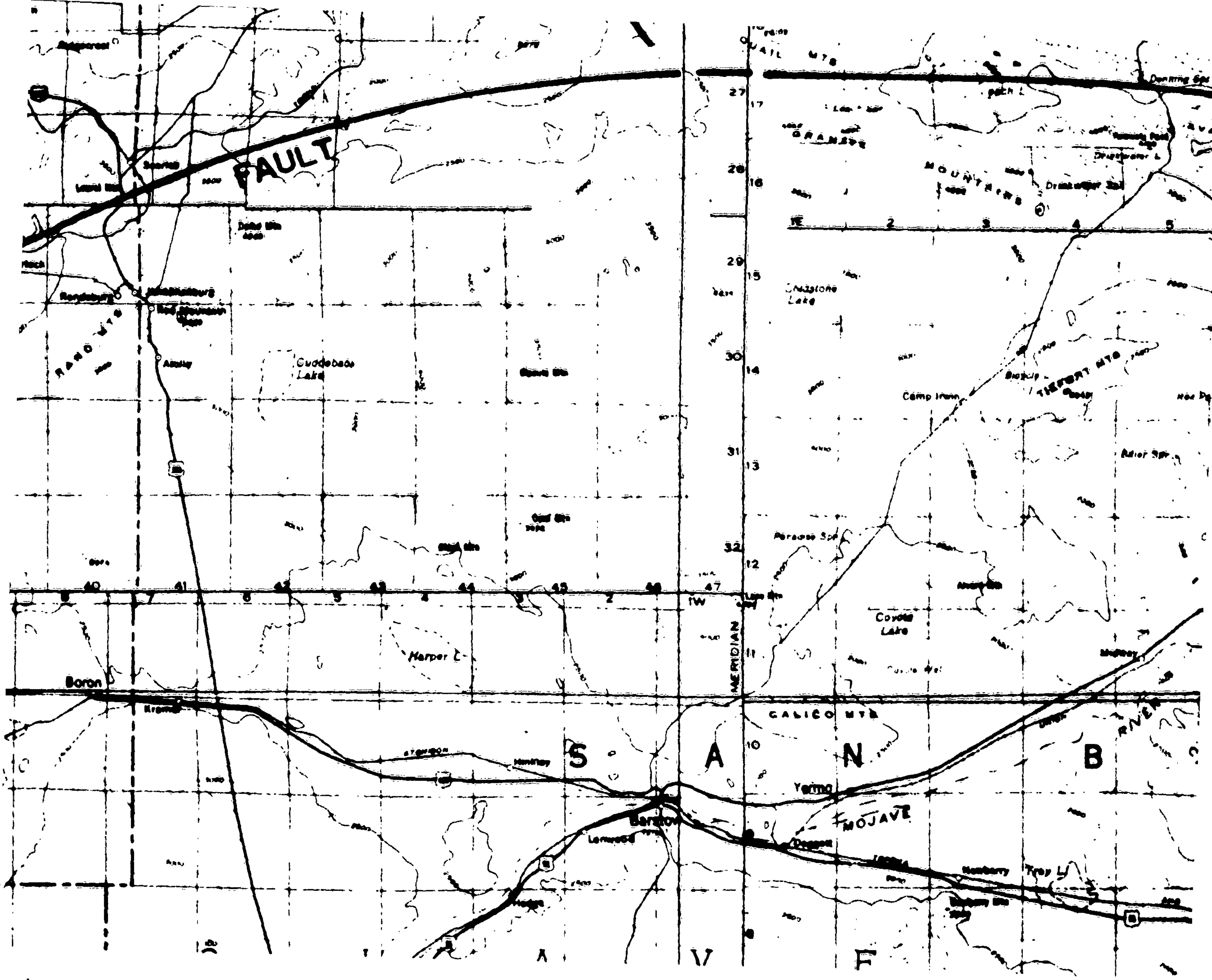

⊕ LOCATIONS OCCUPIED

9

INITIAL FIELD SITE
PROJECT VT/078
POINT ARGUELLO TO
DEATH VALLEY, CALIFORNI/

40 Miles

30 Kilometers

FIG

Contour interval 500 feet
Datum is mean sea level

Depth curves at 100 fathom interval

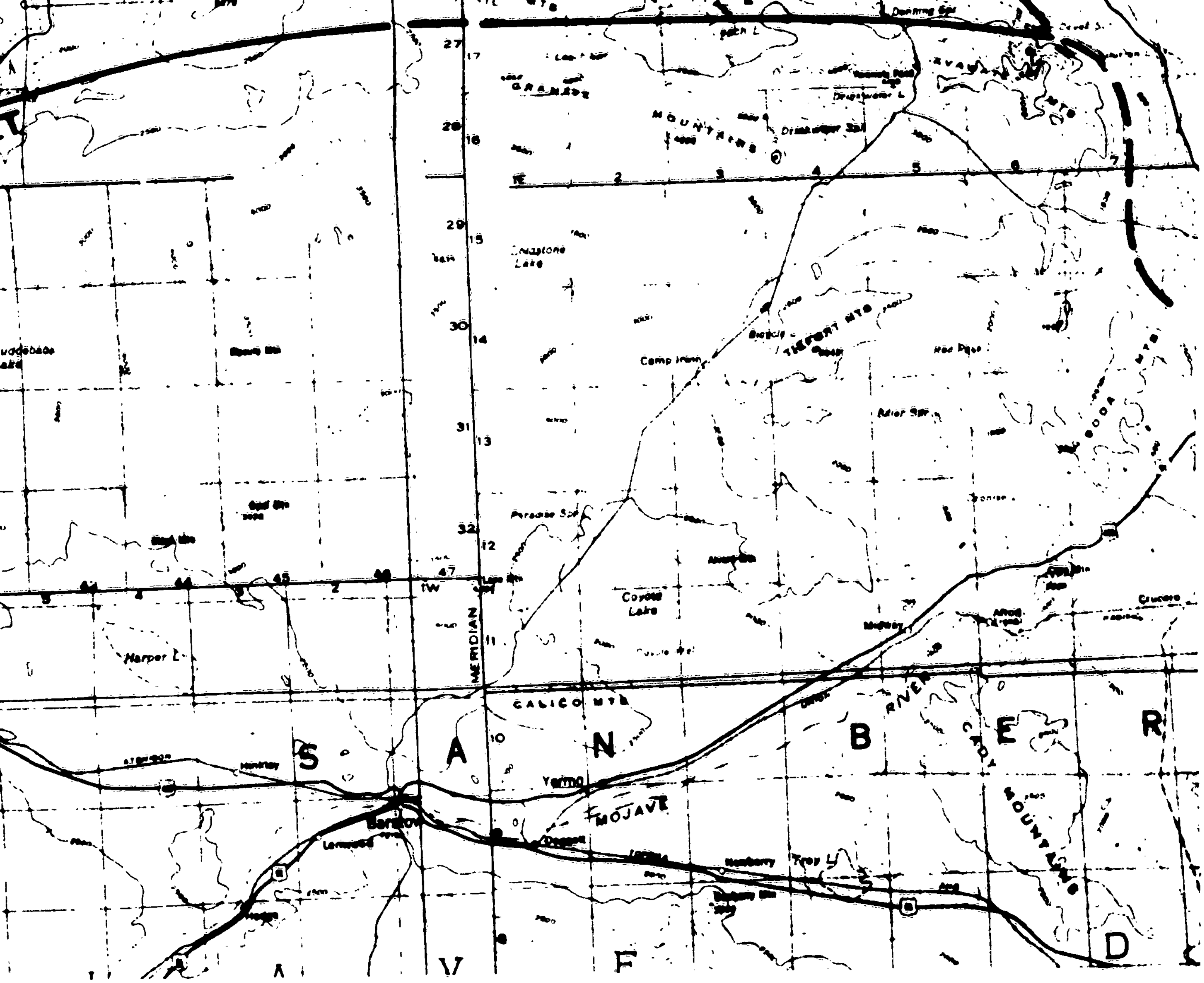

ATIONS OCCUPIED

INITIAL FIELD SITE
PROJECT VT/078
POINT ARGUELLO TO
DEATH VALLEY, CALIFORNIA

10

20 30 40 Miles

20 30 40 50 Kilometers

FIGURE 1.3

rval 500 feet

100 fathom interval

Fault. The Carrizo site is located in the Salinas-Cuyama basin and the Huasna River site is near the Suey Fault about halfway between the coast and the Nacimiento Fault.

Topographically, the Coast Range is a series of sharply divided ridges and valleys with an average elevation difference of about 600 meters. These ridges and valleys are generally an echelon (see for example, the relation of Cuyama Valley and the Carrizo plain as shown on Figure 2.2).

In addition to the major right-lateral strike slip faults which trend northwesterly parallel to the topographic trends, there are a number of normal and reverse faults. The Cuyama Valley oil field, where quite close control is available, illustrates the complex local geology of the Coast Range.

There is a good discussion of the general area of the Carrizo and Huasna River Slave Station sites in Habitat of Oil[1]. This reference is the principal source material for the previous discussion.

Figures 1.4 and 1.5 are photographs of the Huasna River Slave Station site which illustrate the topography. Figure 1.6 illustrates the complex geology of the area. There are several ridges such as that illustrated in Figure 1.6 in the area, which indicate the presence of forces to produce normal, reverse and lateral faulting.

Figures 1.7 and 1.8 are photographs of the Carrizo Slave Station site. This area is somewhat more arid than the Huasna River location.

Figure 1.9 is a photograph of a recent fault trace which occurs in the zone east of the Carrizo site where the San Andreas rift cuts through the Temblor Range.

1.3 Geology and Topography of the Elk Hills and Mannot Creek Locations.

Two slave station locations occur in the San Joaquin Valley, the northwesterly trending valley which divides the Coast Range and the Sierra Nevada. The Elk Hills site is on the south-

1. Habitat of Oil - Geologic Environment of Cuyama Valley Oil Fields, California, by Schwade, Carlson and O'Flynn - American Association of Petroleum Geologists, 1958 pgs. 78-98

Figure 1.4 Huasna River Slave Station site. The ridges on the horizon appear to be fault scarps.

Figure 1.5 Detail photograph of the Huasna River site. Dense stands of scrub oak occur in the valleys.

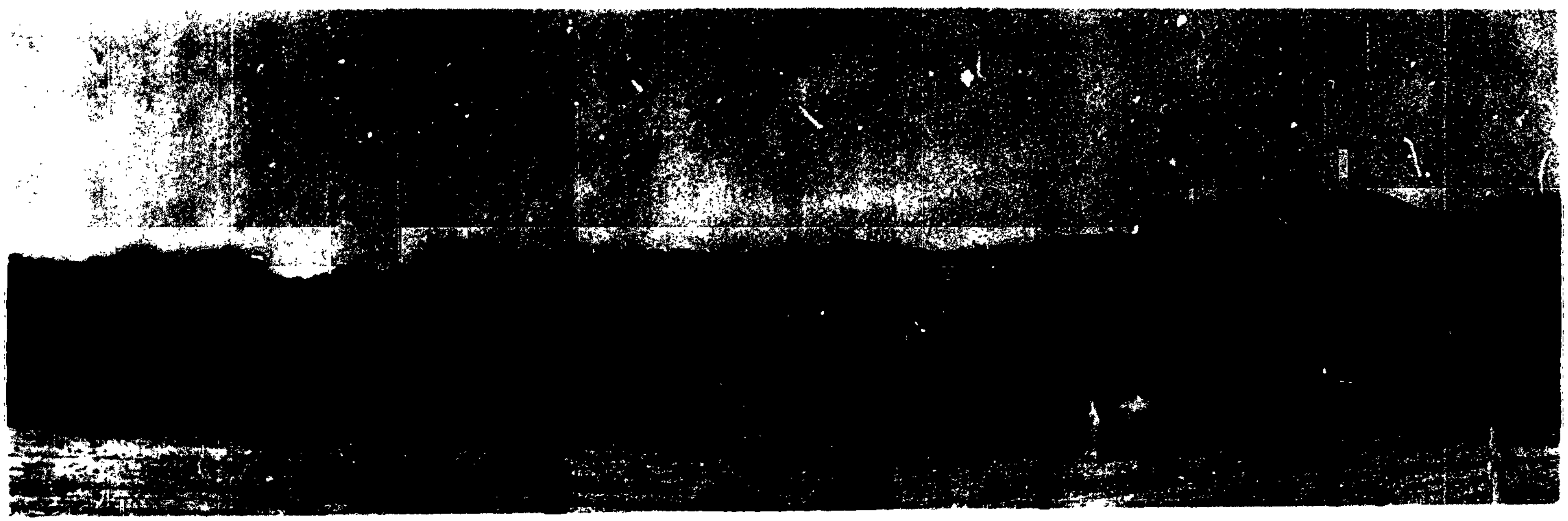

Figure 1.6 Composite photograph of a ridge about three miles west of the Huasna River site, illustrating the complex geology of the area.

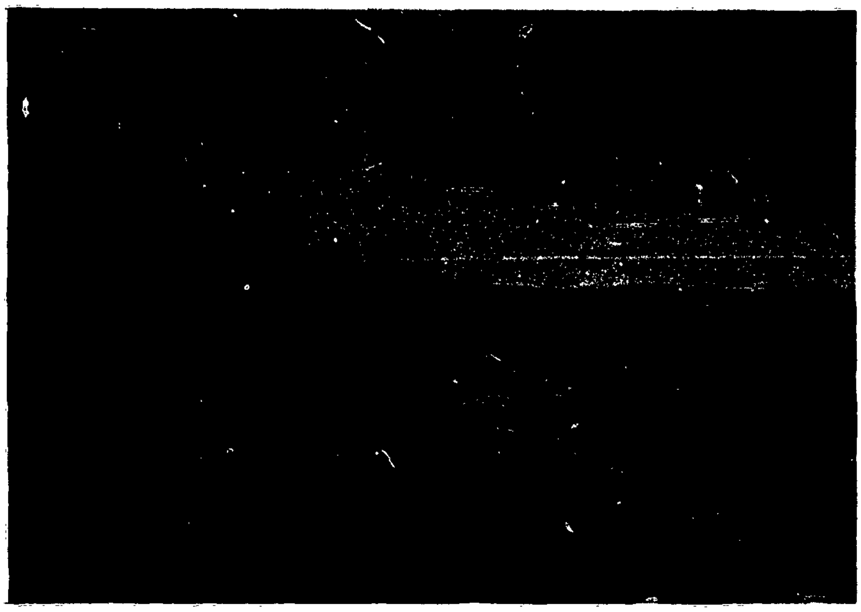

Figure 1.7 Carrizo Slave Station site. The Nacimiento fault, a major right-lateral fault, is parallel to the ridge on the horizon and the slope opposite this photograph.

Figure 1.8 Carrizo Slave Station site. There is a fault scarp at the apex of the first hill in the center of the photograph.

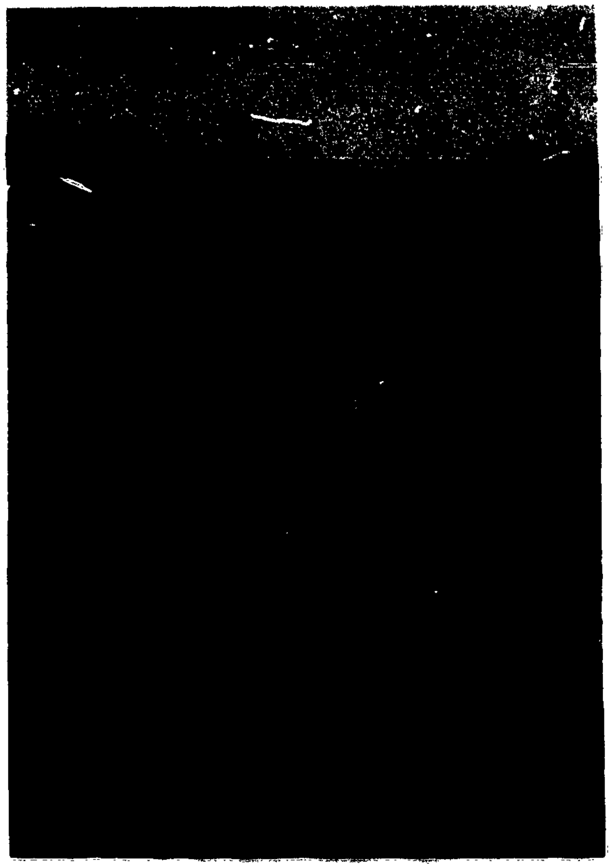

Figure 1.9 Fault trace of a segment of the San Andreas rift in the Temblor Range 20 kilometers northeast of the Carrizo Slave Station.

west side of the valley and the Mannot Creek site on the northwest. Geologically, the San Joaquin is a wedge of Tertiary sedimentary rock (principally sand and shale) which thickens spproximately linearly from zero to about 8000 meters. The deepest portion is northeast of the Temblor Range on the southwest side of the valley. Topographically, the valley is nearly lying, except near its margins, where foothills occur.

The Elk Hills Slave Station is located north of the Elk Hills which is topographic and structural anticline in the Tertiary sediments of the valley. Estimated depth to granite is 7100 meters. This estimate was obtained from one of the oil companies operating in the San Joaquin Valley and is considered reliable. At the Mannot Creek location, depth to granite is about 900 meters.

Figures 1.10, 1.11 and 1.12 are photographs of the Elk Hills and Mannot Creek Slave Station sites.

1.4 Geology and Topography of the Stations in the Sierra Nevada.

Three stations were located in the Sierra Nevada, which is a major granite intrusive. This intrusion occurred during Jurassic time and is the source of the Tertiary sediments in the San Joaquin and Sacramento Valleys. The Sierra Nevada extends from the latitude of Bakersfield nearly to the northern boundary of California. Two stations were located near the western edge of the uplift at elevations of about 900 meters and one is in the central part of the uplift at about 2700 meters. These are Round Mountain, Cedar Creek and High Sierra respectively. The station at Round Mountain was the Master Station, remaining fixed in location from March through November 1961. The topography is gently rolling hills. The surface rock is weathered granite. At the Master Station it was possible to dig through the weathered layer about a meter to hard granite. There is some Quarternary sedimentation in creek valleys.

Figures 1.13 and 1.14 are photographs of the recording equipment at the Master Station and at Cedar Creek about 5 kilometers northeast.

The High Sierra Station was occupied to determine the effect of elevation on seismic noise level. Because of various factors, the attempt failed. Firstly, the local effect of a filled lake caused very high noise levels, secondly, it was necessary to abandon the site because of danger to equipment and personnel from lightning. Some data was obtained and will be discussed in a later section of this report. Figure 1.15 is a photograph of the High Sierra site.

UNITED ELECTRODYNAMICS, INC.
PASADENA CALIFORNIA

Figure 1.10 Elk Hills Slave Station site looking south towards the elk Hills.

Figure 1.11 Elk Hills Slave Station site from the Elk Hills. The approximate center of the area occupied is marked with an X.

Figure 1.12 Mannot Creek Slave Station. This photograph illustrates the rolling topography of the Sierra foothills. Depth to granite is about 900 meters.

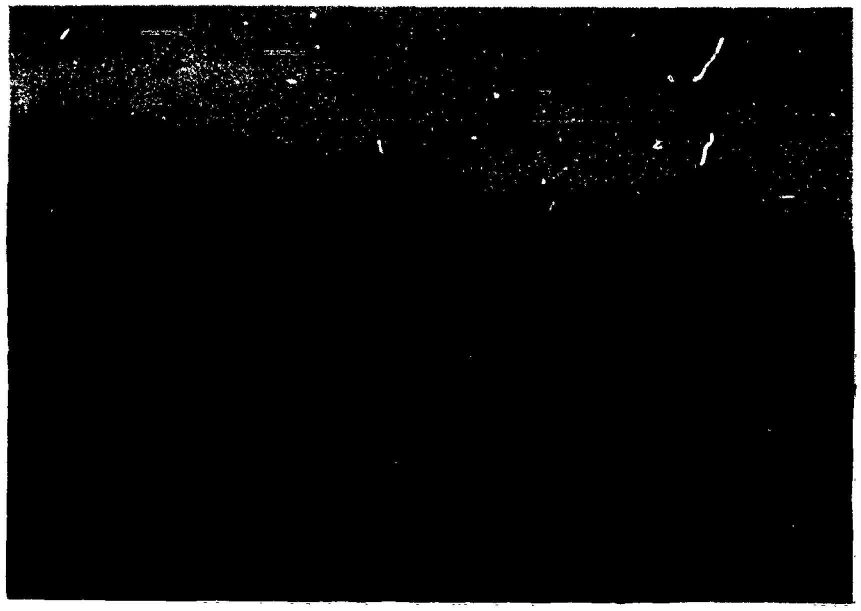

Figure 1.13 Master and Slave Recording Systems at Round Mountain during initial check-out.

Figure 1.14 Cedar Creek Slave Station. The Cedar Creek and Round Mountain sites are 5 kilometers apart.

Figure 1.15 High Sierra Slave Station. The foreground is a meadow,apparently a lake filled during recent times. The trees are growing on a granite outcrop. The noise level of seismometers planted in the filled lake was about 100 times higher than noise on the granite at the edge. The filled lake apparently acts as a gelatinous material.

1.5 Geology and Topography of the Darwin Slave Station Site.

West of the Sierra Nevada, the detail geology is somewhat less well known than in the San Joaquin Valley. However, because of desert conditions, outcrops are well exposed and the principal features of the geology are known.

The Darwin Slave Station site is in a topographic saddle between the Inyo Mountains and Argus Range east of Owens Valley. The principal rocks in the Inyo Mountains and Argus Range are Jurassic granite which form an uplift axis parallel to the Sierra Nevada. Owens valley, which separates the parallel uplifts, is a graben. Kane and Pakisor[1] have concluded that the valley fill (principally Tertiary rocks) vary from 300 to 1500 meters and that the margins of the valley are steeply dipping faults.

Locally, the Darwin site is a north-south trending valley with a thin layer of Quaternary sediments. The east side of the valley is Pennsylvanian limestone and the west side is Quarternary volcanics. The Darwin Tear Fault crosses the array about 0.3 kilometer north of the center. There are inactive copper mines in the Pennsylvanian rocks east of the site.

Figure 1.16 is a photograph of the Darwin Slave Station site.

1.6 Geology and Topography of the Panamint and Death Valley Slave Station Sites.

Northeasterly from the Darwin Slave Station, the profile along which the slave stations are located crosses Panamint Valley, the Panamint Mountains and Death Valley. The Panamint Station is near the apex of the Panamint Mountains. The Death Valley station is on the floor of Death Valley on the west side. These two stations thus occupy sites on the up and down thrown sides of the major down to the northeast fault, the scarp of which forms the northeast face of the Panamints. This fault scarp is about 1500 meters. The core of the Panamints is a granitic intrusive with a cap of older Paleozoic sediments. Death Valley is a fill of Tertiary and recent sedimentation to a depth of about 2000 meters (P. B. King op.cit. pg 157). The net vertical displacement of the Death Valley Fault is thus about 3500 meters.

1. M. F. Kane and L. C. Pakiser – Geophysical Study of Subsurface Structure in Southern Owens Valley, California - Geophysics Vol. XXVI, pgs 12-26.

Figure 1.16 Darwin Slave Station. This photograph is taken from the Pennsylvanian outcrop east of the Darwin site. The hills in the background are Quarternary volcanics.

In detail, the Panamint site is a fenster which exposes granite, the upper plate is Cambrian limestone. There is a veneer of Quaternary alluvium in the valley in which the array center is located.

The Death Valley site is located partially on the valley floor, which is silt and salt and partially on an alluvial from the Panamint Mountains. The alluvial fan is a poorly consolidated conglomerate.

Figures 1.17 and 1.18 are photographs of the Panamint and Death Valley Slave Stations.

Figure 1.17 Slave Station site in Death Valley. The Panamint Mountains are in the background.

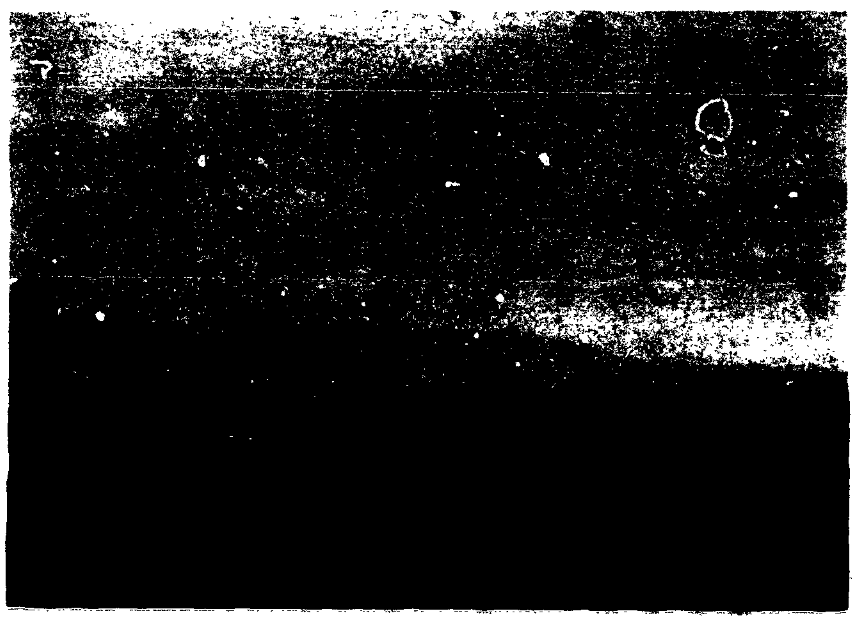

Figure 1.18 Death Valley. This photograph is of the Panamints and north portion of the valley.

Figure 1.19 Panamint Slave Station. There are a number of abandoned mines in this area.

2. Washington Profile

During October 1961, as the work in California neared completion, it was proposed to occupy a profile in the Pacific Northwest as the second major work area. This is part of the program as originally proposed, namely; that various sites in the continental United States be occupied to determine the relation of seismic noise to geology and topography. (Ref. 1).

A letter was written on 17 October 1961 (Ref. 21), requesting permission to occupy a profile line extending from Gray's Harbor on the Pacific Coast of Washington southeasterly to the Blue Mountains in northeastern Oregon. Permission was granted 25 October 1961. (Ref. 23).

2.1 General Geology of the Pacific Northwest.

Figure 2.1 illustrates the relation of both the California and Pacific Northwest profiles to the regional geology at western North America. The Pacific Northwest profile extends from the Tertiary sediments across the Puget Sound-Willamette trough, through the Cascade Mts. south of Mt. Ranier, and across the Columbia basaltic plateau into the granite outcrop area in the Blut Mountains. Figure 2.1 is adapted from P. B. King[1] and illustrates the relation and marked difference between the geology in California and Pacific Northwest profile. Figure 2.2 is a more detailed geologic map of the northwest which illustrates the interpreted re-entrant in the Nevadan orogenic belt. This figure is also adapted from King (op.cit). From both a topographic and geologic aspect, the most striking phenomena in the northwest is the line of recently active volcanic peaks about 150 kilometers from the coast line and eleven to twelve hundred kilometers in a north-south extent. It is interesting to note that this volcanic trend crosses the Nevadan orogenic belt and thus has a distinctly different set of geologic forces as its origin.

In an earlier report (Ref. 24), the controversy concerning the origin of the northwest volcanic province was briefly discussed. From all that can be determined, the concept of an off-shore volcanic archipeligo seems to be unnecessary mechanism. Also, there is no residual evidence in sea floor topography of

1. King, P. B. - The Evolution of North America - Princeton University Press, 1959

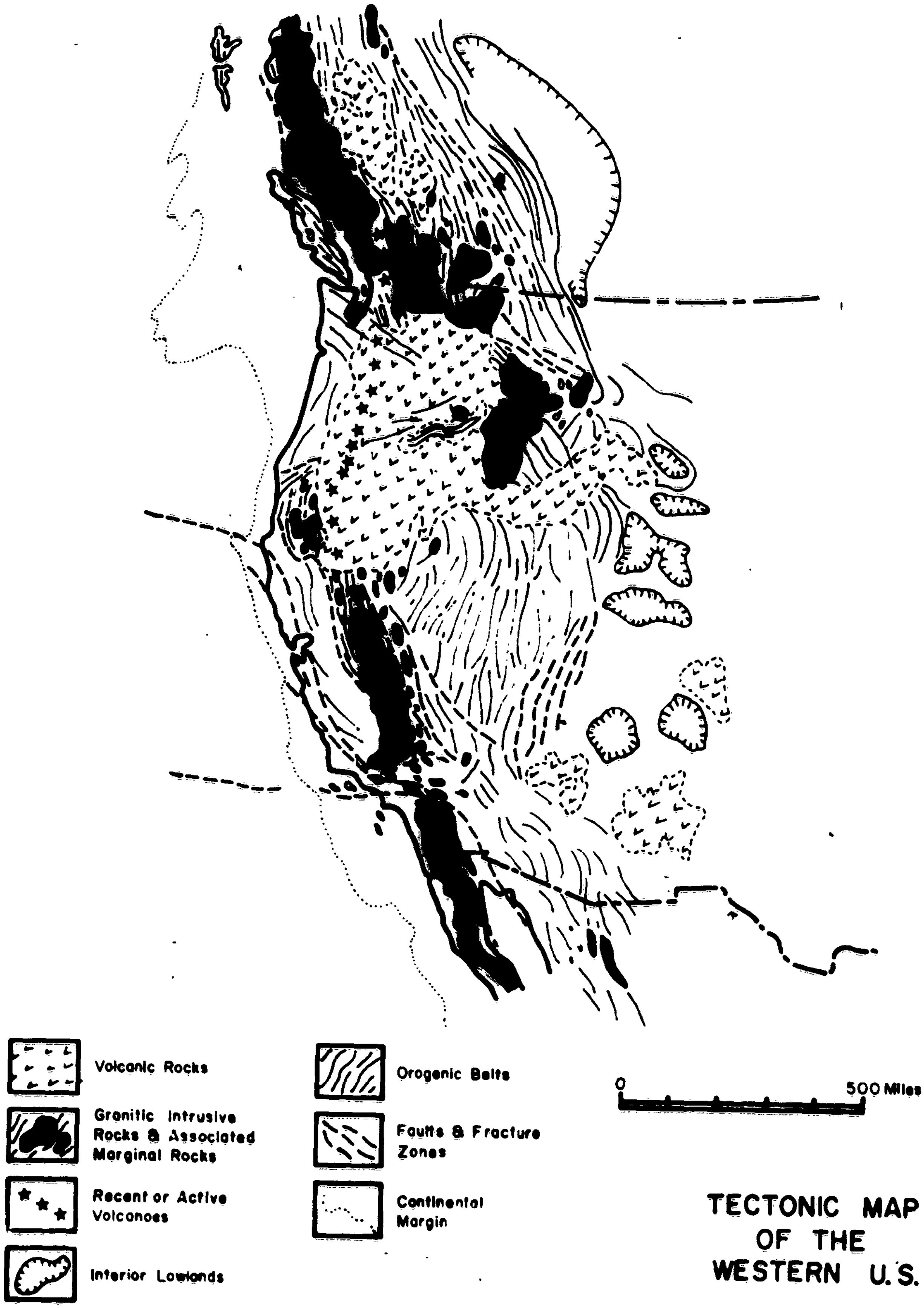

TECTONIC MAP OF THE WESTERN U.S.

FIGURE 2.1

UED
H-10,962 1-15-62
UNITED ELECTRODYNAMICS INC

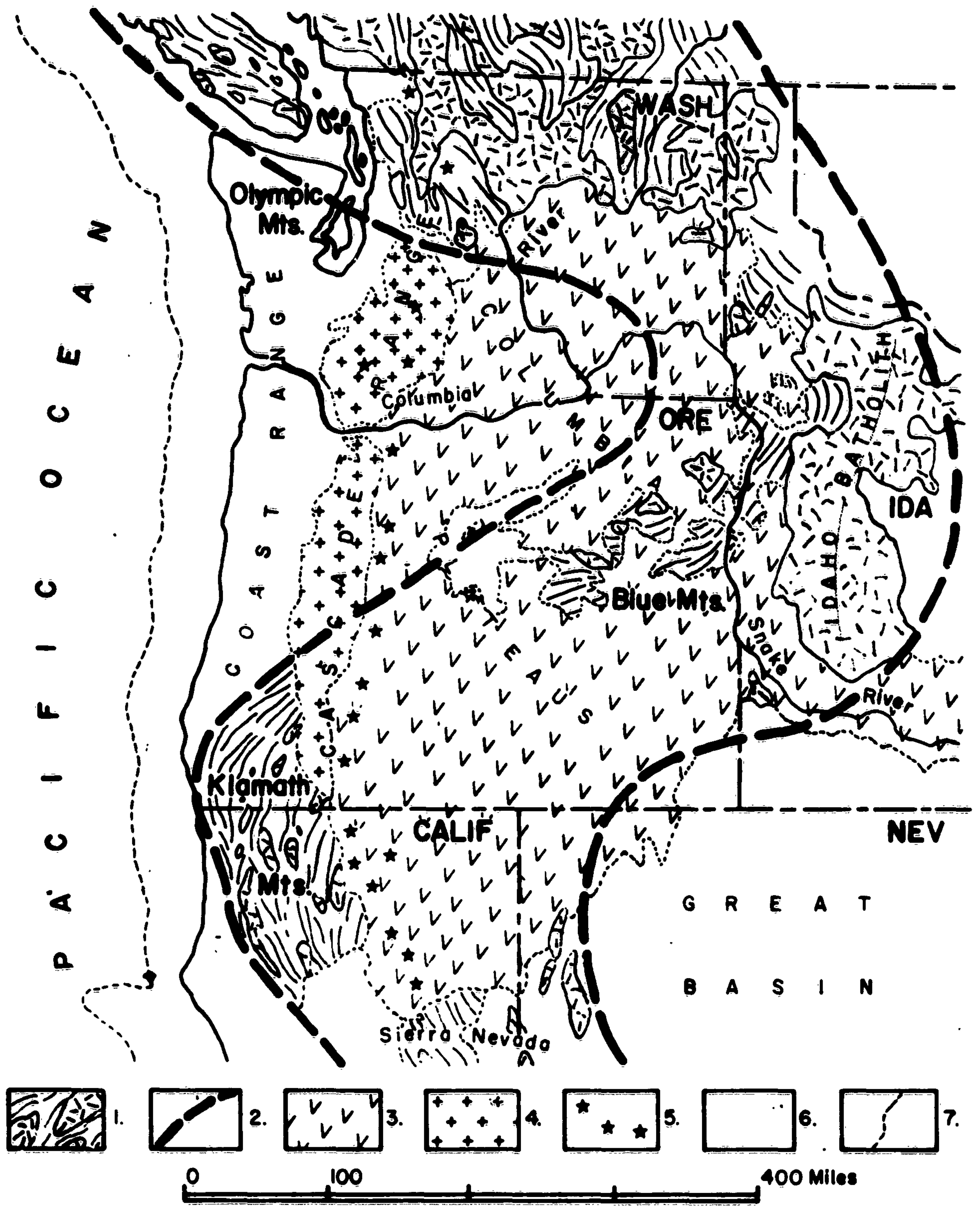

1. Nevadan Basement Complex
2. Margins of Nevadan Orogenic Belt
3. Miocene & Later Aged Basalts
4 Andesitic Volcanics of Cascade Range
5 Recent or Active Volcanos
6 Other Rock-Mesozoic & Tertiary Sediments
7. Continental Edge

Tectonic and Geomorphic Map of Oregon and Washington
FIGURE 2.2

UED H-10,960 Date 1-12-62
UNITED ELECTRODYNAMICS, INC.
PASADENA, CALIFORNIA

its existence. From the point of view of this work, the present land-form situation is of greater interest.

In contrast to California where considerable is known concerning the geology from commercial oil and gas development, the results of oil and gas drilling in Washington are quite limited. A number of shallow (less than 300 meters) wells have been drilled. These, although widespread, are so poorly logged as to be nearly unuseable for geologic control.

From west to east the Pacific Northwest can be divided into geomorphological provinces which, from a seismic noise study aspect, seem to be significant. These provinces are illustrated in Figure 2.3 in the form of a diagrammatic cross section,because of lack of well control depths as shown are questionable.

Preliminary locations have been made to occupy each of these provinces with a slave station location. They are from west to east (see Figure 2.3); the costal Tertiary province, the Puget Sound-Willamette trough, which is both a structural and topographic trough and the axis line of late Tertiary and Quaternary volcanism illustrated in Figure 2.2 The tentative Slave Station locations in the Cascade Mountains and west have been located only by map study. The stations east of the Cascades have been visited on the ground and permission obtained for their occupancy. From the Cascades east the Slave Station sites are on the east slope of the mountains, near the axis of the basin east of the mountains, in the Blue Mountains where the granite is several thousand feet below in the surface, and in the eastern Blue Mountains on a granite outcrop.

2.2 Detail Geology and Topography of Master Station Site East of the Cascades.

The Master Station is located 73 kilometers nearly due east of Mt. Adams (3750 meters-elevation), one of the major volcanic peaks of the Cascades. This places the station on the topographic east slope of the mountains and about 65 kilometers west of the topographic axis of the Columbia River Basin. The station is located on an east-west trending ridge, one of several that cross central Washington. These ridges have steep to overturned north flanks and relatively gentle dipping south flanks. There is some faulting along the north flanks. Dips are defined in successive layers of basalt. Several wells have been drilled near the axis of these folds in an effort to penetrate the presumed underlying Tertiary sedimentary sequence. One such test located in the Rattlesnake Hills 85 kilometers northeast of the

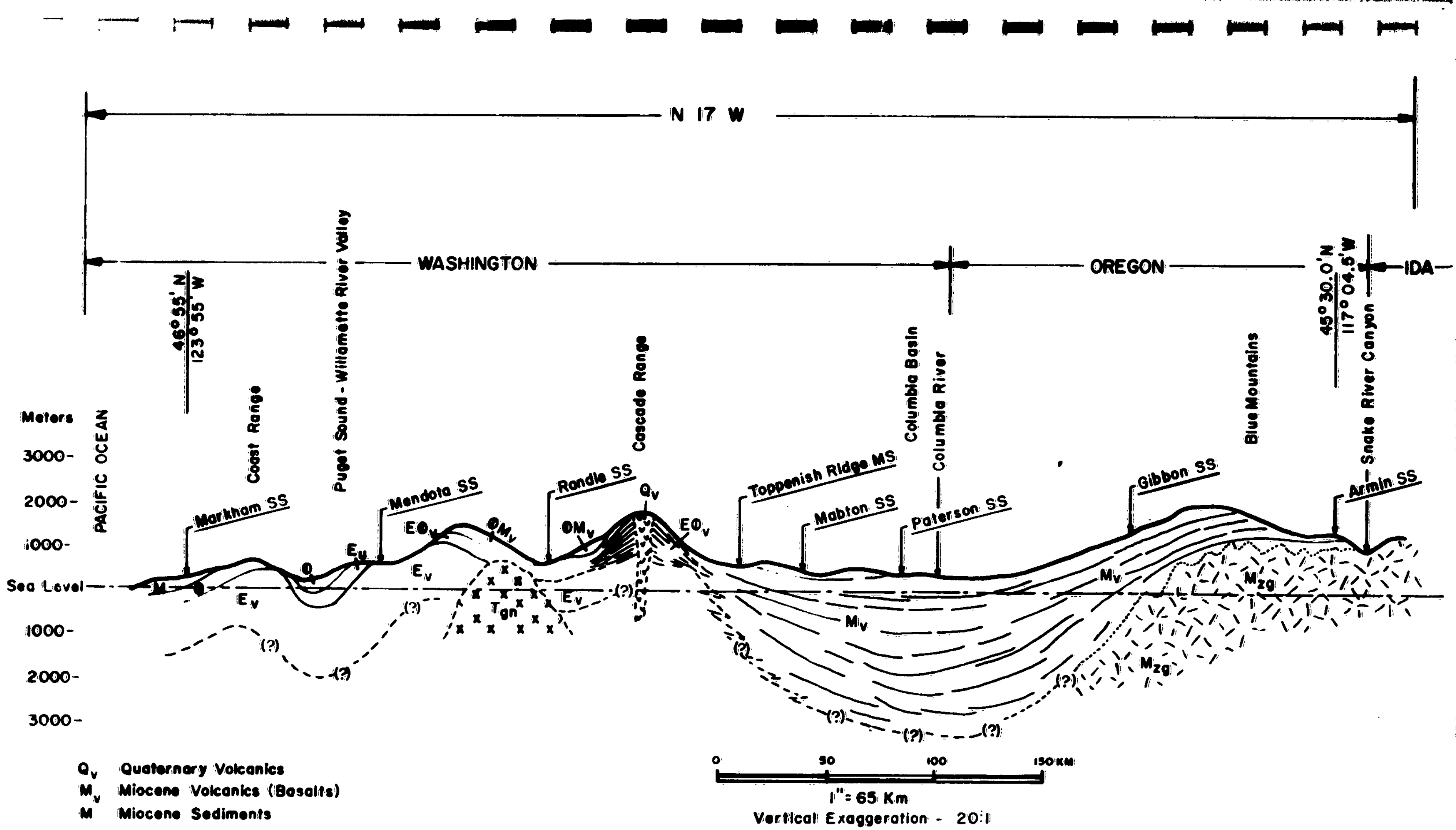

Q_v Quaternary Volcanics
M_v Miocene Volcanics (Basalts)
M Miocene Sediments
ΘM_v Oligocene-Miocene Volcanics
Θ Oligocene Sediments
$E\Theta_v$ Eocene-Oligocene Volcanics
E_u Upper Eocene Sediments
E_v Eocene Volcanics
T_{gn} Tertiary Granite
M_{zg} Mesozoic Granite (Nevadan)

UED H-10,968 Date 1-18-62
UNITED ELECTRODYNAMICS, INC
PASADENA CALIFORNIA

DIAGRAMMATIC CROSS SECTION OF PACIFIC NORTH WEST FROM GREYS HARBOR, WASH., TO IDAHO BORDER

FIGURE 2.3

Master Station was abandoned in basaltic rock at 3250 meters. Figure 2.4 illustrates the location of several of these ridges and the course of the Columbia River during recent geologic time. A recent publication of the Washington State Division of Mines by J. Hoover Mackin[1] is of interest. Of particular relevance is his description of methods of identification of particular basaltic flows. From his description, each of the flows has upon careful examination, a distinctive pattern which can be identified over considerable distance. This publication is also of interest from the aspect of the geologic methods used in a lava flow area. Figures 2.4 and 2.5 are photographs which illustrate the rolling topography of Toppenish Ridge near the Master Station. These photographs were taken in late November during the initial test period at the Master Station. This location is about 8 kilometers south of the steep north flank of the Toppenish Ridge.

One of the features of the Master Station is elongate east-west trending captive dunes of loess soil. Locations were made on hard basaltic rock without resorting to blasting to obtain a pit for the seismometers by making the locations fall on one of these dunes. They are two to three feet above hard rock level, the right distance for the seismometer pits. Figure 2.6 is a photograph of one of the dunes. The surface is rough with occasional lava boulders. The sage brush is sparse and attains a maximum height of about 0.5 meters. Figure 2.7 is a photograph of rigging-up operations at the Master Station array center.

2.3 Geology and Topography of the Mabton Site.

Following a preliminary checkout period when both the Master and Slave instrumentation systems occupied the Toppenish Ridge Site, the Slave Station was moved 19.5 kilometers S 75°E to the Mabton Site. Occupancy at this site began 4 December and was completed 23 December. Total recording time was about 210 hours.

The Mabton Site is located on the steep north side of the Horse Heaven Hills. These hills are an approximate east trending ridge with steep north slope and gentle south slope which are described in Section 2.1. The center of the Mabton Site is about 6 kilometers north of the apex of the ridge.

1. Mackin, J. Hoover - A Stratigraphic Section in Yakima Basalt and the Ellensburg Formation in South-Central Washington - Washington Division of Mines and Geology, 1961

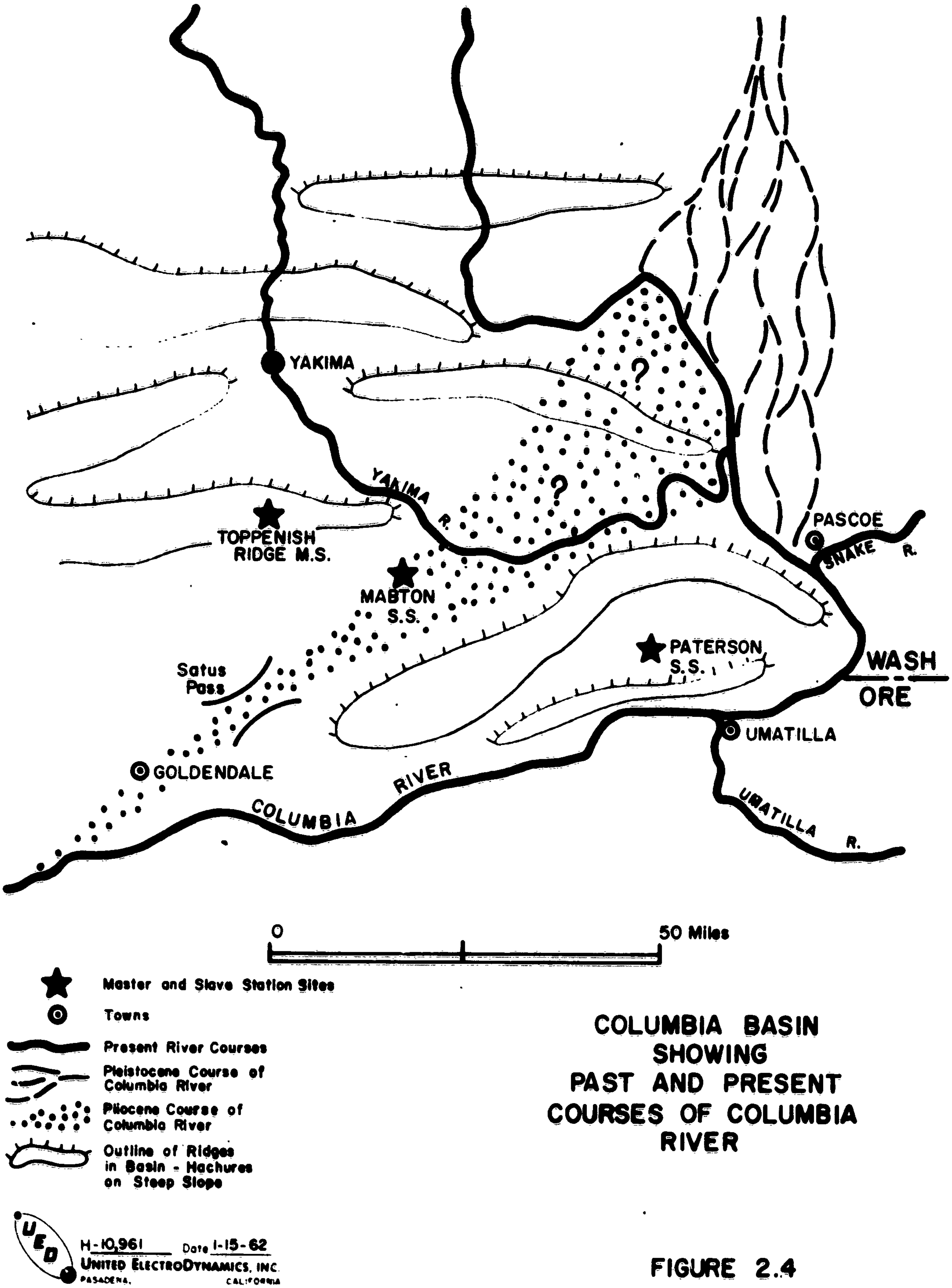

COLUMBIA BASIN
SHOWING
PAST AND PRESENT
COURSES OF COLUMBIA
RIVER

FIGURE 2.4

Figure 2.4   Topography near the Master Station at Toppenish Ridge.

Figure 2.5   Looking north from the Master Station. The hill in the background is the apex of Toppenish Ridge. The north slope of this hill is relatively steep.

Figure 2.6 Captive easterly trending "dune" of loess soil near the Master Station. The rock is barren lava between the "dunes". There was snow on the ground when this photograph was taken.

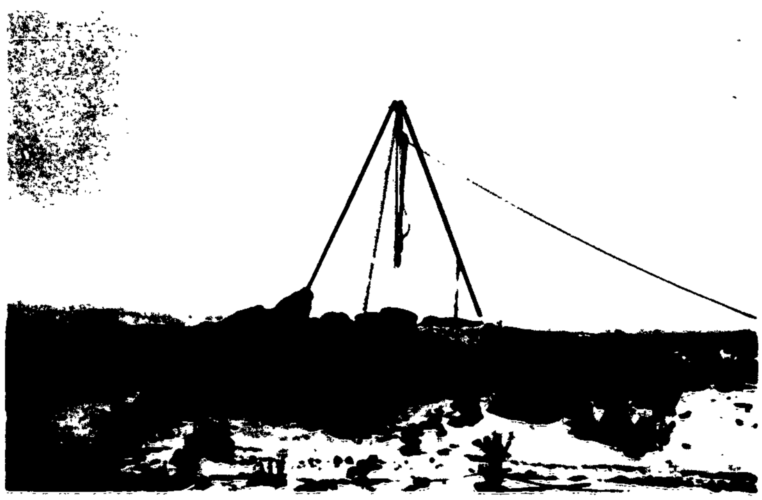

Figure 2.7 Rigging-up operations at the array center of the Master Station. The ridge of loess allowed buried seismometer locations without blasting.

A conglomerate is exposed in the canyons near this site. These have been interpreted as originating from the Pliocene channel of the Columbia River (see Figure 2.4). Figure 2.8 is a photograph of the Mabton site.

The basalt is probably at least 3000 meters thick at this point.

2.4 <u>Geology and Topography of the Paterson Slave Station Site.</u>

The Paterson Slave Station site is located on the south flank of the Horse Heaven Hills (see Figure 2.4). This station with Mabton and Toppenish Ridge are located to occupy the south slope, the steep north flank and the apex respectively of the easterly trending ridge topography of south-central Washington.

Occupany of this station is scheduled to begin 2 January, with actual recording beginning 8 January.

The topographic basin east of the Cascades is rather poorly defined as to its margins; however, in over-all aspect, it is a definite topographic low. The Paterson site is roughly at the center of this basin. It is located in an area where the course of the Columbia has been moved east by the rise of the Horse Heaven Hills. It is approximately 50 kilometers due south of a deep test for petroleum, which was in basalt from the surface to total depth. Although some authors have hypothesized a zone of Tertiary sedimentary rocks underlying the basalt layers, there is no real evidence for its existence. The nearest outcrop evidence is east in the Blue Mountains where the basalt overlies granite. It would seem that projecting this information to the center of the basin, near Paterson, would be ill-advised.

Figures 2.9 and 2.10 are photographs of the Paterson site. They illustrate the flat to slightly rolling topography and the grassland cover. The soil in this area is mineral rich and in a less arid climate, would be excellent farm land.

2.5 <u>Gibbon and Arnim Slave Station Sites</u>.

Two additional Slave Station sites have been located and permitted to the east of the Paterson site. They are both in the Blue Mountains which are rather poorly defined as to their extent. Approaching the area from the west there is a gradual increase in elevation and of the ruggedness of the topography.

Figure 2.8 Mabton Area. The Mabton Slave Station Site is located on the near slope of the ridge on the left horizon of the photograph.

Figure 2.9 Paterson Slave Station Site looking northeast.

Figure 2.10 Paterson Slave Station Site looking northwest.

The Gibbon site is located about 15 kilometers southeast of Milton-Freewater, Oregon in a wooded area. There is an estimated 800 to 1000 meters of loess and basaltic layers on top of the granite.

The Arnim site is the eastern extremity of the Pacific Northwest profile and is 35 kilometers from the Oregon-Idaho boundary and 50 kilometers south of the Washington-Oregon boundary. It is on a granite outcrop.

The locations of both the Arnim and Gibbon sites are tentative. Their geology and topography will be discussed in more detail in later reports.

2.6 Metereological Conditions in the Pacific Northwest.

In the Pacific Southwest during the summer, there are very few changes in the weather. There is little or no rain, the days are monotonously hot. From one aspect of noise analysis this is fortunate since it allows analysis of seismic noise that is little affected by weather. However, since in most areas there are weather changes and frontal movements, the Pacific Southwest presents a limited area to study the effects of weather changes on seismic noise level. This is one of the reasons the Pacific Northwest was recommended as a second area for a profile line to study noise. The area has considerable weather contrast from west to east and has considerable frontal movement.

The Cascade Mountains, in conjunction with the Rocky Mountains, separate the northwestern United States into three distinct meteorological provinces. These are the costal province west of the Cascades which is strongly affected by Pacific storms; the intermontane area between the Cascades and the Rockies which is in a sense, a "weather trap" tending to hold weather, particularly a cold air mass; the Rocky Mountain area and east which is strongly influenced in winter months by cold fronts moving in from Canada. Only the western slope of the Cascades and the intermontane area will be the locale of test-sites of the Pacific Northwest Profile.

The mechanism of weather changes in the Pacific Northwest is controlled along the coast (west of the Cascades) by Pacific fronts which bring rain and occasional snow to the Seattle area. They have an approximate cycle of every 3 to 4 days.

The intermontane area is controlled in part by cold air from Canada that originates from the northeast quadrant and fills the basin. The frontal systems from the Pacific are warm relative to this cold air mass. They can do one of two things in a general way, either sweep the cold air out of the intermontane area as a surface front, or ride over the cold air and exist only as a front aloft.

It is the relation of this weather pattern to seismic noise levels that is of interest in the Pacific Northwest.

3. Operational Setup.

The noise analysis system consists of three separate operating units. These are the Master Station, the Slave Station, and the Analysis Group. The Master Station and Slave Stations are essentially identical. Figure 3.1 is a block diagram of these recording systems. The difference is in the manner of use. The Master Station remains in a fixed location for each profile. The Slave Station is moved about once a month to a new site which has been selected to obtain noise level under certain geologic or topographic conditions. The instruments used were described in detail in Report No. VT/078-10 (Ref. 16).

The field setup at the Master Station is illustrated by Figure 3.2, at the Slave Station by Figure 3.3.

Work on the California line was completed 10 November and the initial work in Washington State began on 27 November 1961. By the end of the year, the recording at the first Slave Station location was completed.

The office analysis system presently located in Pasadena, is essentially as described in the semiannual report for the period ending 30 June 1961. Figure 3.4 is a block diagram of the office analysis system. The only change in this system which has occurred, is the addition of cross spectral analysis equipment which was received 29 December 1961.

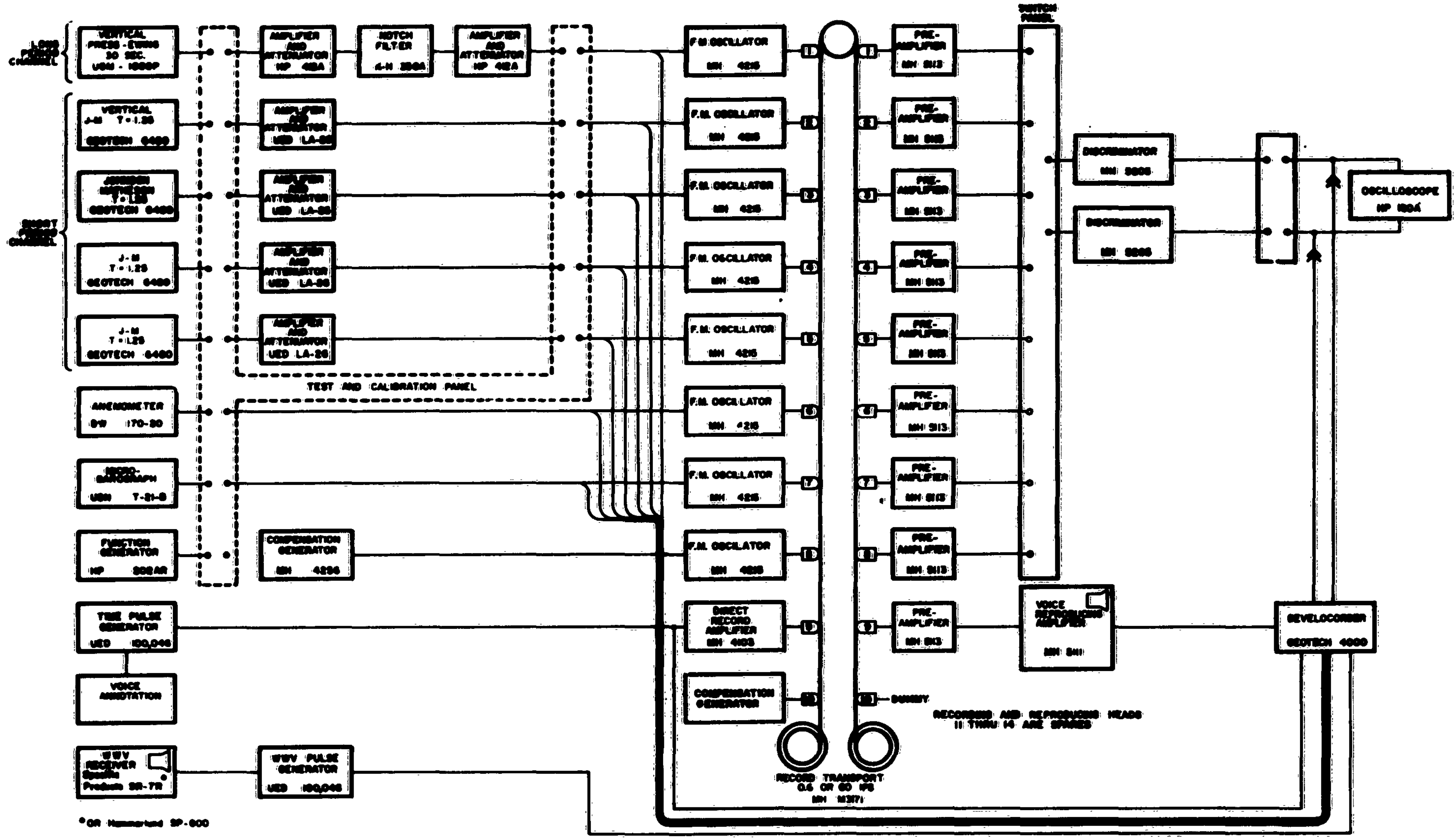
VERTICAL PRESS-EWING 30 SEC. UGM - 1080P
VERTICAL J-M T=1.25 GEOTECH 6480
J-M T=1.25 GEOTECH 6480
J-M T=1.25 GEOTECH 6480
ANEMOMETER BW 170-30
MICRO-BAROGRAPH UGM T-21-B
FUNCTION GENERATOR HP 202AR
TIME PULSE GENERATOR UED 100,046
VOICE ANNOTATION
WWV RECEIVER Products SR-7R
*OR Hammarlund SP-600
AMPLIFIER AND ATTENUATOR HP 462A
NOTCH FILTER
AMPLIFIER AND ATTENUATOR UED LA-26
TEST AND CALIBRATION PANEL
COMPENSATION GENERATOR MH 4236
WWV PULSE GENERATOR UED 100,046
F.M. OSCILLATOR MH 4215
DIRECT RECORD AMPLIFIER MH 4103
COMPENSATION GENERATOR
PRE-AMPLIFIER MH 5113
DUMMY
RECORD TRANSPORT 0.6 OR 60 IPS MH M3171
RECORDING AND REPRODUCING HEADS 11 THRU 14 ARE SPARES
SWITCH PANEL
DISCRIMINATOR MH 5605
VOICE REPRODUCING AMPLIFIER MH 5411
OSCILLOSCOPE HP 150A
SEVELOCORDER GEOTECH 4000

FIGURE 3.1

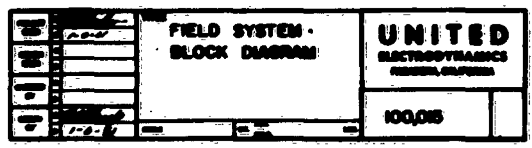
FIELD SYSTEM · BLOCK DIAGRAM
UNITED ELECTRODYNAMICS
100,015

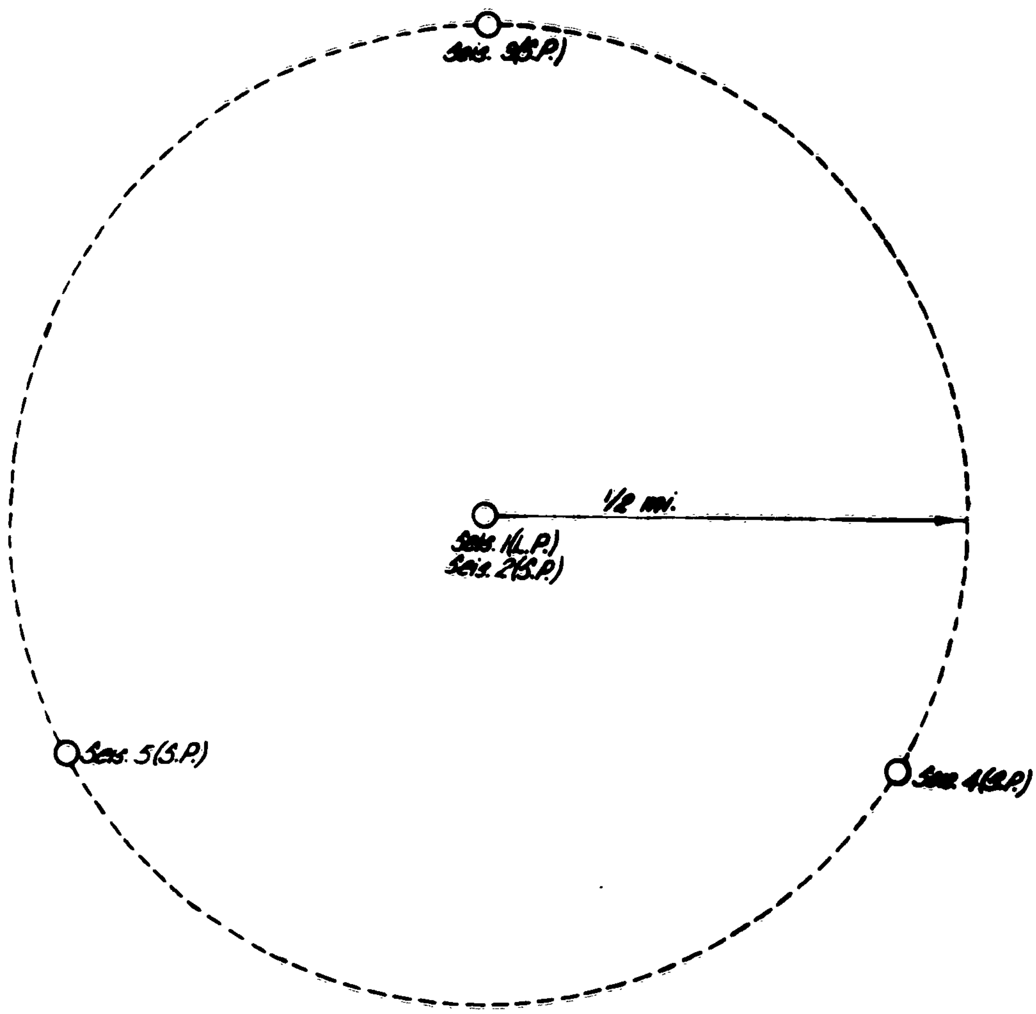

MASTER STATION
SEISMOMETER ARRAY

Fig. 3.2

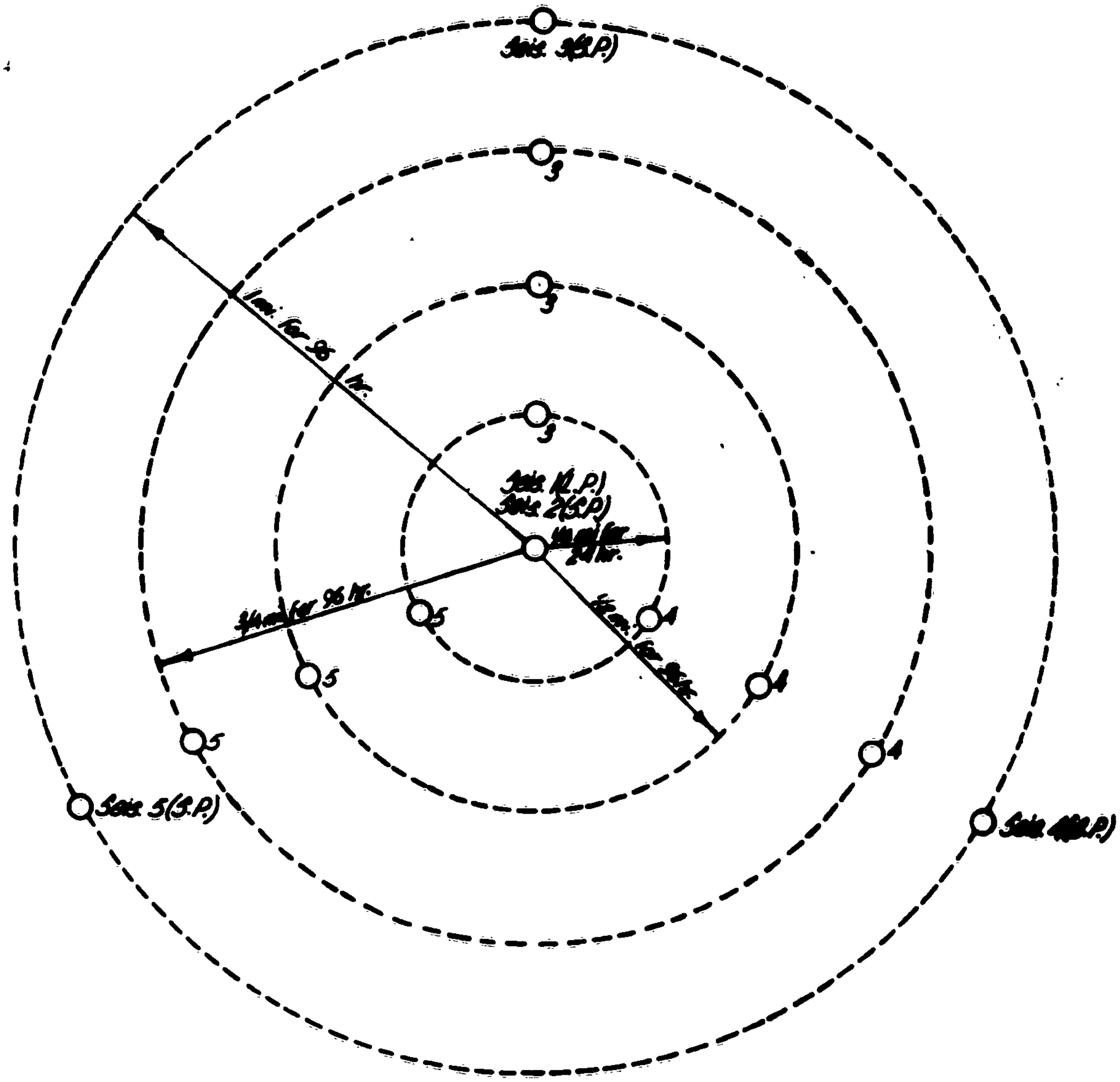

SLAVE STATION
SEISMOMETER ARRAYS
Showing
Radius & Duration
of each array

Fig. 3.3

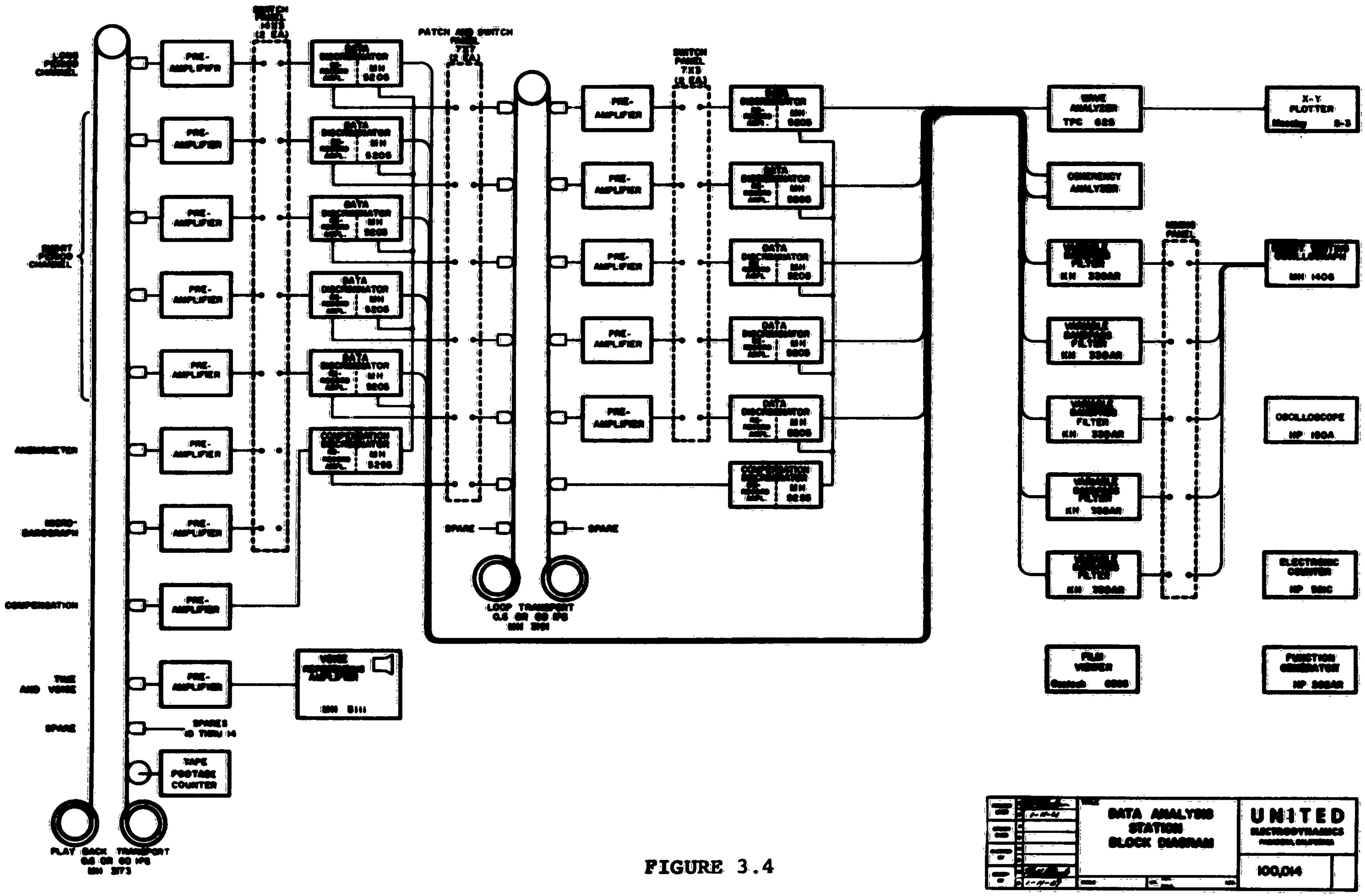

PRE-AMPLIFIER
DATA DISCRIMINATOR
PATCH AND SWITCH PANEL
SPARE
LOOP TRANSPORT
PLAY BACK TRANSPORT
TAPE FOOTAGE COUNTER
ANEMOMETER
COMPENSATION
TIME AND VOICE
WAVE ANALYZER TPC 625
X-Y PLOTTER
COHERENCY ANALYZER
VARIABLE FILTER
OSCILLOSCOPE HP 150A
ELECTRONIC COUNTER
FUNCTION GENERATOR
FILM VIEWER
DATA ANALYSIS STATION BLOCK DIAGRAM
UNITED ELECTRODYNAMICS
100,014

FIGURE 3.4

4. Seismic Noise and Its Analysis

The word noise has its primary use in ordinary speech as something disharmonious or unpleasant to hear. It is a common experience that noise to one person is music to another, or that sounds may be pleasant under certain circumstances and unpleasant under others. This brief discussion emphasizes that noise is subjective.

From the aspect of this project, noise is the continuous motion of the earth that interferes with the recognition of the amplitude and phase characteristics of earth motion resulting from earthquakes and explosions. It is also the purpose of this project to relate this interference to geologic, geographic and weather parameters. It is thus necessary in the final analysis, to determine a signal to noise ratio.

The procedure followed has been to separate insofar as possible, noise and signals for analysis purposes and combine the results as a final step. This section of the report is limited to noise. It is recognized that earthquake signals, particularly a large number of local earthquake signals, may be "noise" as far as recognition of signals from more distant earthquakes is concerned.

There are two broad categories of noise analysis methods. These are machine methods and visual methods. Each of these methods has certain advantages and disadvantages which will be discussed in the following section.

4.1 Advantages and Disadvantages of Alternate Noise Analysis Methods

As will be developed in this section, the advantages of machine analysis methods seemed to outweigh its disadvantages and was therefore chosen as the method to be used.

The advantages of machine methods are:

1) The rapid processing of large quantities of data

2) The capability of more detailed separation of a complex wave into its various components

3) Its ability to do a routine job without fatigue or boredom

4) The ability to recognize lower amplitudes, lower frequency noise in a background of high frequency noise.

The disadvantages of machine methods are:

1) The addition of machine variable and machine calibration problems

2) The inability of the machine to recognize an erroneous input

The advantages of visual methods are:

1) Better control of the data being analyzed insofar as signal and noise separation is concerned

2) The filtering and judgment that a skilled observer uses in recognition of amplitude and phase

The disadvantages of visual methods are:

1) The practical limitations of frequency separation unless extreme photographic enlargement of the recorded trace is used

2) The fact that to obtain statistical reliability, large quantities of data need to be processed, the work is commonly delegated to unskilled personnel, and the advantage listed under 2) above is lost.

During the equipment assembly period of this project, the above advantages and disadvantages were compared. It was decided to use machine methods largely because of the machine's ability to process large quantities of data rapidly.

4.2 Comparison of Results by Machine and Visual Methods

There are several machine methods and manners of presenting results as well as different visual methods. It is the purpose of this section to compare two specific methods and the results obtained. It will be concluded that because of differences in method that the results must be interpreted with respect to each other and cannot be directly compared. This difference results when reduced to essentials from the fact that one method determines the peak value of the noise and the other determines the average.

The machine method in use on this project produces a power spectral density of a noise sample in the form of a plot on semi-log paper with frequency as one axis and voltage squared per cycle as the vertical axis. This data can then be corrected

for system response and converted to ground motion as a function of frequency or period. A later section will clarify the details and how the machine works.

The visual method selects from a series of samples by visual inspection, the maximum amplitude that occurs in a given period band, commonly 0.3 to 1.5 seconds period. This data is then assembled in the form of an S-curve which shows the probability of noise occurring at a given location at or less than a given seismogram amplitude.

The results are not readily compared, since one method looks at all periods between 0.3 and 1.5 and the other separates frequencies or periods into quite narrow bands and corrects to unit band width. However, in the following example there is a dominant frequency for the entire one hour period studied. The results can be presented in the form of an S-curve for the visual method and a vertical line which establishes the average level of the particular frequency which has the greatest amplitude.

The first step in the analysis is to establish magnification levels of the particular one hour sample analyzed. The sample was chosen at random except that it was an hour when visual inspection of the records indicated that there were no earthquakes recorded. The seismometer used was at the center of the Master Station array at Round Mountain. It is a Johnson-Matheson seismometer, - Serial No. 6. The sample chosen was between 0850 and 0950 G C T on the 226th day of 1961 (14 August). Calibration control is based on driving the seismometer through its calibrate coil at three frequencies (nominally 0.5, 2.0 and 8.0 cps).

The results of the calibration as viewed on the Film Viewer are:

Period	Amplitude (p-p)	ma Drive
1.0/8	5.5 mm	3.9
8.2/16	22.0 mm	7.8
8.25/4	9.5 mm	6.2

Using the formula[1]

$$\mu = \frac{G\ i\ 1404}{f^2}$$

to determine equivalent ground motion, where μ is equivalent motion in microns (p-p), G is the calibration coil motor constant, i is calibration coil current in amperes (p-p), and f is the frequency of the calibrate signal, results in the following data:

Frequency	Equivalent Ground Motion
8 cps	1.24 mμ
1.95 cps	41.8 mμ
0.485 cps	535 mμ

Since film viewer amplitudes are double the (5cm = 10 seconds) normal magnification used, the observed amplitudes are divided by 2 and the following magnifications computed:

Frequency	Magnification
8 cps	$\frac{2.75\ \text{mm}}{1.24\ \text{m}\mu} = 2.22 \times 10^6$
1.95 cps	$\frac{11.0\ \text{mm}}{41.8\ \text{m}\mu} = 2.63 \times 10^5$
0.485 cps	$\frac{4.75\ \text{mm}}{535\ \text{m}\mu} = .888 \times 10^4$

The attenuator level was set at -40db during calibration and operating level was -20 db. The magnifications have been increased by a factor of 10 to compensate for this difference and plotted on Figure 4.1.

Determination of the maximum amplitude that occurred in each minute between 0850 and 0950 resulted in the following data:

1. Operation and Maintenance Manual, Johnson-Matheson Vertical Seismometer, Model 6480, pg. 11

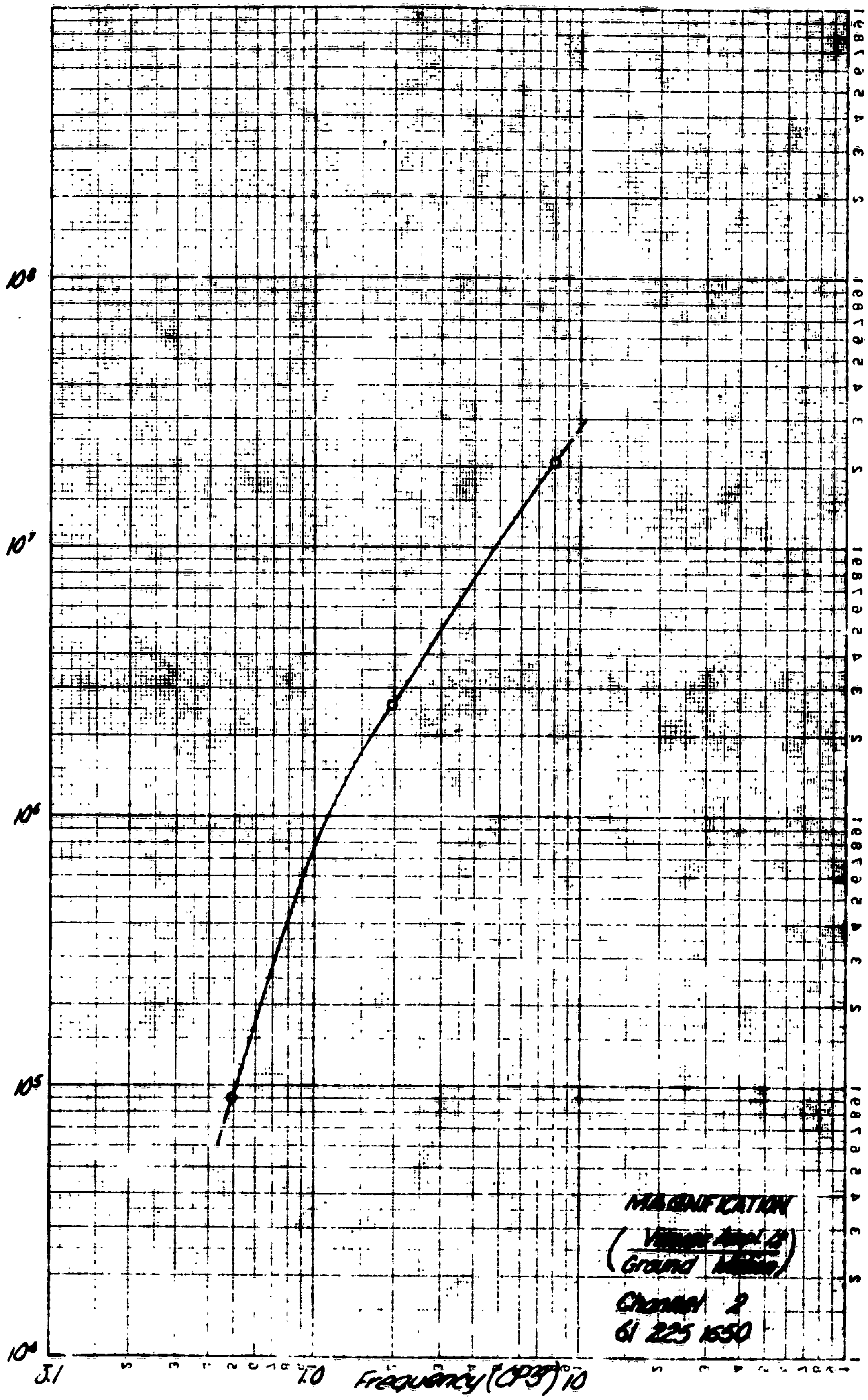

MAGNIFICATION
(Vibrator Ampl. (R) / Ground Motion)
Channel 2
61 225 1650
10^8
10^7
10^6
10^5
10^4
.1
1.0
10
Frequency (CPS)

Fig. A.1

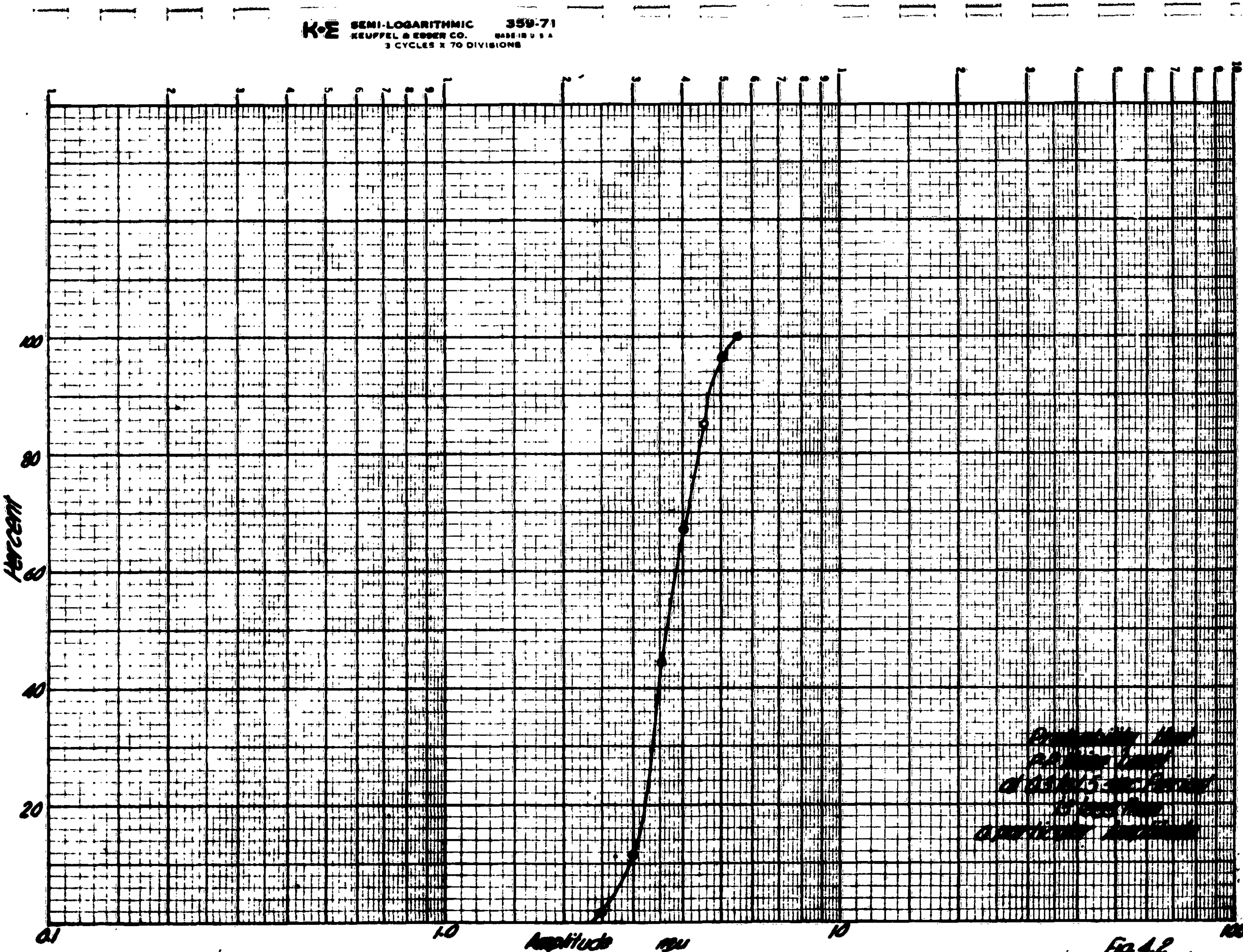
K•E SEMI-LOGARITHMIC 359-71
KEUFFEL & ESSER CO. MADE IN U.S.A.
3 CYCLES X 70 DIVISIONS
Percent
100
80
60
40
20
0.1
1.0
10
100
Amplitude mu

Fig. 4.2

Amp. (mm)	Occurrences	Occurrences Minimum Ampl.	% Minimum Ampl.	Ampl.x10^{-6}
2.5	1	1	1.64	2.5
3.0	6	7	11.5	3.0
3.5	20	27	44.3	3.5
4.0	14	41	67.2	^.0
4.5	11	52	85.2	4.5
5.0	7	59	96.7	5.0
5.5	2	61	100.0	5.5

Figure 4.3 is a record sample of one of the records used to obtain the above data.

In order to obtain a comparison between the visually analyzed data and data from the wave analyzer, power spectra were made at the beginning, middle and end of the one hour period analyzed by visual means. Figures 4.4 to 4.6 are these spectra. The system response curve has been plotted on Figure 4.4 as a dashed line. An examination of these spectra shows that the highest power level occurs near the upper end of the period band studied by the visual method at 0.70 cps or 1.4 seconds period. The vertical scale of these plots is in $(m\mu/sec)^2/cps$ at 2.0 cps. An additional correction is required for system response. There will be a discussion of the wave analyzer and how it works in a later section of the report. The read values of "Power" at about 0.7 cps are:

MS 226 0850	$(3.10\ m\mu/sec)^2/cps$	1.76 $m\mu$/sec/cps
MS 226 0920	$(2.76\ m\mu/sec)^2/cps$	1.66 $m\mu$/sec/cps
MS 226 0946	$(2.36\ m\mu/sec)^2/cps$	1.54 $m\mu$/sec/cps

The third column is the square root of the Power, that is the velocity value corresponding to input voltage into the analyzer. The average value is 1.65 $m\mu$/sec/cps. The voltage which the analyzer sees is proportional to velocity of the ground, since the Johnson-Matheson has voltage output proportional to ground velocity in the flat portion of its response curve. The analyzer is calibrated at 2cps.

In order to obtain a correction from voltage out of the amplifier to ground motion, it is necessary to divide the magnifications computed for view screen (5 cm = 10 sec) amplitude by $2\pi f$, where f is the frequency of the sinusoidal drive used into the calibrate coil. This "magnification" is plotted in Figure 4.7. It supplies a factor to correct the velocity at 0.7 cps to that at

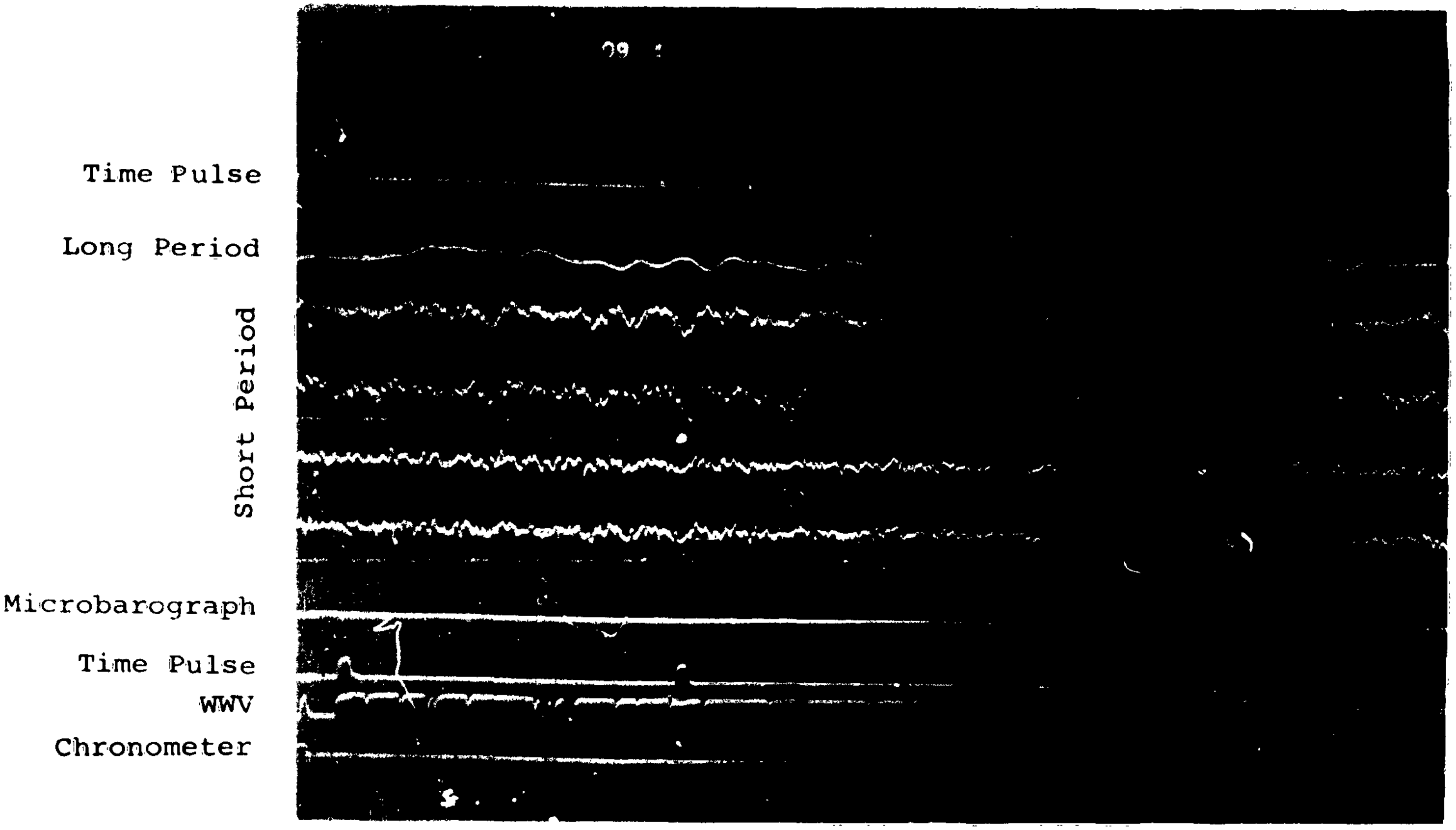

Figure 4.3 Record sample of data used to obtain S-curve plot Figure 4.2
MS 226 0941

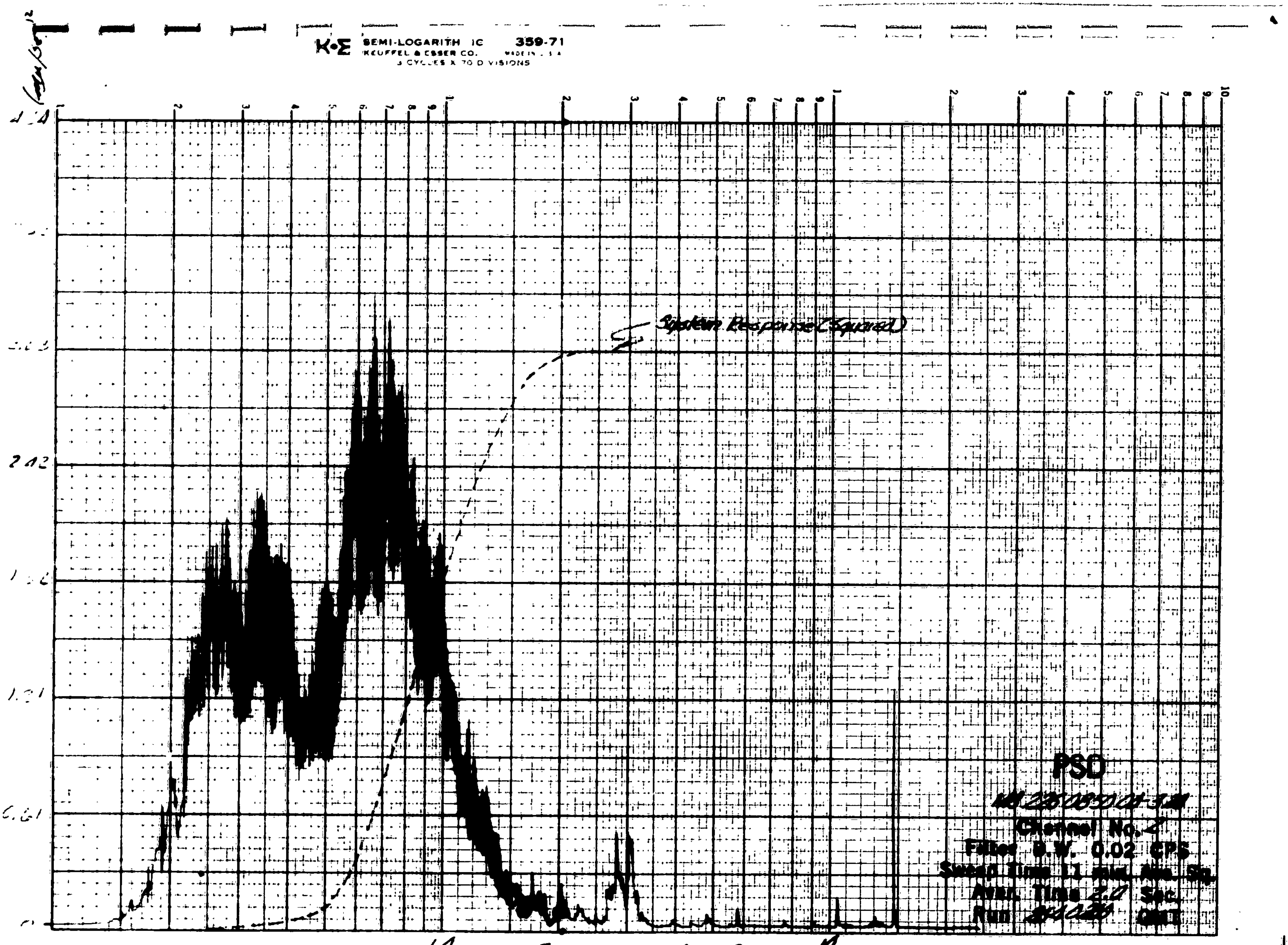
K•E SEMI-LOGARITHMIC 359-71
KEUFFEL & ESSER CO.
3 CYCLES X 70 DIVISIONS
System Response (Squared)
PSD
Channel No. 2
Filter B.W. 0.02 CPS
Avgr. Time 2.0 Sec.
1.0
Frequency in CPS
10

Fig. 4A

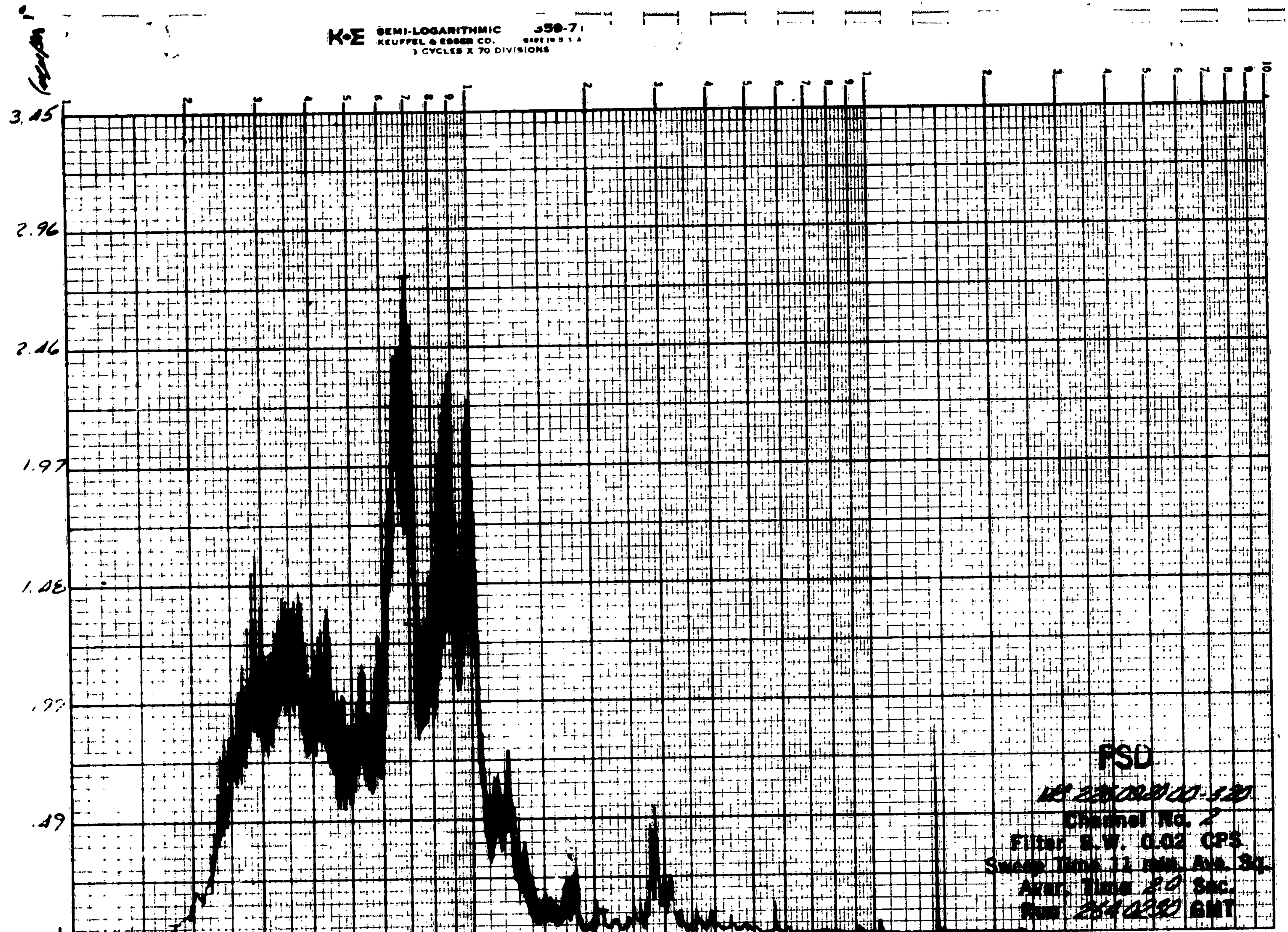
K•E SEMI-LOGARITHMIC 359-71
KEUFFEL & ESSER CO.
3 CYCLES X 70 DIVISIONS
3.15
2.96
2.16
1.97
1.08
.99
.49
0
1.0
Frequency in CPS
10
FSD
Channel No. 2
Filter B.W. 0.02 CPS
Sweep Time 11 min. Ave. Sq.
Aver. Time 20 Sec.
GMT

Fig. 4.5

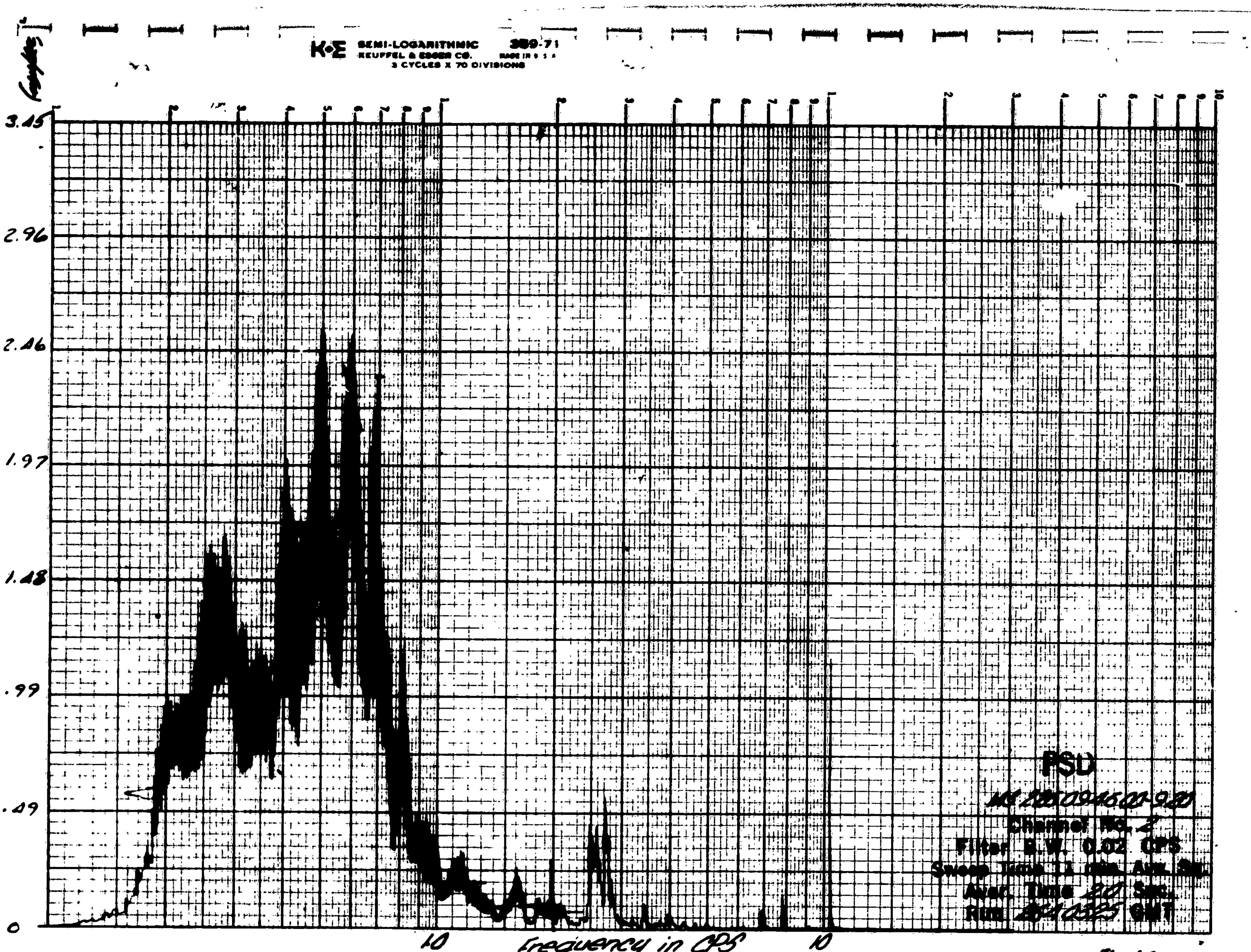

K+E SEMI-LOGARITHMIC 359-71
KEUFFEL & ESSER CO. MADE IN U.S.A.
3 CYCLES X 70 DIVISIONS
3.15
2.96
2.46
1.97
1.48
.99
.49
0
10
10
Frequency in CPS
PSD
Channel No. 2
Filter B.W. 0.02 CPS
Ave. Time 20 Sec.
GMT

Fig. 46

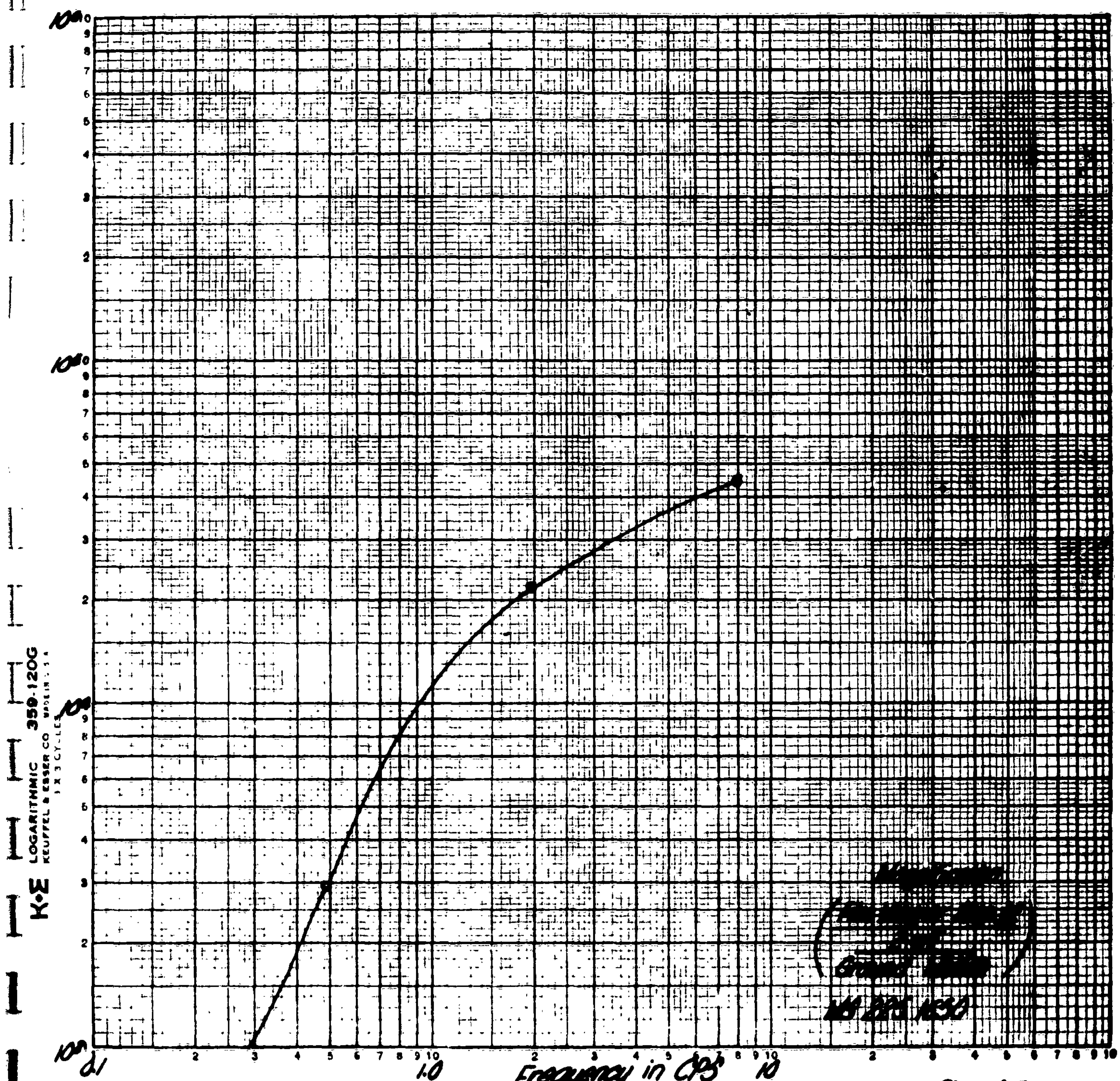
K•E LOGARITHMIC 359-120G
KEUFFEL & ESSER CO. MADE IN U.S.A.
3 X 3 CYCLES
0.1
1.0
10
Frequency in CPS

Fig. 4.7

2.0 cps.

From the curve Figure 4.7, the magnification at 0.7 cps is 6.0×10^3, at 2.0 cps it is 2.15×10^4. The ratio is 3.58. This is the correction to be applied to 1.65 mμ/sec/cps.

1.65 mμ/sec/cps x 3.58 = 5.90 mμ/sec/cps.

Since this is velocity at 0.7 cps, it can be converted to amplitude by dividing by $2\pi f$.

$$\frac{5.90\ \mathrm{m\mu/sec/cps}}{2\quad \times 0.7} = 1.35\ \mathrm{m\mu/cps}$$

The analyzer writes rms value; however, it is calibrated by ratio to a sinusoidal input that automatically corrects the output to mμ(p-p).

This last step is possible since at any given frequency, the analyzer output is a DC analogue of nearly a single sinusoidal frequency.

Figure 4.8 combines the results of the two methods of obtaining noise level. This shows that the average level of noise in the one hour sample by visual means (50% level) is 3.6 mμ, 2.7 times the level by machine analysis.

This result is probably only valid for this particular example. In general, if a higher frequency band of noise is considered,using the visual method, the machine method will give a lesser result by a factor of $2\pi f$, the value of f depending on where in the band the dominant noise frequency occurs.

The machine analysis method has the advantage of noise separation by quite narrow bands and seems a better way of determining absolute noise level as a function of frequency. However, if relative noise level of two locations is the prime consideration, then either method will give the same relative level. It should be emphasized that this comparison is for only two methods of analysis.

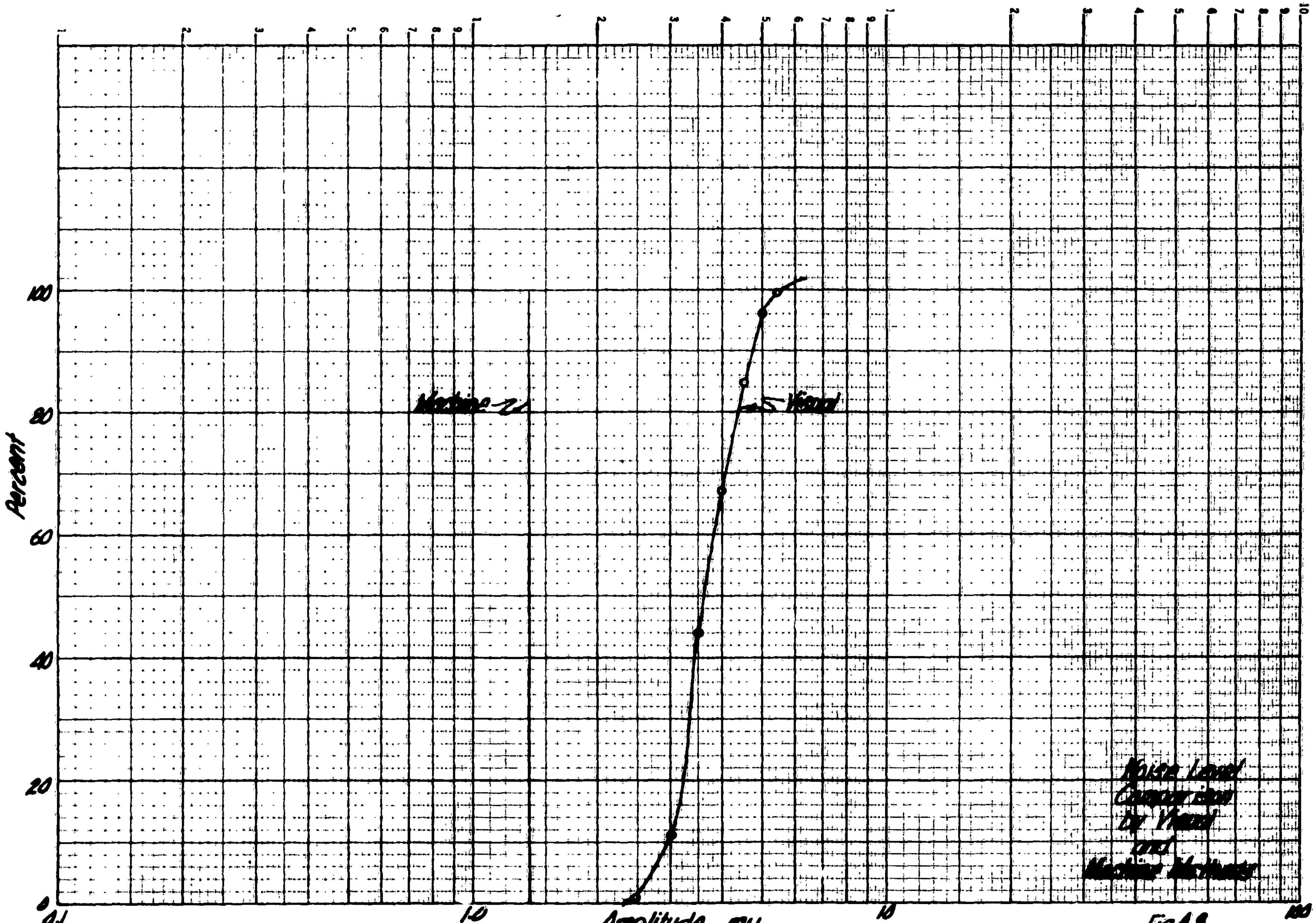
Percent
100
80
60
40
20
0
0.1
1.0
10
100
Amplitude mu
Machine 2.1
5 Visual
Noise Level
Comparison
by Visual
and
Machine Methods

Fig 4.8

5. The Wave Analyzer and How It Works.

This section of the report is a discussion of Wave Analyzers in general and the Technical Products Wave Analyzer in use on Project VT/078. An attempt is also made to clarify certain of the mathematical aspects of the analysis.

5.1. Power as Related to Fourier Transform Theory.

In order to obtain a definition of power spectral density and add meaning to the word "power" as it appears in the definition, it is necessary to develop a certain amount of mathematical background.

Let

$$y_1(t) = \int_{-\infty}^{\infty} c_1(f_1) e^{j2\pi f_1 t} df_1 \tag{1.1}$$

and

$$y_2(t) = \int_{-\infty}^{\infty} c_2(f_2) e^{j2\pi f_2 t} df_2 \tag{1.2}$$

Then the product of these two functions, which in the case of seismic noise analysis are random processes is

$$y_1(t)y_2(t) = \int_{-\infty}^{\infty}\int_{-\infty}^{\infty} c_1(f_1)c_2(f_2) e^{j2\pi(f_1+f_2)} df_1 df_2 \tag{1.3}$$

The following development is based largely on that of W. R. Bennett.[1] It is possible to change the order of integration etc., in these functions because as recorded the seismic noise wave does not have singularities or sudden jumps in value.

Now, let

$$f_1 + f_2 = f$$

then

$$y_1(t)y_2(t) = \int_{-\infty}^{\infty}\int_{-\infty}^{\infty} c_1(f_1)c_2(f - f_1) e^{j2\pi ft} df_1 df$$

[1] William R. Bennett, Electrical Noise, McGraw-Hill, 1960 pp.204-207

and if

$$c_{12}(f) = \int_{-\infty}^{\infty} c_1(f)c_2(f - f_1)df_1 \tag{1.4}$$

then

$$y_1(t)y_2(t) = \int_{\infty}^{\infty} c_{12}(f)\varepsilon^{j2\pi ft}df \tag{1.5}$$

The integral in (1.4) is by definition the convolution of the functions c_1 and c_2 and is designated $c_1 * c_2$.

Symbolically

$$c_{12}(f) \equiv c_1(f) * c_2(f_1) \tag{1.6}$$

or in words, the Fourier transform of two functions of time is the convolution of their individual Fourier transforms.

By inversion of (1.5)

$$c_{12}(f) = \int_{-\infty}^{\infty} y_1(t)y_2(t)\varepsilon^{-j2\pi ft}dt \tag{1.7}$$

Combining the two equations involving $c_{12}(f)$, (1.7) and (1.4) gives

$$\int_{-\infty}^{\infty} y_1(t)y_2(t)\varepsilon^{-j2\pi ft}dt = \int_{-\infty}^{\infty} c_1(f_1)c_2(f - f_1)df_1 \tag{1.8}$$

If in this equation $f = 0$ and $y_1(t) = y_2(t)$, then

$$\int_{-\infty}^{\infty} y^2(t)dt = \int_{-\infty}^{\infty} |c(f)|^2 df \tag{1.9}$$

The following paragraph is quoted directly from Bennett (op. cit.). "If in (1.8) we set $y_1(t)$ as a voltage $E(t)$ and $y_2(t)$ as a current, then the integral on the left represents the total energy over all time represented by this voltage and current pair. The formula says that this energy can be computed by integrating the product of the Fourier transform of one and the conjugate of the Fourier transform of the other throughout all frequencies. Likewise

if y(t) in (1.9) represents a voltage or current, the integral on the left is the total energy dissipated per mho or ohm, respectively, in the circuit. The formula says that this energy can be calculated by integrating the squared magnitude of the Fourier transform over all frequencies. In this sense the function $|c(f)|^2$ thus represents an energy density on the frequency scale.

5.2. <u>Power Spectral Density</u>.

If a finite segment of y(t) is considered, say from -T to T, then if

$$c_T(f) = \int_{-T}^{T} y(t)\varepsilon^{-j2\pi ft}dt = \int_{-\infty}^{\infty} y_T(t)\varepsilon^{-j2\pi ft}dt \tag{2.1}$$

where

$$y_T(t) = y(t) \quad -T \le t \le T$$

and

$$y_T(t) = 0 \qquad t < -T \quad \text{and } t > T$$

This limitation of consideration of the function y(t) to a limited time corresponds to practical considerations such as that portion which can be put on a loop of magnetic tape. It also avoids questions concerning infinite power which would result from integration over all time.

The average power S_T into a 1 ohm load, providing y(t) is a voltage, becomes

$$S_T = \frac{1}{2T}\int_{-T}^{T} y^2(t)dt = \frac{1}{2T}\int_{-\infty}^{\infty} y_T^2(t)dt$$

$$S_T = \frac{1}{2T}\int_{-\infty}^{\infty} |c_T(f)|^2 dt \tag{2.2}$$

from Parseval's Formula (1.9).

The average power in a frequency interval Δf at f, involves the assumption of an ideal band pass transmittance function, i.e.

a constant non-zero value in the band-pass and zero elsewhere (see Bennett op. cit. Paragraph 2.2). Let $W_y(f,T,\Delta f)$ be the average power in the frequency interval Δf, then

$$\int_{f-\frac{\Delta f}{2}}^{f+\frac{\Delta f}{2}} \frac{|c_T(\lambda)|}{2T\Delta f}\, d\lambda = W_y(f,T,\Delta f) \tag{2.3}$$

As T approaches infinity

$$W_y(f,\Delta f) = \lim_{T\to\infty} \int_{f-\frac{\Delta f}{2}}^{f+\frac{\Delta f}{2}} \frac{|c_T(\lambda)|^2}{2T\Delta f}\, d\lambda \tag{2.4}$$

The power spectral density is defined as the limit $\Delta f \to 0$, thus

$$\text{Power Spectral Density} \equiv W_y(f) = \lim_{\Delta f\to 0} \left[\lim_{T\to\infty} \int_{f+\frac{\Delta f}{2}}^{f+\frac{\Delta f}{2}} \frac{|c_T(\lambda)|^2}{2T\Delta f}\, d\lambda \right] \tag{2.5}$$

This definition is equivalent to definitions in terms of the cross correlation function. (See for example, Lee p. 58.)[2] It is left in this form since it is more readily used in terms of the analyzer system.

5.3. <u>Practical Limitations</u>.

It is necessary and practical when working with an electronic wave analyzer to avoid such things as allowing the filter band-width to approach zero. The power spectral density determinations in actuality become

$$W_y(f,T,\Delta f) = \int_{f-\frac{\Delta f}{2}}^{f+\frac{\Delta f}{2}} \frac{|c_T(\lambda)|^2}{2T\Delta f}\, d\lambda \tag{3.1}$$

[2] Y. W. Lee, <u>Statistical Theory of Communication</u>, Wiley, 1960.

It thus becomes necessary to determine the adequacy of this approximation which is a sample taken from the entire time series. This involves sampling theory and will be discussed in a later section.

It is also easier to work with the squared value of the time series than its Fourier transform, therefore the form

$$W_y(f,T,\Delta f) = \int_{-T}^{T} \frac{y^2(t)dt}{2T\Delta f}$$

is used.

5.4. Filtering.

The first step is to limit the power to a finite band width Δf. In the Technical Products Wave Analyzer in use on Project VT/078 this is accomplished by multiplying the audio signal by a high frequency sinusoid generated by an oscillator. This oscillator has a frequency range centered at 97kc and is calibrated in terms of the audio range 0 to 250 cps, 0 to 2500 cps, or 0 to 25.kc depending on the range selected.

The system is shown in block diagram form in Figure 1.

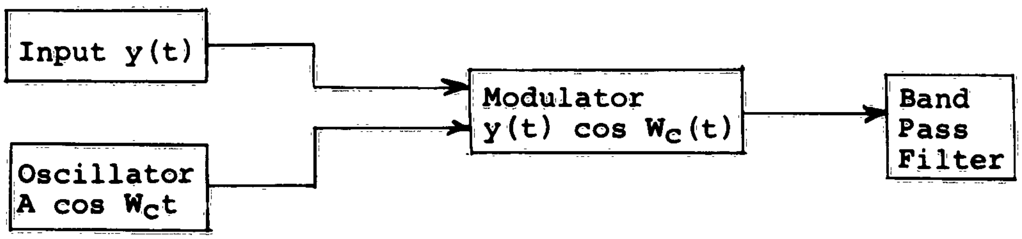

If y(t) is the input function, then its Fourier transform is

$$\Phi(w) = \int_{-\infty}^{\infty} y(t)e^{-jwt}dt \qquad (4.1)$$

and the Fourier transform of y(t) multiplied by the carrier A cos $W_c t$

$$\Phi_1(w) = \int_{-\infty}^{\infty} y(t)Ae^{-jwt} \cos W_c t dt \qquad (4.2)$$

which becomes, when the cosine is written in terms of the exponential

$$\Phi_1(w) = \frac{A}{2}\left\{\int_{-\infty}^{\infty} e^{-j(W_c - w)t} y(t)dt + \int_{-\infty}^{\infty} e^{-j(W_c + w)t} y(t)dt\right\}$$

$$= \frac{A}{2}\left\{\Phi(W_c - w) + \Phi(W_c + w)\right\} \tag{4.3}$$

This means that the original input audio frequency distribution has been converted to a frequency distribution of the upper and lower side-band of the oscillator frequency.

The output of the modulator is then passed through a filter of band width Δw which is displaced from the carrier frequency W_c by a frequency w. This acts to select from the modulator output those frequencies between

$$(W_c - w - \frac{\Delta w}{2}) \quad \text{and} \quad (W_c - w + \frac{\Delta w}{2}) \tag{4.4}$$

By equation (4.3) this amounts to selecting the lower side band from the modulated audio input. Since the oscillator is calibrated in terms of w the output has the same frequency distribution as the audio input.

The output of the filter at any given moment (fixed carrier) is thus a sinusoid of frequency w and amplitude proportional to the amplitude of the component of the original input frequency w. This proportionality is constant if the system is flat in the radio frequency range about the modulated carrier. It is strictly true only for $\Delta f \to 0$, however, it is an adequate description if Δf is small relative to the band of frequencies occurring in y(t).

5.5. Squaring.

The next step in determining the power spectral density of the system is to square the filter output.

Let $R(t) \cos W_\alpha t$ be the input to the squaring device, where W_α is the center frequency of the filter. The initial stage of the squaring device is a paraphase amplifier[3] which provides two

[3] Samuel Seely, Electron-Tube Circuits, McGraw-Hill, 1950, p. 187.

equal output channels which are 180° out of phase. These outputs are then applied through a transformer to the grids of a twin triode, which are then combined to form the output. Seely (op. cit., p. 151) illustrates one way of accomplishing this. In the Technical Products Analyzer this is accomplished by using a 12Au7 twin triode.

If the plate current in ½ the twin triode can be represented by

$$i_{p1} = a_1 e_{g1} + a_2 e_{g1}^2 + a_3 e_{g1}^3 + \ldots \tag{5.1}$$

then for the other half

$$i_{p2} = a_1(-e_{g1}) + a_2(-e_{g1})^2 + a_3(-e_{g1})^3 \tag{5.2}$$

Then

$$i_p = i_{p1} + i_{p2} = 2a_2 e_{g1}^2 + 2a_4 e_{g1}^4 + \ldots \tag{5.3}$$

which, if terms fourth order and greater can be neglected, becomes

$$i_p \sim 2a_2 e_{g1}^2 \ .$$

If R_k is the resistance into which i_p is connected,

$$e_o \sim R_k 2a_2 e_{g1}^2 \ .$$

In words, this states that in the circuit output, voltage is proportional to square of the inputs.

5.6. Averaging.

The next step in the determination of the power spectral density is to determine the average of the output. This is essentially a smoothing amplifier as shown in the following simplified diagram:

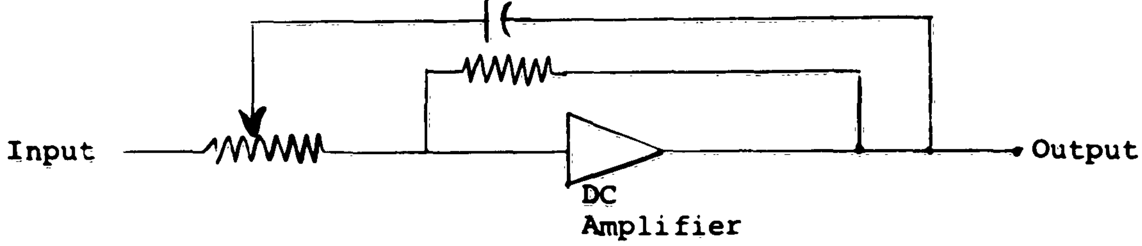

The capacitor in the feedback loop has three values controllable by a switch. The result is continuous averaging time from 0.1 to 100 seconds. An averaging time of 2.0 seconds (equivalent to one revolution of the 200 second real time sample) is commonly used. This averaging time was established experimentally.

5.7. Band-Width Divisor Circuitry.

In the integrator portion of the analyzer there is a series of attenuators corresponding to the filters with which the analyzers are equipped. In the case of the analyzer in use on Project VT/078, the filters are 2, 10, 50 and 200 cps wide. The attenuators are calibrated to compensate for the larger amount of energy which the broader filter "lets through" the system, reducing the amplitude for random inputs to that of the narrowest filter.

The next logical question concerning the operation of the analyzer has to do with sampling theory. Most of the available literature approaches the problem from a negative aspect (see for example, Davenport and Root, p. 107).[4] However, from a practical aspect, consistent results have been obtained using a 200 second sample. Work is continuing in an attempt to clarify the rather involved mathematics.

[4] Davenport and Root, An Introduction to the Theory of Random Signals and Noise, McGraw Hill, 1958.

6. Station Factor and Signal Levels in California

The purpose of this section is to discuss the results obtained concerning a measure of the relative signal to noise ratio of various sites in California. It also includes a more detailed discussion of signal ratio and how the data concerning signals was obtained.

In brief, the results are that the Station Factor is 1.0 or greater from the Sierra Nevada east and deteriorates to 0.3 at the two sites less than 50 kms from the coast. The station at Darwin had the highest factor 1.4. Data is normalized to a value 1.0 at the Master Station at Round Mountain.

6.1 Relative Signal-Noise Level of California Sites

In order to present the data in summary form concerning the relative signal to noise ratio for the various sites in California, it is necessary to make certain simplifying assumptions. These assumptions are that the noise is limited to that between 0.8 to 1.0 seconds period and the signal to that with a measured period of 1.0 seconds in the first or second phase. The effect is to limit the spectrum much as if the noise and signal were recorded through a sharply tuned filter. The consideration of noise or signals in other frequencies is thus eliminated. These assumptions, for reasons that will be discussed in detail in a later section, have a marked effect on the signal portion of the factor. For example at Panamint, if instead of a 1.0 second signal, that at 0.8 is chosen, the signal ratio has an average value of 2.3 compared to 1.4 at 1.0 seconds.

Figure 6.1 is a plot of the Station Factor which in approximate terms is a measure of the average signal to noise improvement that can be expected between one site and another. The data is normalized to the Master Station at Round Mountain which has been given unit value. This results from the signal data amplitudes as recorded at each site to that at the Master Station at Round Mountain. Figure 1.3 is a map of station locations. The data on which Figure 6.1 is based is listed in Table 6.1.

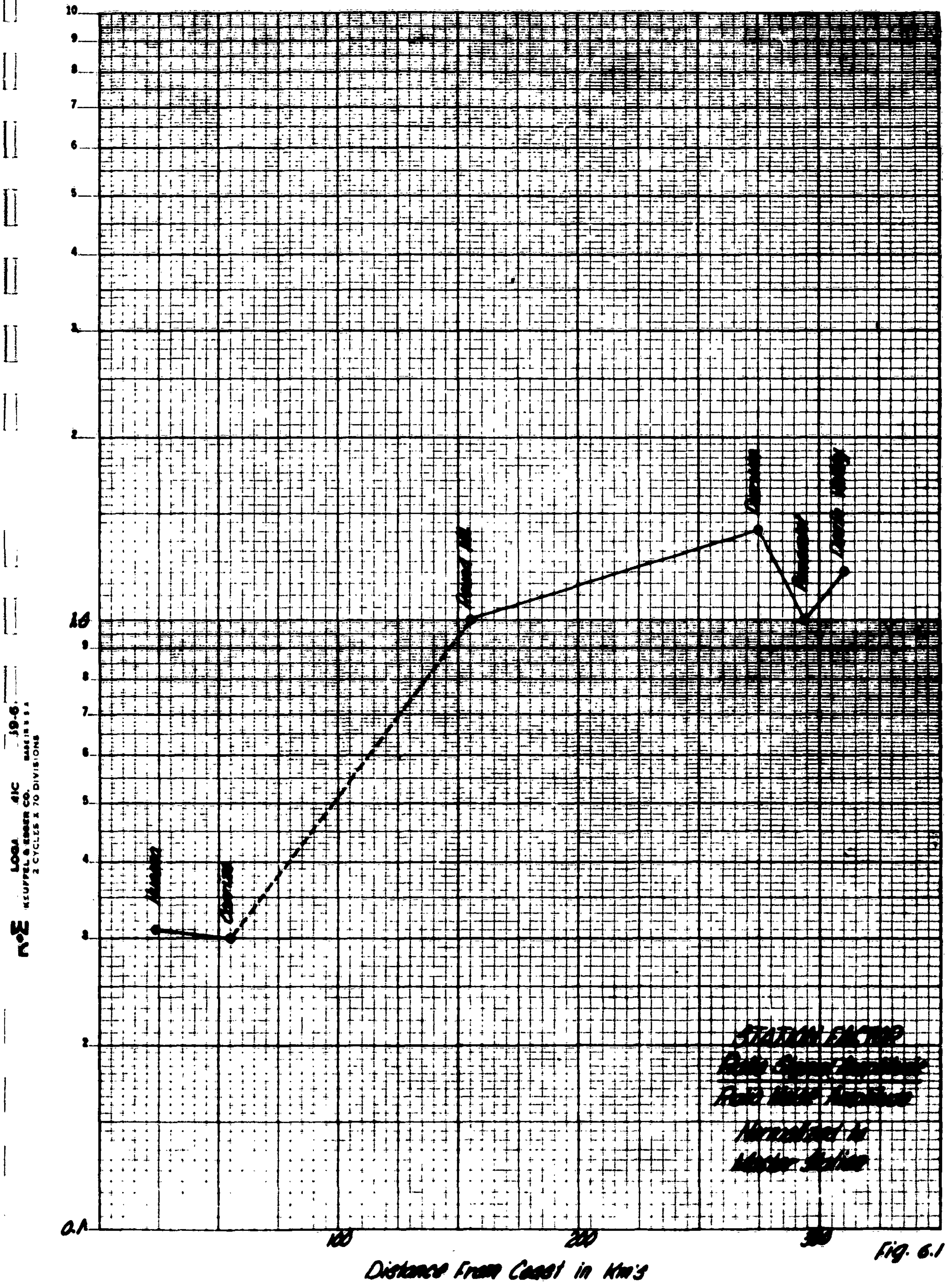

10
9
8
7
6
5
4
3
2
1.0
9
8
7
6
5
4
3
2
0.1
100
200
300
Distance From Coast in Km's
STATION FACTOR
LOG4 41C 19-6
KEUFFEL & ESSER CO.
2 CYCLES X 70 DIVISIONS

Fig. 6.1

TABLE 6.1

STATION	AVG. SIGNAL AMPL. RATIO SS/MS AT 1.0 SEC.	AUG.NOISE AMPL. 0.8 - 1.0 SEC.	SIGNAL SS/MS / NOISE SS/MS
Round Mt.	1.0	0.098	1.0
Huasna R.	2.7	0.862	0.31
Carrizo	1.6	0.525	0.3
Darwin	0.9	0.063	1.4
Panamint	1.7	0.165	1.0
Death Valley	2.8	0.225	1.2

Of particular interest in Table 6.1 is the Death Valley station which has both a high signal level and noise level, resulting in a higher Station Factor than the Master Station. Geologically, the contrast is a deep alluvial fill to a massive granitic intrusive. In contrast, although Huasna River has a high signal ratio, the noise level is enough higher to cause an overall degradation in the Station Factor.

Three of the stations occupied are not included in this study. Elk Hills had a high level of apparent man-made noise and has not been analyzed in detail. Mannot Creek will be analyzed. The High Sierra Station was occupied for a relatively short time before its abqndonment because of hazard to personnel and equipment from lightning.

6.2 Signal Level Comparison Slave to Master Station

A visual analysis method was used to obtain amplitude ratios of signals between the Slave and Master Station. Earthquakes are selected that have reasonably well-defined first motion at both stations. The amplitudes ratios of the first two cycles of first motion are compared and plotted as function of period. Since both stations are located in the circum-Pacific belt, about 50% of earthquakes recorded arrive at both stations at nearly the same time. The sample does not have random directionality.

Figure 6.2 is a plot of the signal data obtained at the Huasna River site. These curves illustrate the marked differences which occur as a function of period. Figures 6.3 to 6.6 are the signal amplitude ratio plots for other sites. A comparison of these curves illustrates the marked differences both in amplitude ratio and frequency which occur from one site to another. More work is scheduled in the study of signals and their relation to the parameters. In general, the data concerning noise is better controlled than the signal data.

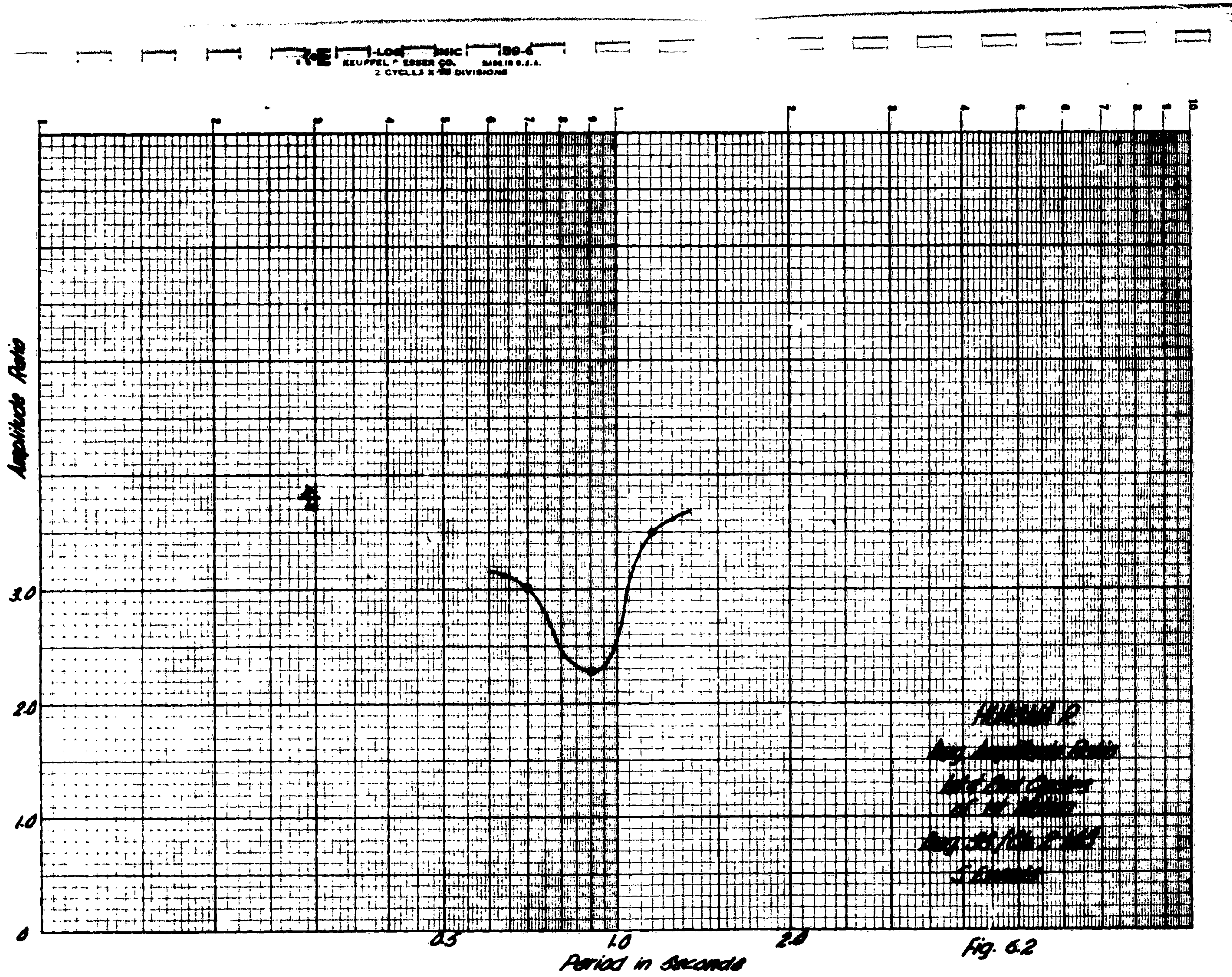

K+E 1-LOG MIC 359-6
KEUFFEL & ESSER CO. MADE IN U.S.A.
2 CYCLES X 10 DIVISIONS
Amplitude Ratio
3.0
2.0
1.0
0
0.5
1.0
2.0
Period in Seconds

Fig. 6.2

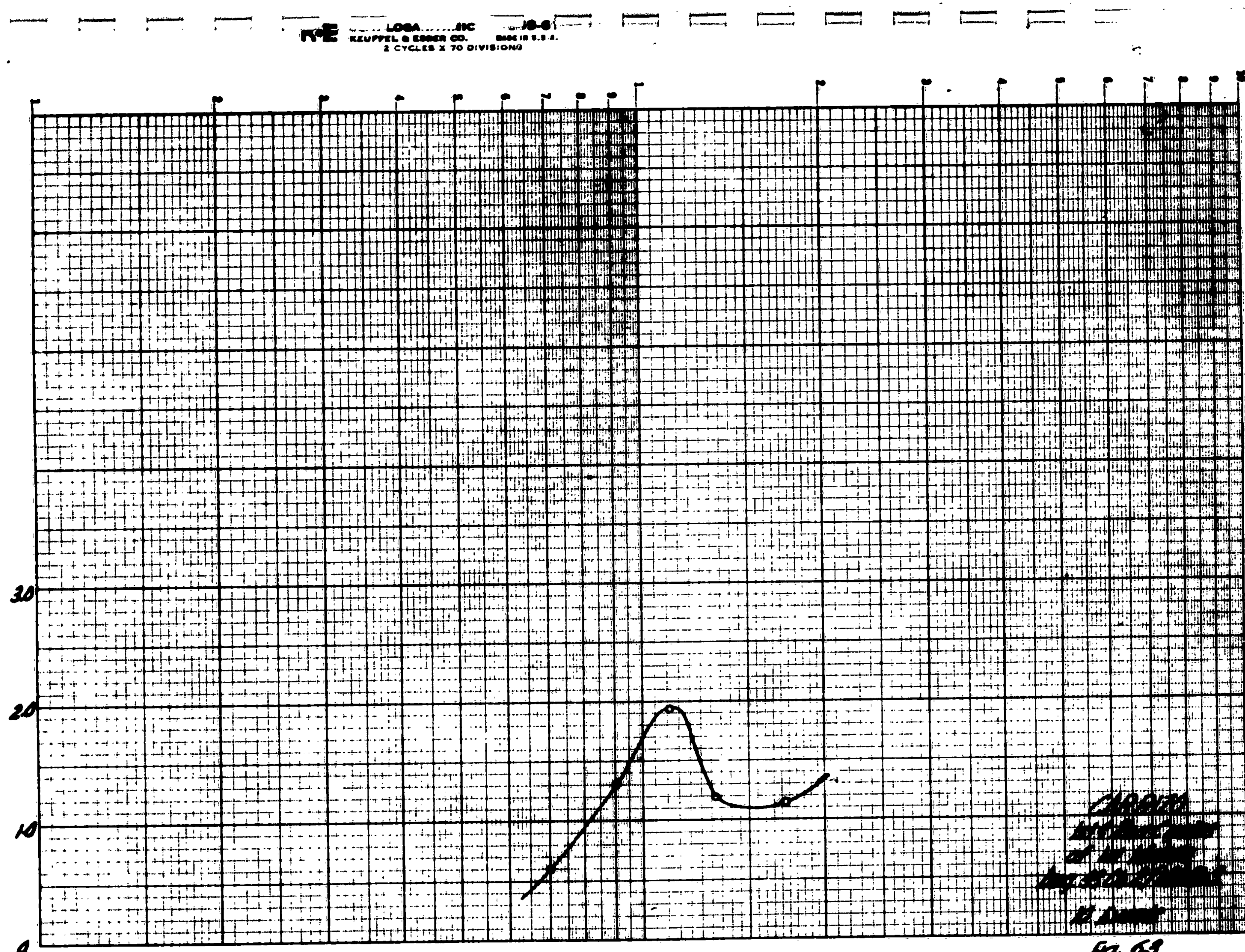

K&E LOGARITHMIC
KEUFFEL & ESSER CO. MADE IN U.S.A.
2 CYCLES X 70 DIVISIONS
30
20
10
0

Fig. 63

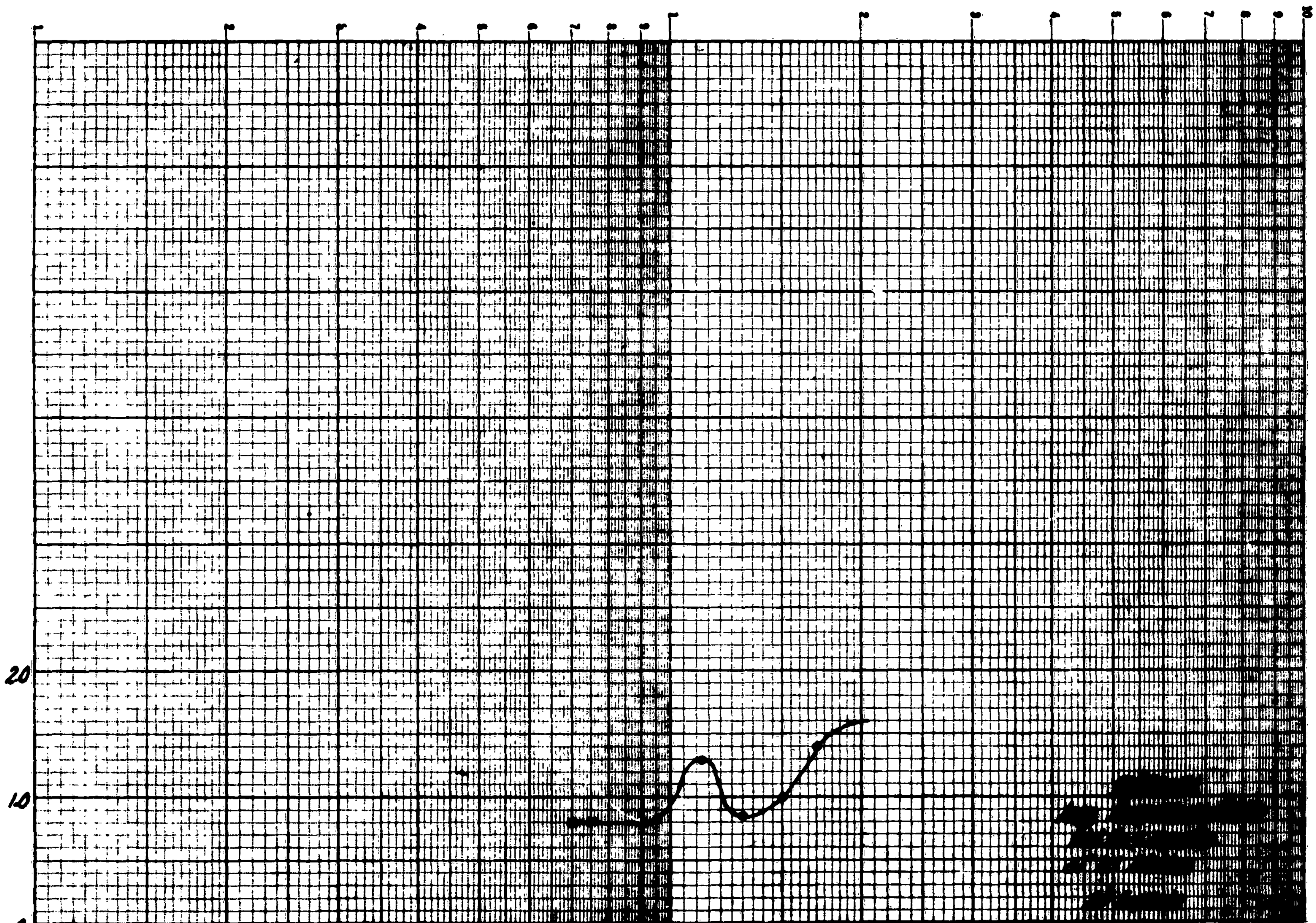

Fig. 6.1

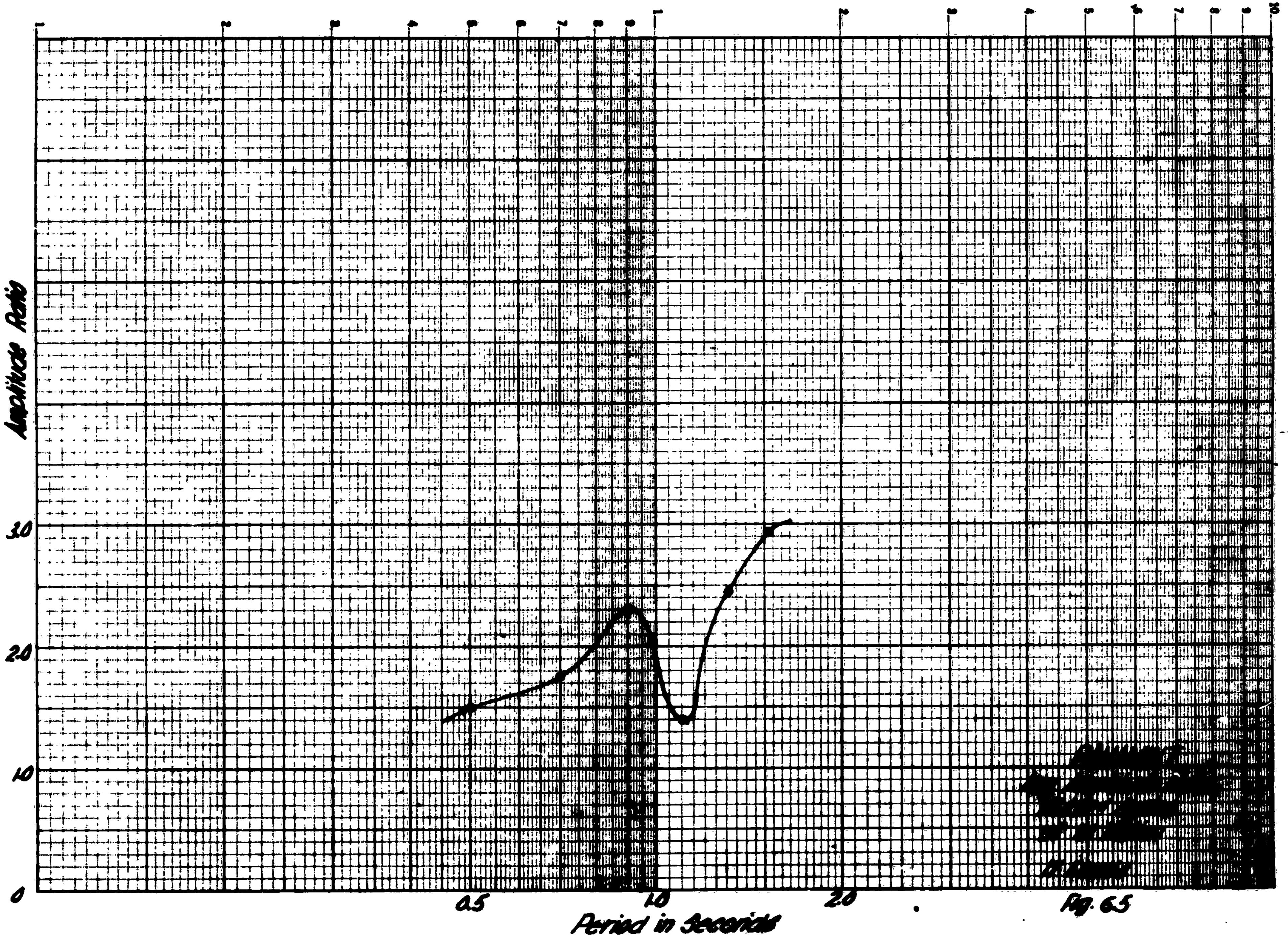

Fig. 6.5

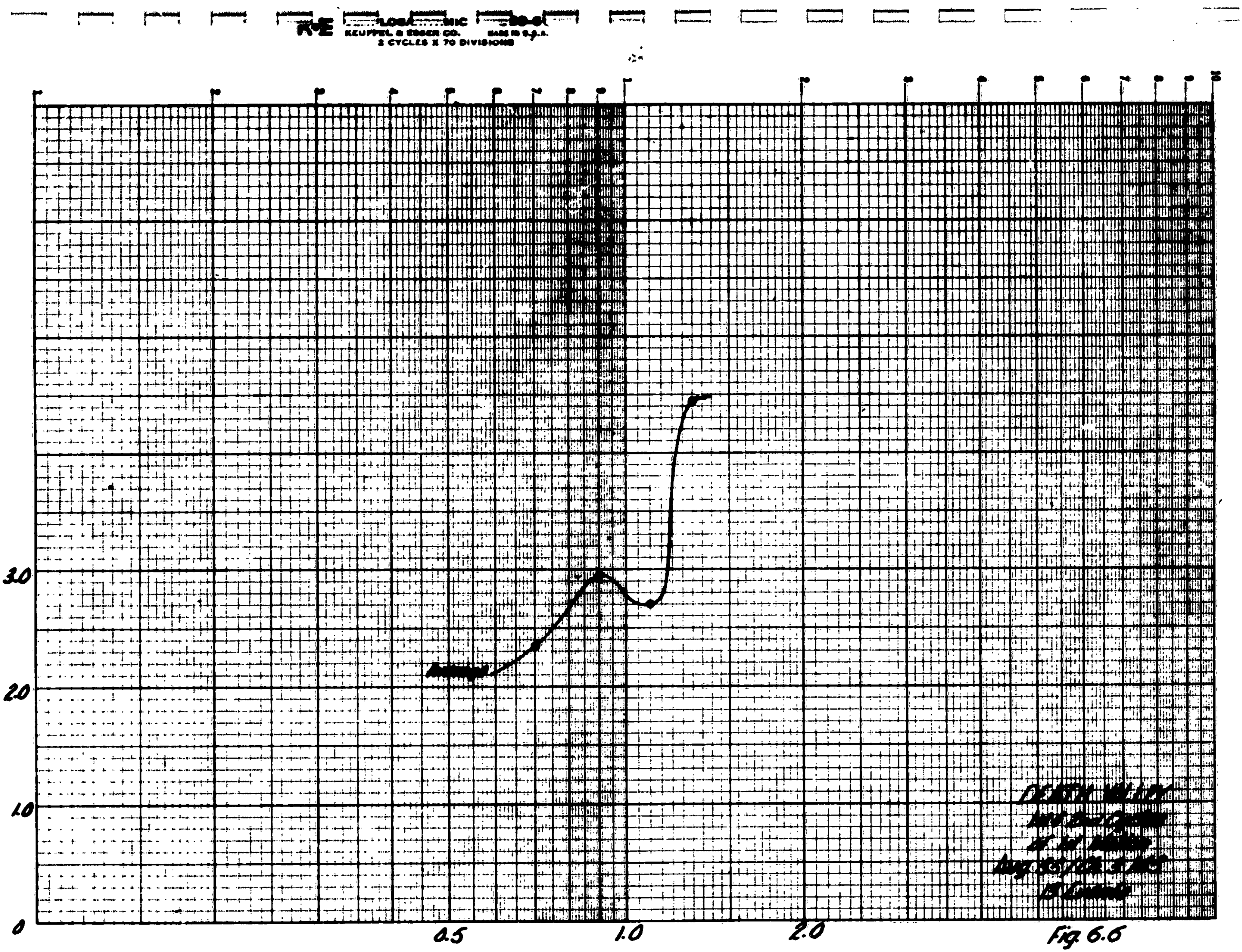
K+E LOGARITHMIC
KEUFFEL & ESSER CO. MADE IN U.S.A.
2 CYCLES X 70 DIVISIONS
3.0
2.0
1.0
0
0.5
1.0
2.0
DEATH VALLEY

Fig. 6.6

7. Seismic Noise Along California Profile

The purpose of this section is to show the relations between seismic noise and geology, topography, wind speed and weather fronts as established along the California Profile from San Luis Obispo Bay to Death Valley.

In general there is a well-defined change in noise at the Sierra Nevada. Sites in and east of the Sierra Nevada had a lower noise level and less variation than those in the San Joaquin Valley and the Coast Range.

Various aspects of noise as studied will be discussed in the following subsections of this section.

7.1 Twenty Four Hour Noise Averages

Figure 7.1 is a plot of the average peak to-peak amplitude of noise by bands of period between 0.2 and 5.0 seconds (0.2 to 5.0 cycles). The horizontal scale is in days of the year and thus represents the order in which various sites were occupied. Also plotted against the day axis is distance to weather front as it appears on the daily weather map published by the Department of Commerce. Distance from Bakersfield was chosen as a parameter. Within the accuracy of the weather maps this represents a workable average distance from the California profile to the usual weather front which is northwest of the profile line and generally parallel to it. Since the California profile was occupied from March to November, only rarely did a front pass through Bakersfield. On the plots the solid is the particular Slave Station being occupied; the dashed line is the Master Station.

7.1.1 Cedar Creek Slave Station

Noise levels at the Cedar Creek Slave Station are nearly identical for periods between 0.3 and 5.0 seconds. This is as expected since the stations are 5 kms. apart. There is some difference in the 0.2 to 0.3 second noise which has no direct correlation with wind speed. Topographically the Cedar Creek Station is in a valley east of and 160 meters lower in elevation than the Master Station at Round Mountain. An interpretation of the higher noise level in the 0.2 to 0.3 second band is that the valley shelters the site from the prevailing wind action against the mountains, even though the recorded wind speeds are comparable. The general trend of the valley is perpendicular to the prevailing wind direction. Geologically both sites are on granite of the Sierra Nevada.

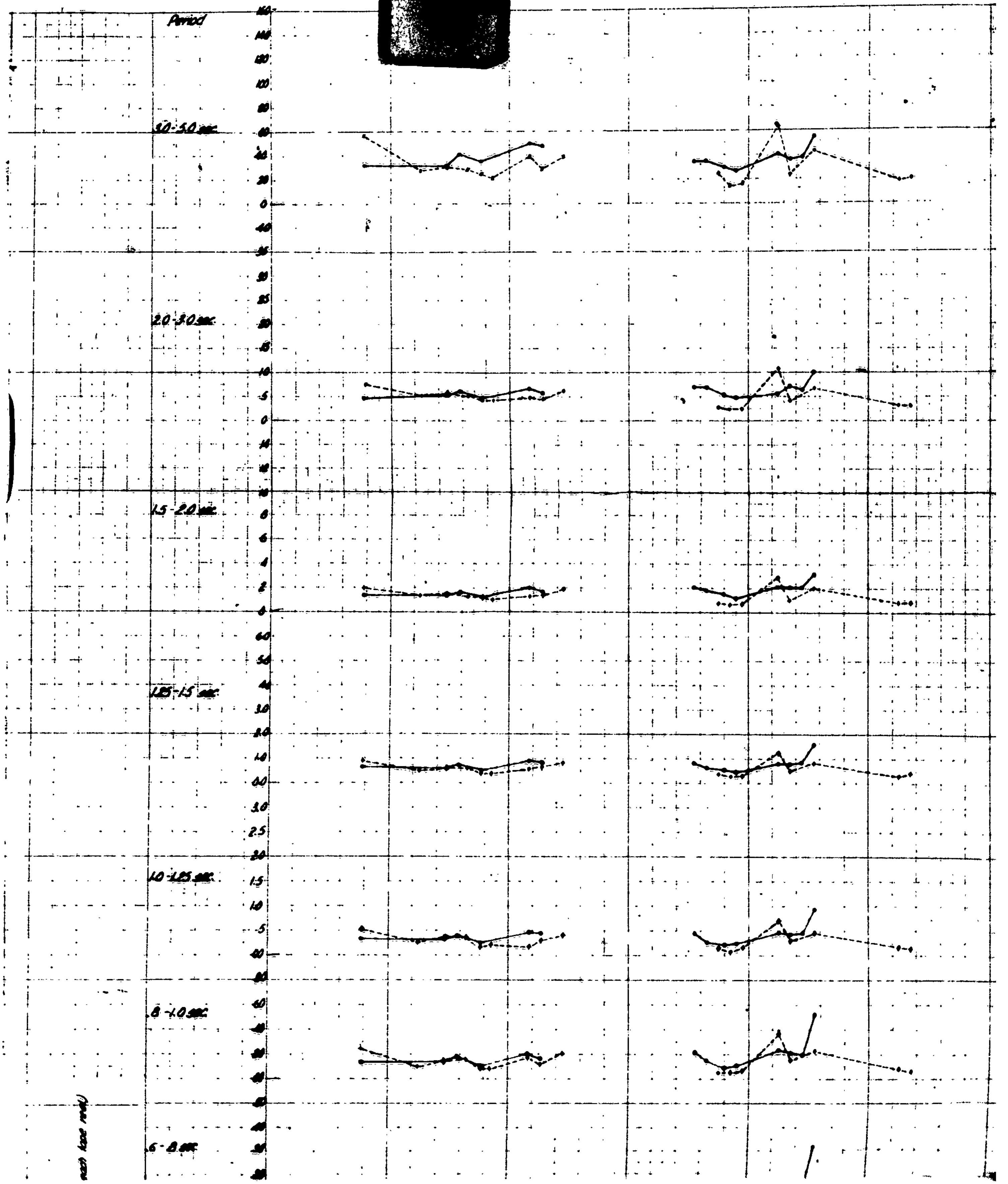

Period
3.0-5.0 sec
2.0-3.0 sec
1.5-2.0 sec
1.25-1.5 sec
1.0-1.25 sec
.8-1.0 sec
.6-.8 sec

2

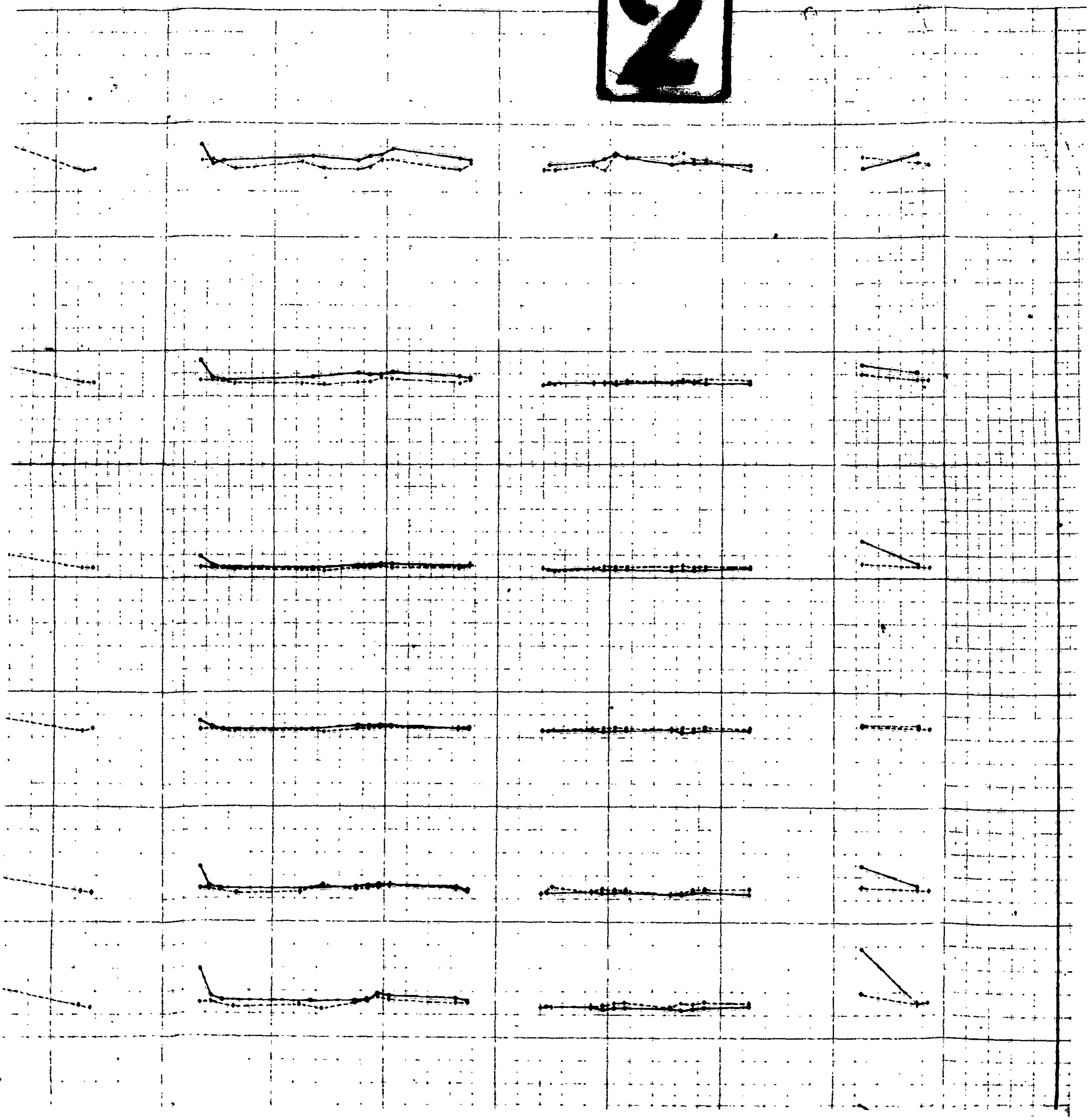

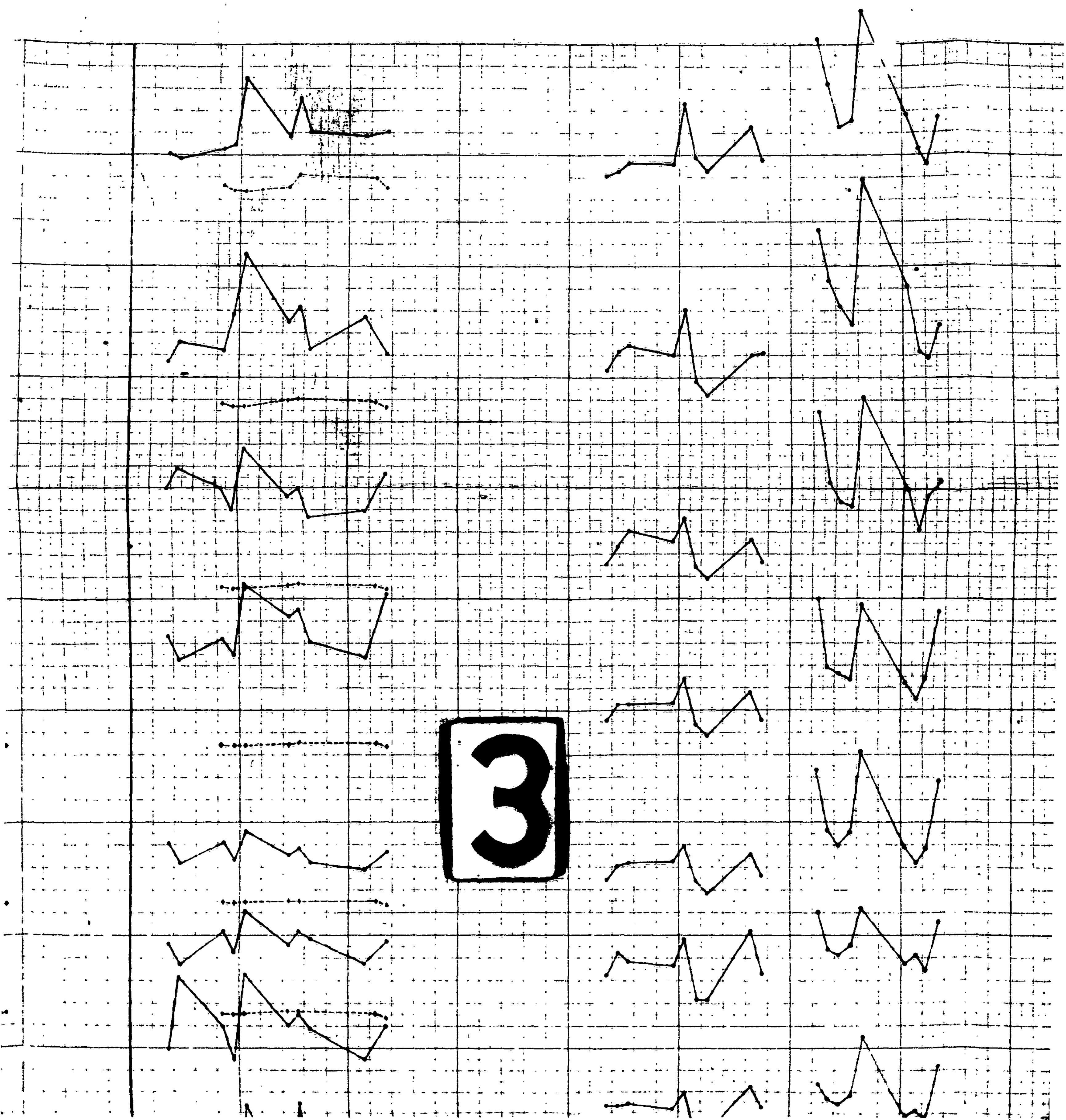
3

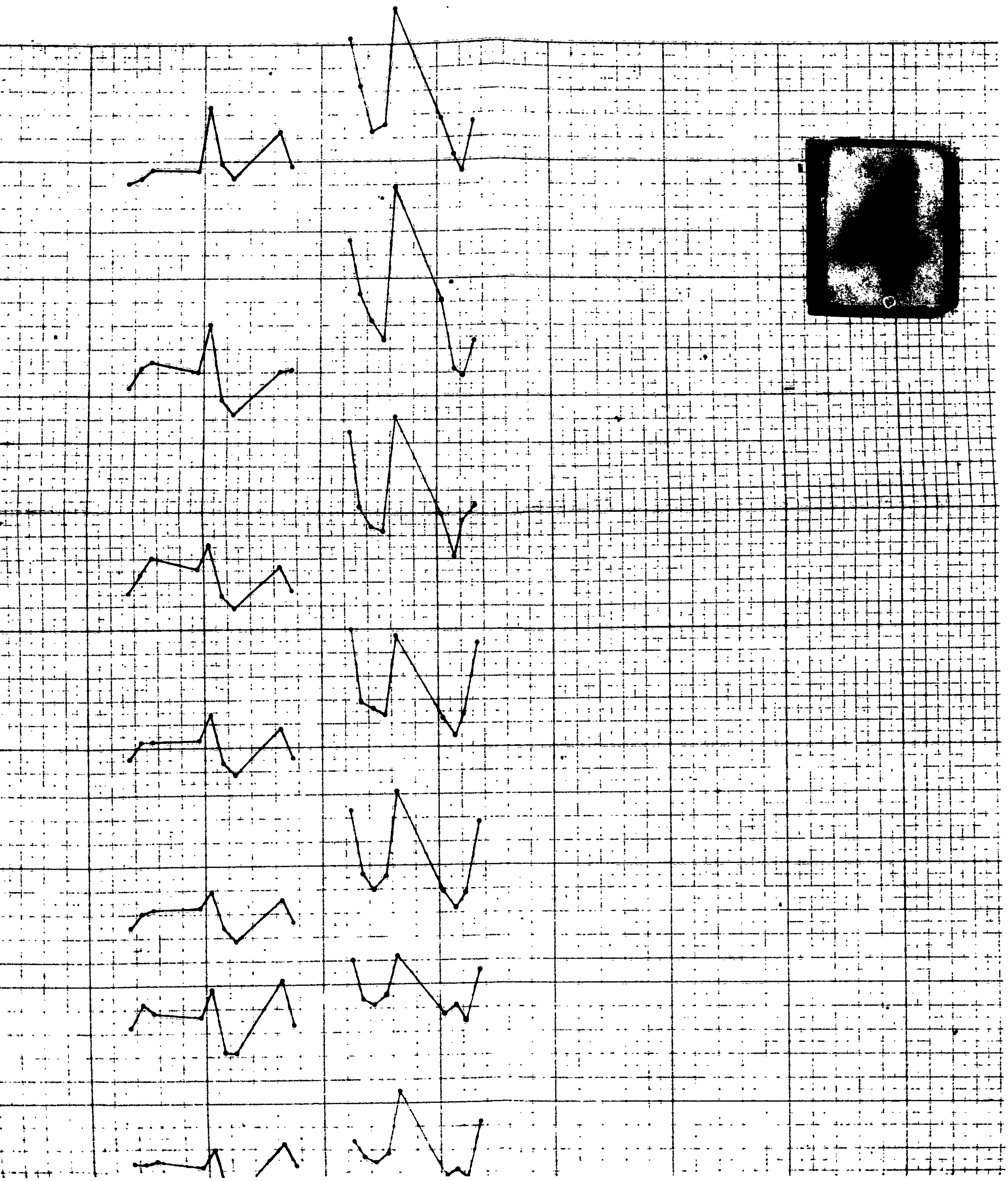

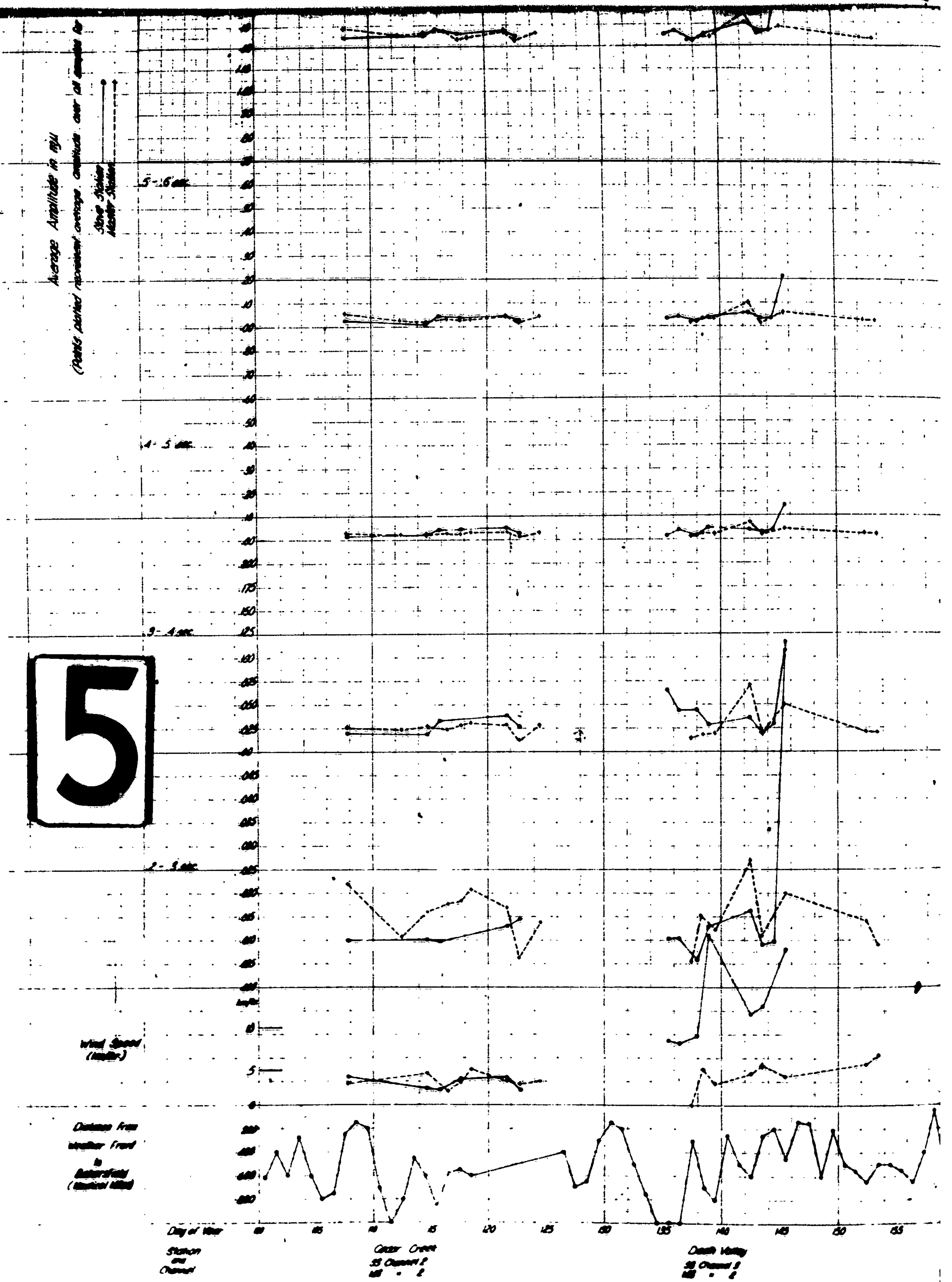

Average Amplitude in mμ
Slave Station
Master Station
5 - 6 sec
4 - 5 sec
3 - 4 sec
2 - 3 sec
Wind Speed (knots)
Distance from Weather Front to Bakersfield (Nautical Miles)
Day of Year
Station and Channel
Cedar Creek
Death Valley

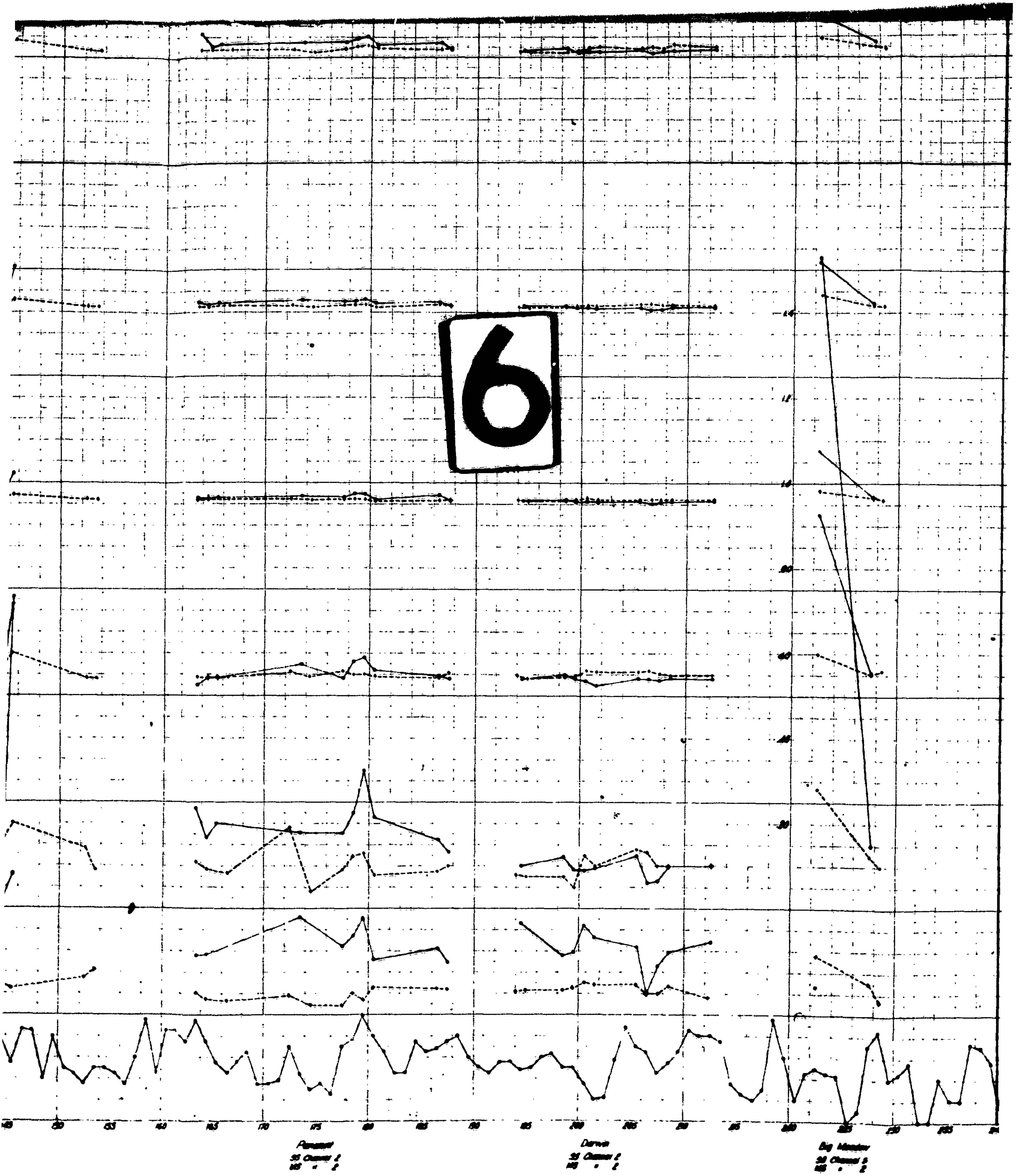
6
Darwin
Big Meadow

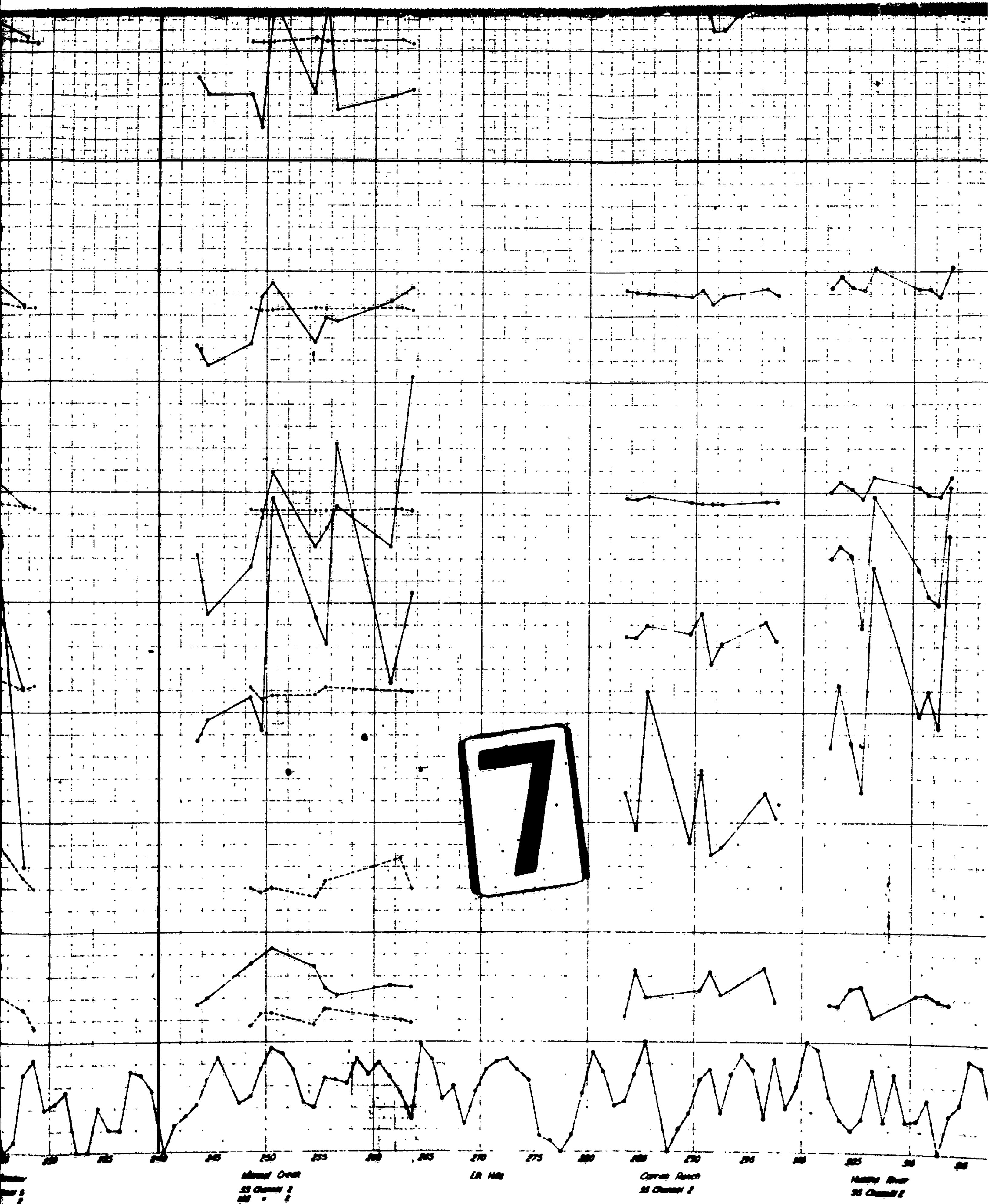

250
270
275
Elk Hills
Carrizo Ranch
SS Channel 2
SS Channel 2

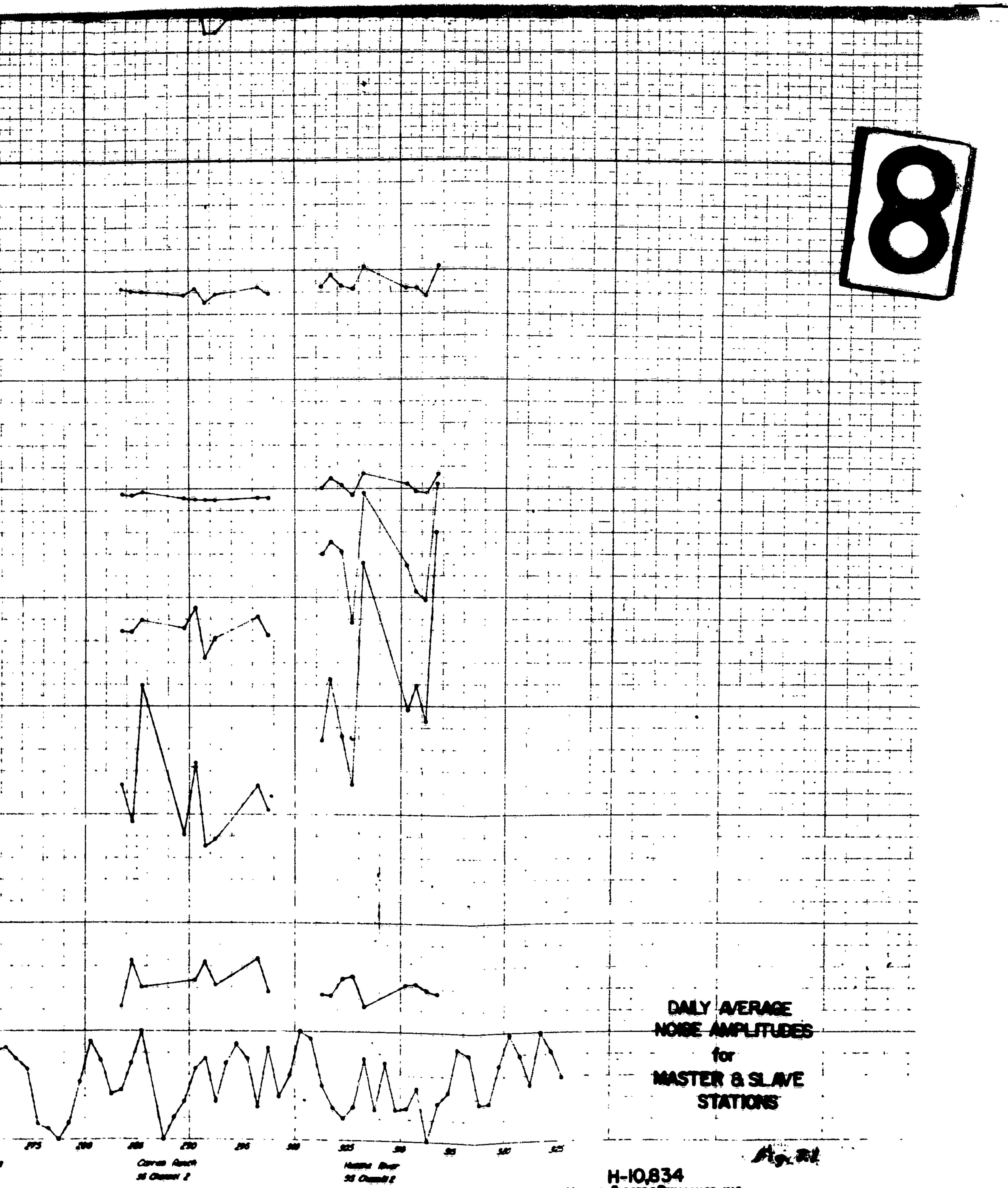

DAILY AVERAGE NOISE AMPLITUDES for MASTER & SLAVE STATIONS

H-10,834
UNITED ELECTRODYNAMICS, INC.
PASADENA, CALIFORNIA

7.1.2 Death Valley Slave Station

The Death Valley Station is located on the floor of Death Valley, at an elevation of minus 73 meters. At this point the valley is an alluvial fill about 2000 meters thick. Of interest is the greater variation of noise level at the Master Station than at Death Valley for the longer periods (1.0 to 3.0). The wind speed level at Death Valley was high during the time the station was there, averaging about 15 km/hr. There is no well-defined correlation between wind speed and noise level in the higher frequencies. The average noise at this site in the higher frequencies (above 5 cps) showed more correlation with wind speed.

7.1.3 Panamint Slave Station

The Panamint Station, except in the 0.2 to 0.3 second band, had noise level very similar to that at the Master Station. Geologically they are dissimilar (See Section 1.4 and 1.6). There is an indicated correlation between wind speed and the 0.2 to 0.3 second noise. Wind speed and this period of noise do not correlate at the Master Station. As noted earlier (Section 6), the signal/noise ratio of this station is greater than the Master Station.

7.1.4 Darwin Slave Station

From a geological and topographic aspect, the Darwin and Panamint stations are similar. The Darwin station is located on hard metamorphosed Pennsylvanian limestone, with a thin cover of Quarternary alluvium. Volcanics occur west of the area. Darwin had the lowest noise level of all the stations occupied. Of interest is the relatively low level of noise in the 0.2 to 0.3 second band, even though the wind speed was higher than at the Master Station. This station also has a higher signal to noise ratio than the Master Station.

7.1.5 Big Meadow Slave Station

This station is variously referred to as Big Meadow or High Sierra. (See Section 1.4) The very high noise level in the 0.2 to 0.3 second period (1.5 m μ) on the 222nd day, about 5 times the corresponding Master Station amplitude, is interpreted as standing waves in the low velocity material of the recently filled lake. This gelatinous material is similar to the low velocity material found in the filled channels of the Mississippi where P-wave velocities of about 1.0 km/sec occur. It is believed that this low velocity is a result of aeration. The mechanism of these waves is interpreted as similar to that of seiches.

On the 227th day the seismometers were moved to the edge of the meadow on hard granite. Plans to continue recording at this site were abandoned because of severe lightning.

7.1.6 Mannot Creek Slave Station

The Mannot Creek site is located on the west side of the San Joaquin Valley on Tertiary fill about 800 meters thick (see Section 1.3). The noise level was higher than the Master Station 22 kms northeast. The principal source of man-made noise in the area appeared to be pumping oil wells with a period of about 3.0 seconds. The fact that a markedly higher level of noise did not occur at this period indicates that the noise is not man-made. The visual records were dominated by the 0.2 to 0.4 second noise.

7.1.7 Elk Hills Slave Station

This station was occupied in an attempt to determine noise levels on the east side of the valley. The difficulties locating a station in this area free of man-made noise are formidable. The site was selected as far as possible from sources of man-made noise. The effort was unsuccessful.

7.1.8 Carrizo Slave Station

This station is located in the Coast Range (see Section 1.2). Of interest both at this station and the Huasna River Station is the relatively low level between 0.4 and 0.6 seconds in contrast to higher and lower periods which are significantly greater than the Master Station level. During this period (October) noise levels at the Master showed more variation than they did through the spring and summer.

7.1.9 Huasna River Station

The Huasna River Station was located as close to the ocean as practical (16 kms.). There is a major highway, railroad and several towns which precluded a site closer to the beach. There appears to be a weak correlation between changes in level at this and that at the Master Station. Of interest in this regard is the 0.6 and longer period noise at Carrizo, where the correlation is better defined.

7.2 Mean Noise Amplitude vs Distance From the Coast

In order to emphasize the variation of noise of a particular period as a function of distance from the coast, Figures 7.2 to 7.10 are plots of the average peak to-peak noise plus and minus one standard deviation, at each site against distance from the coast. This is essentially the same data as presented in Section 7.1.

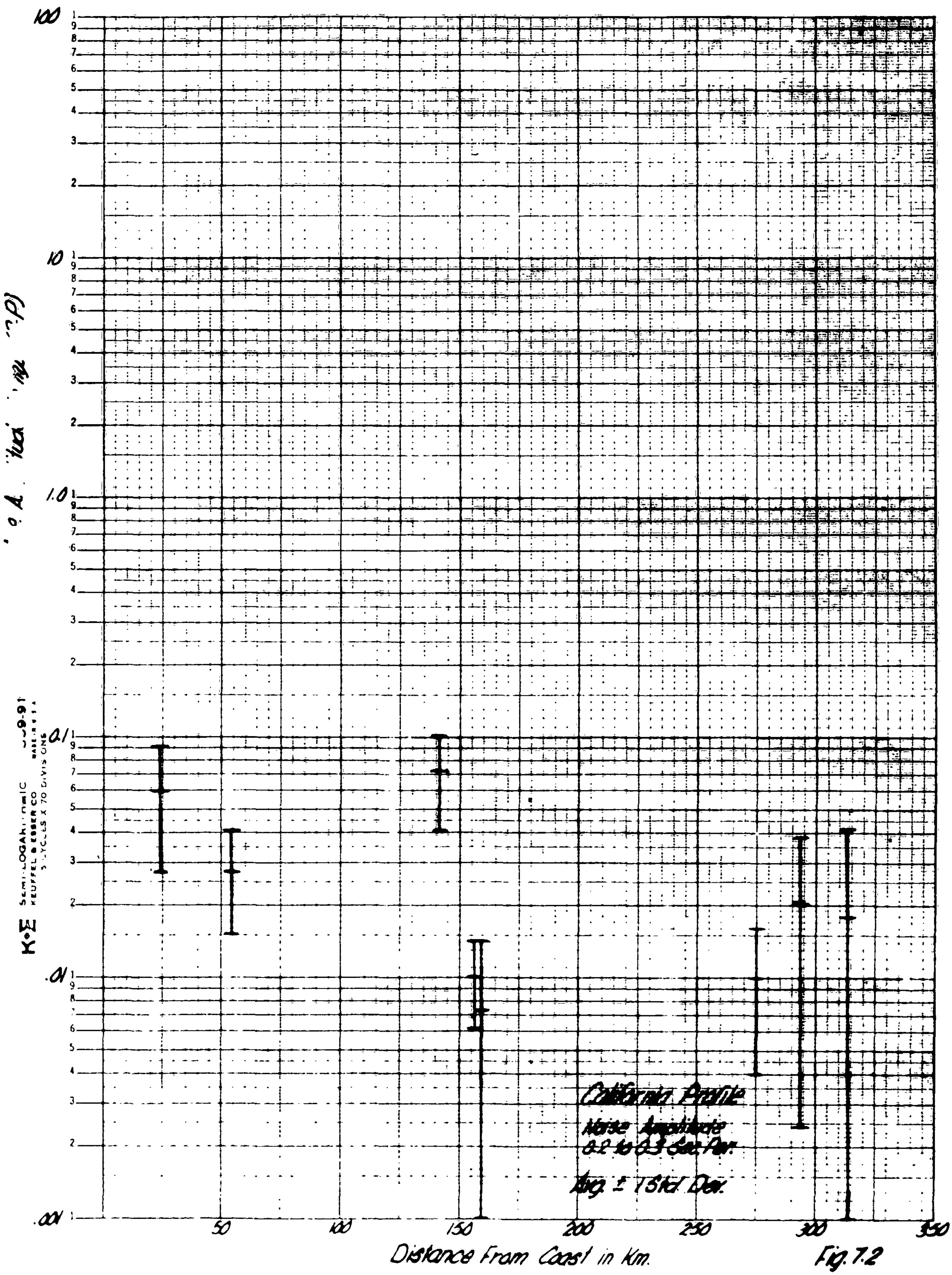

100
10
1.0
0.1
.01
.001
50
100
150
200
250
300
350
Distance From Coast in Km.
California Profile
Noise Amplitude
0.2 to 0.3 Sec Per.
Avg. ± 1 Std Dev.
K-E SEMI-LOGARITHMIC 359-91
KEUFFEL & ESSER CO.
5 CYCLES X 70 DIVISIONS

Fig. 7.2

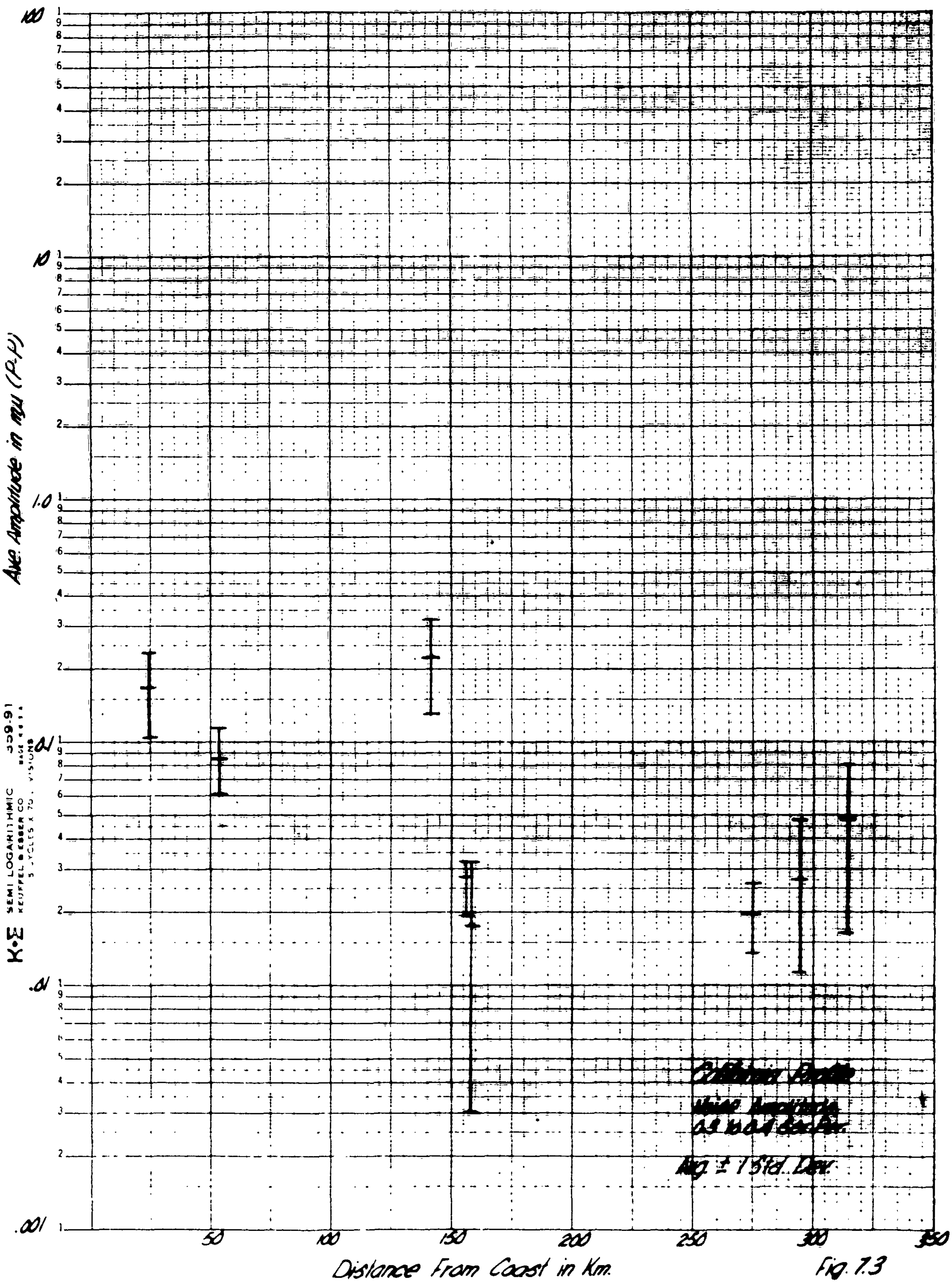

100
10
1.0
.01
.001
Ave. Amplitude in mμ (P-P)
K·E SEMI LOGARITHMIC 359-91
KEUFFEL & ESSER CO.
5 CYCLES X 70 DIVISIONS
50
100
150
200
250
300
350
Distance From Coast in Km.
Avg. ± 1 Std. Dev.

Fig. 7.3

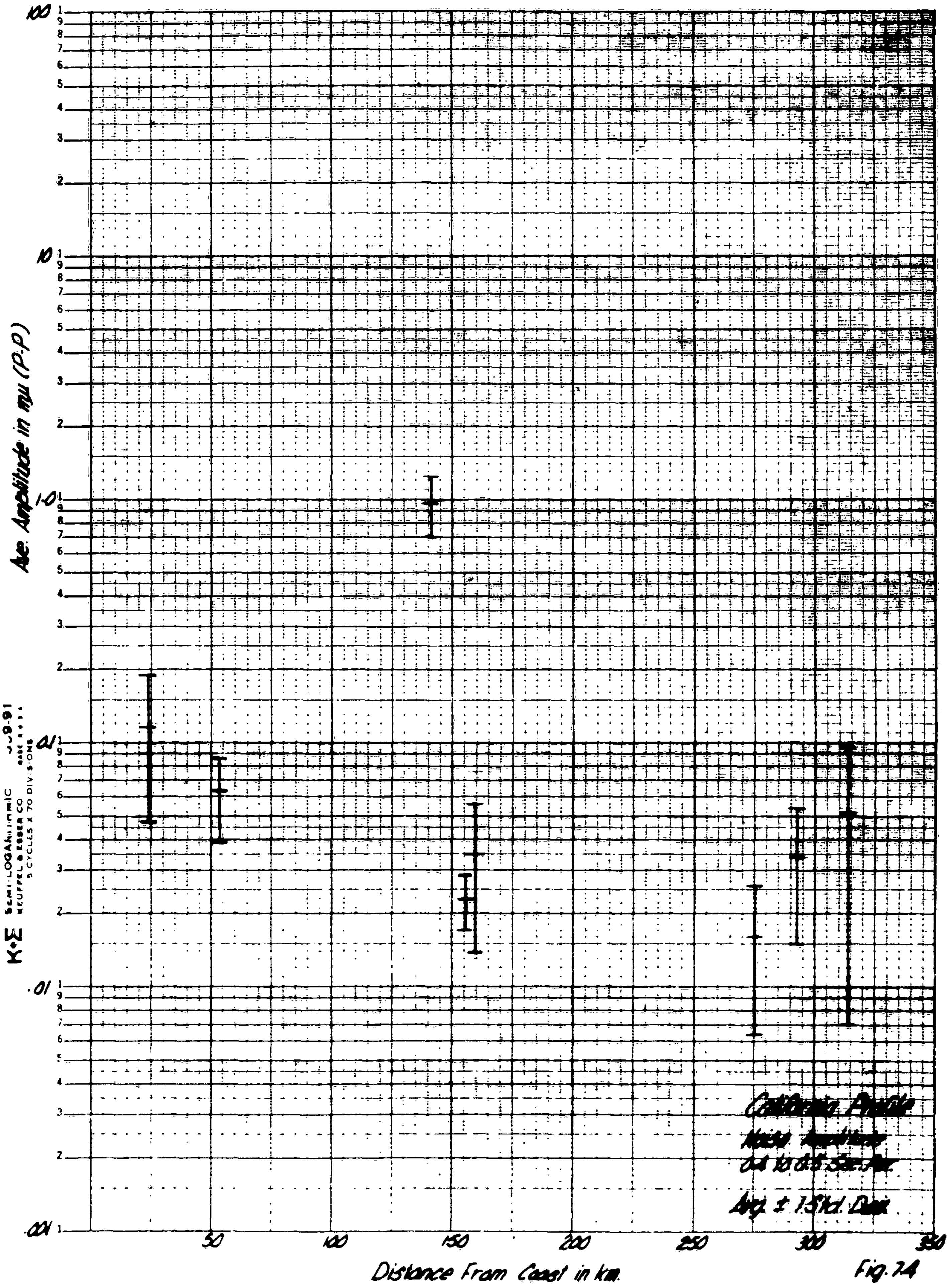
Ave. Amplitude in mμ (P-P)
100
10
1.0
.01
.001
50
100
150
200
250
300
350
Distance From Coast in km.
K·E SEMI-LOGARITHMIC
KEUFFEL & ESSER CO.
5 CYCLES X 70 DIVISIONS

Fig. 7A

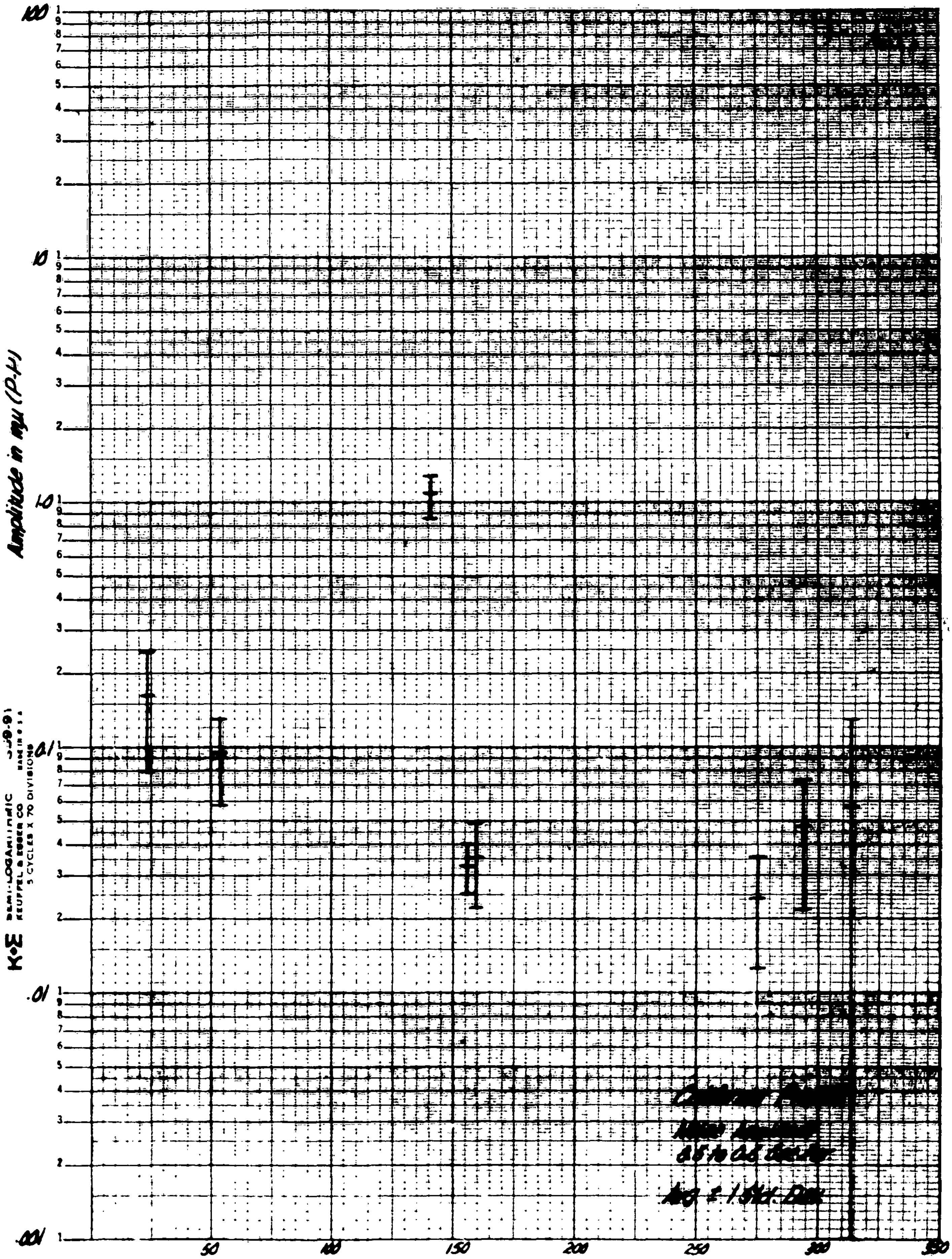
Amplitude in mμ (P-P)
100
10
1.0
0.1
.01
.001
50
100
150
200
250
300
350
Distance from Coast in km.
K·E SEMI-LOGARITHMIC
KEUFFEL & ESSER CO.
5 CYCLES X 70 DIVISIONS

Fig. 7.5

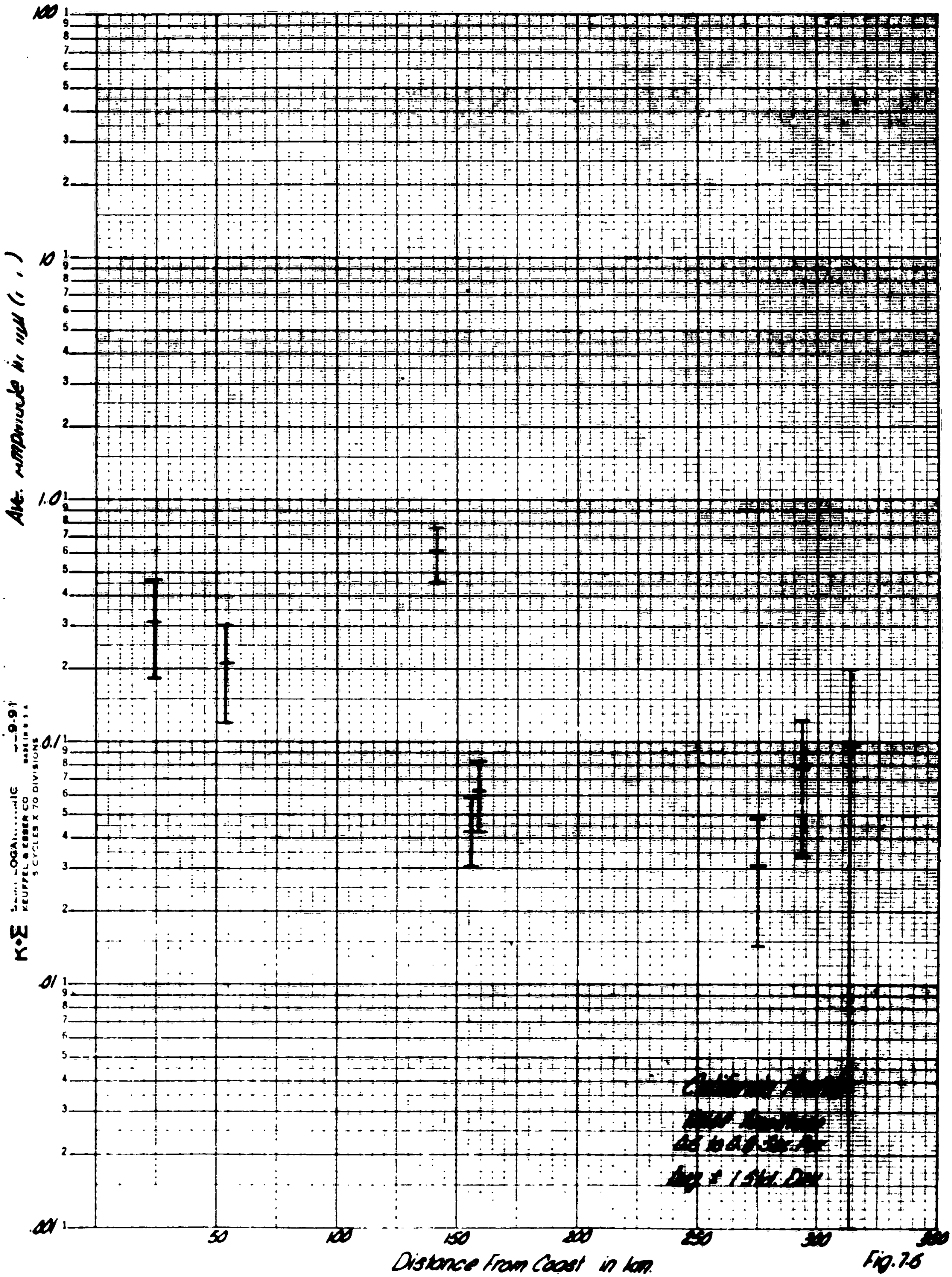

100
10
1.0
0.1
.01
.001
Ave. Amplitude in mμ
50
100
150
200
250
300
350
Distance From Coast in km.
K•E
KEUFFEL & ESSER CO.
5 CYCLES X 70 DIVISIONS

Fig. 7-6

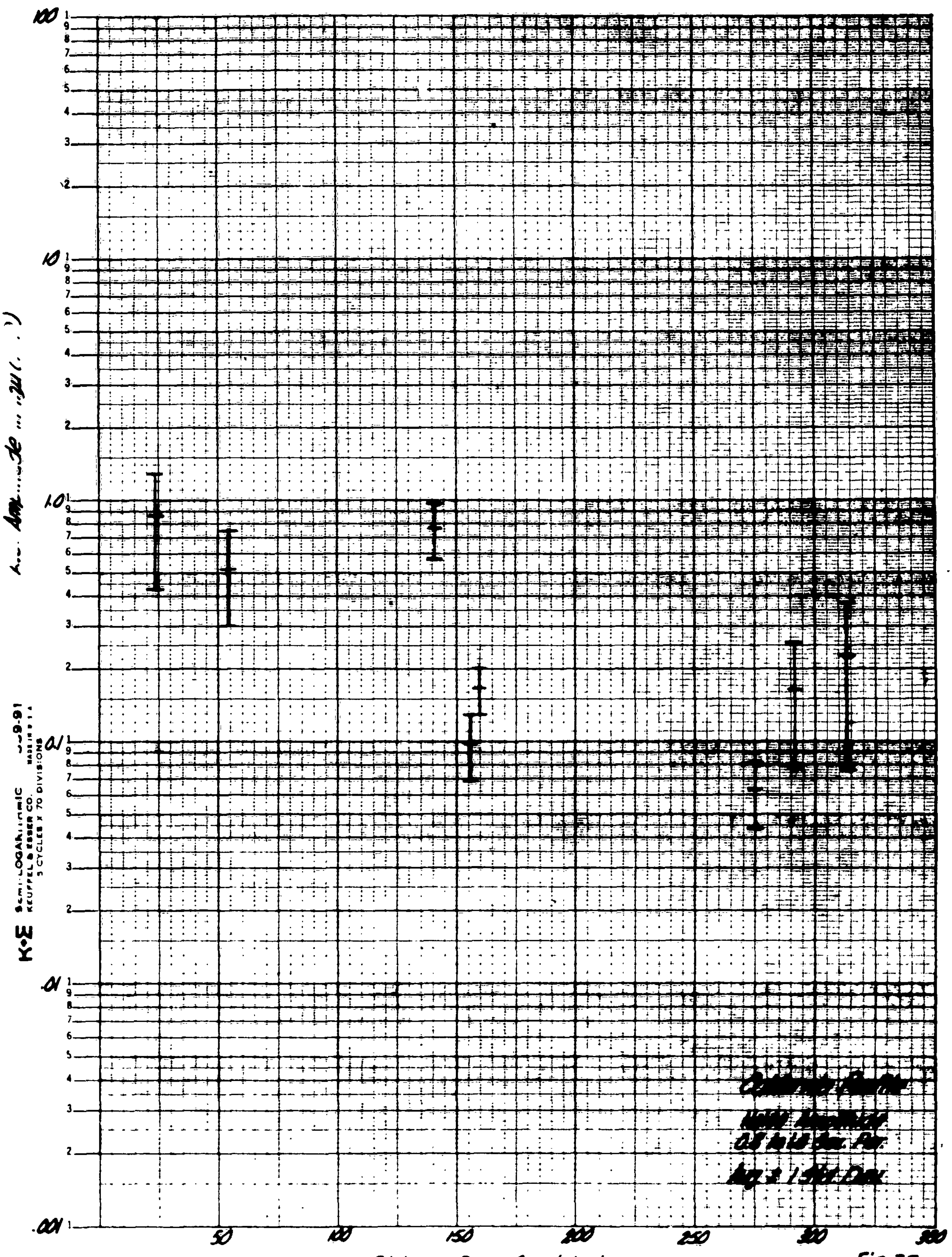
100
10
1.0
0.1
.01
.001
50
100
150
200
250
300
350
Distance From Coast in km.
Fig. 7.7

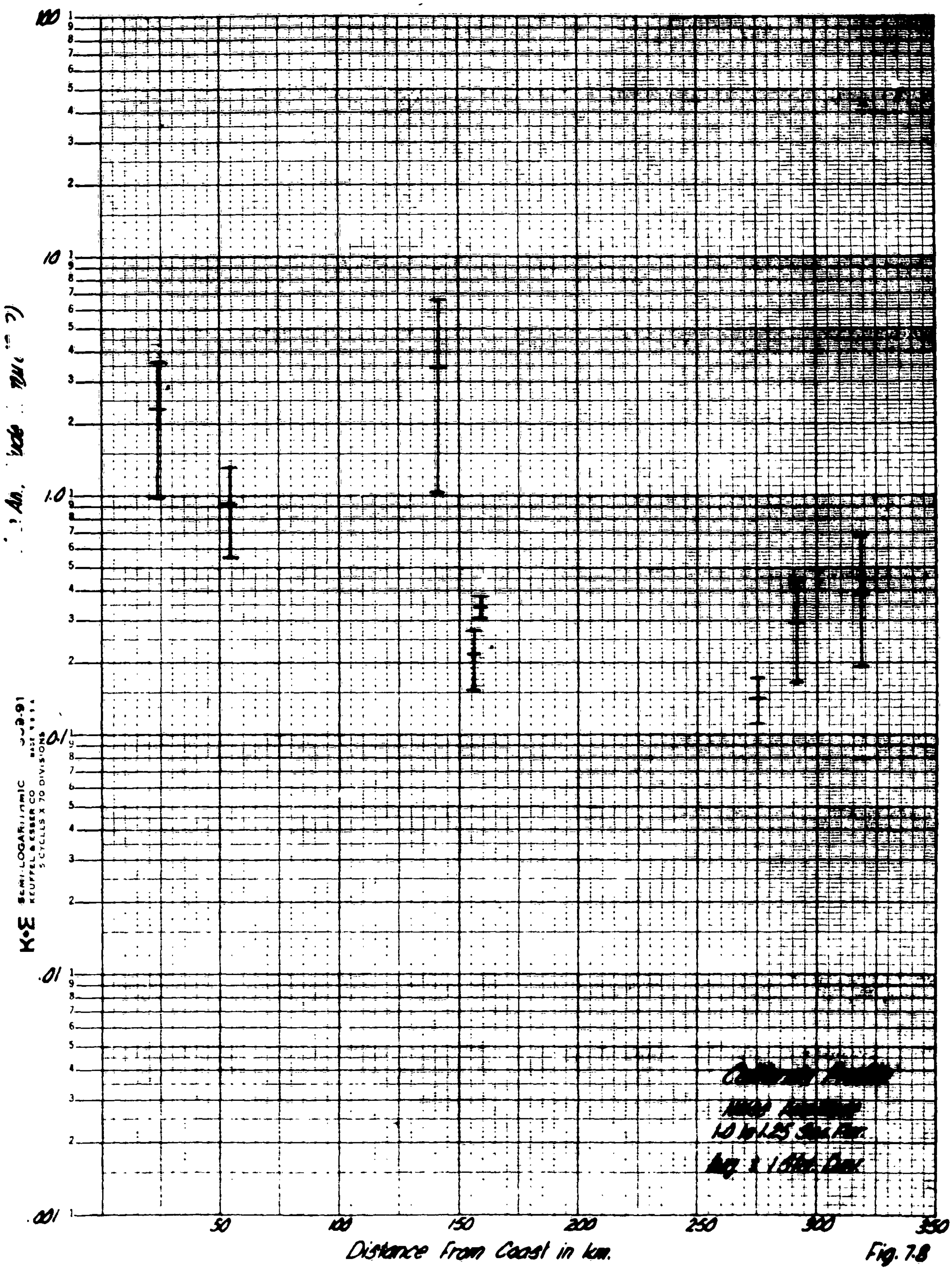
100
10
1.0
0.1
.01
.001
50
100
150
200
250
300
350
Distance From Coast in km.
K•E SEMI-LOGARITHMIC
KEUFFEL & ESSER CO.
5 CYCLES X 70 DIVISIONS

Fig. 7.8

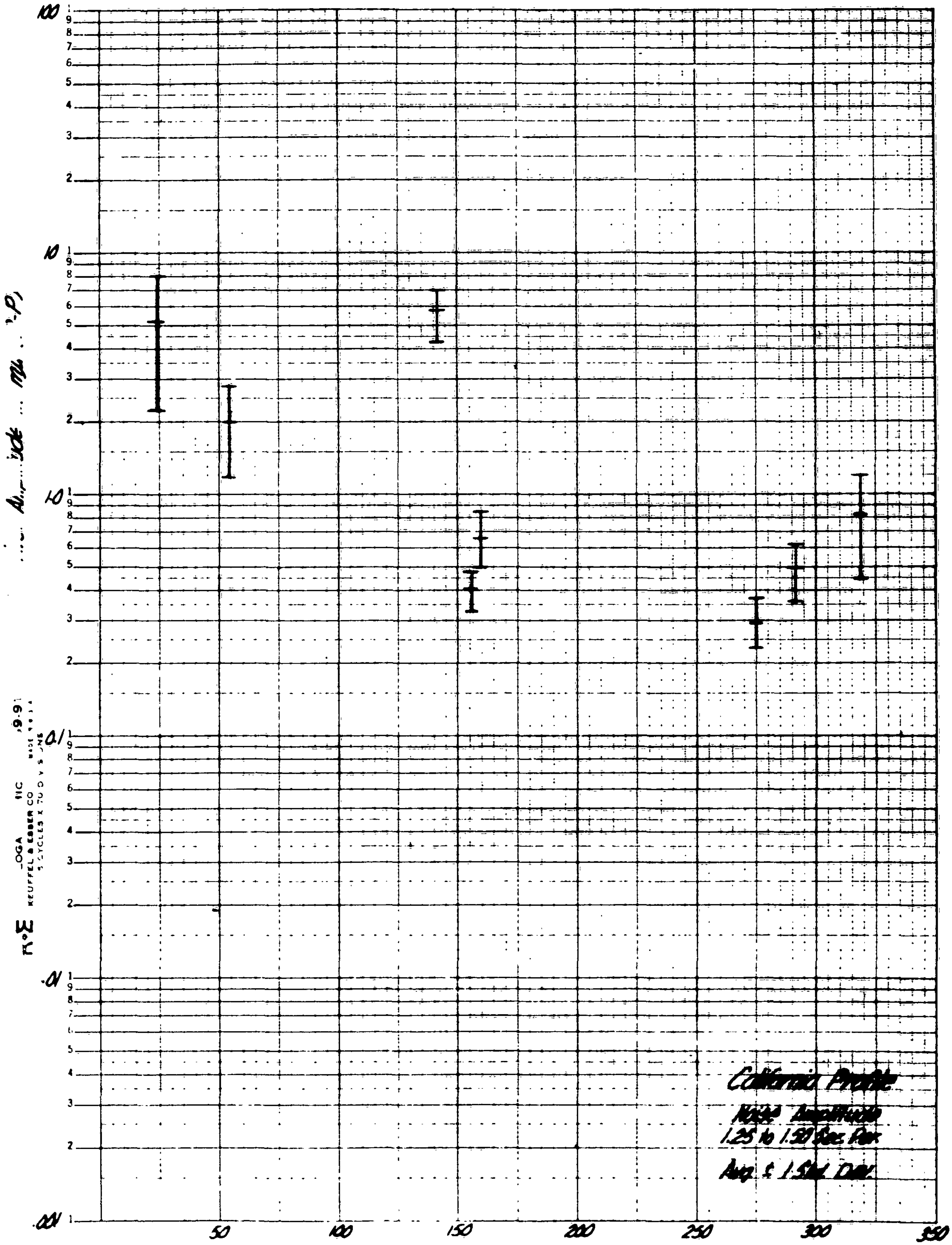

California Profile
Noise Amplitude
1.25 to 1.50 Sec. Per.
Avg. & 1 Std. Dev.
Distance From Coast in km.
50
100
150
200
250
300
350
100
10
1.0
0.1
.01
.001

Fig. 7.9

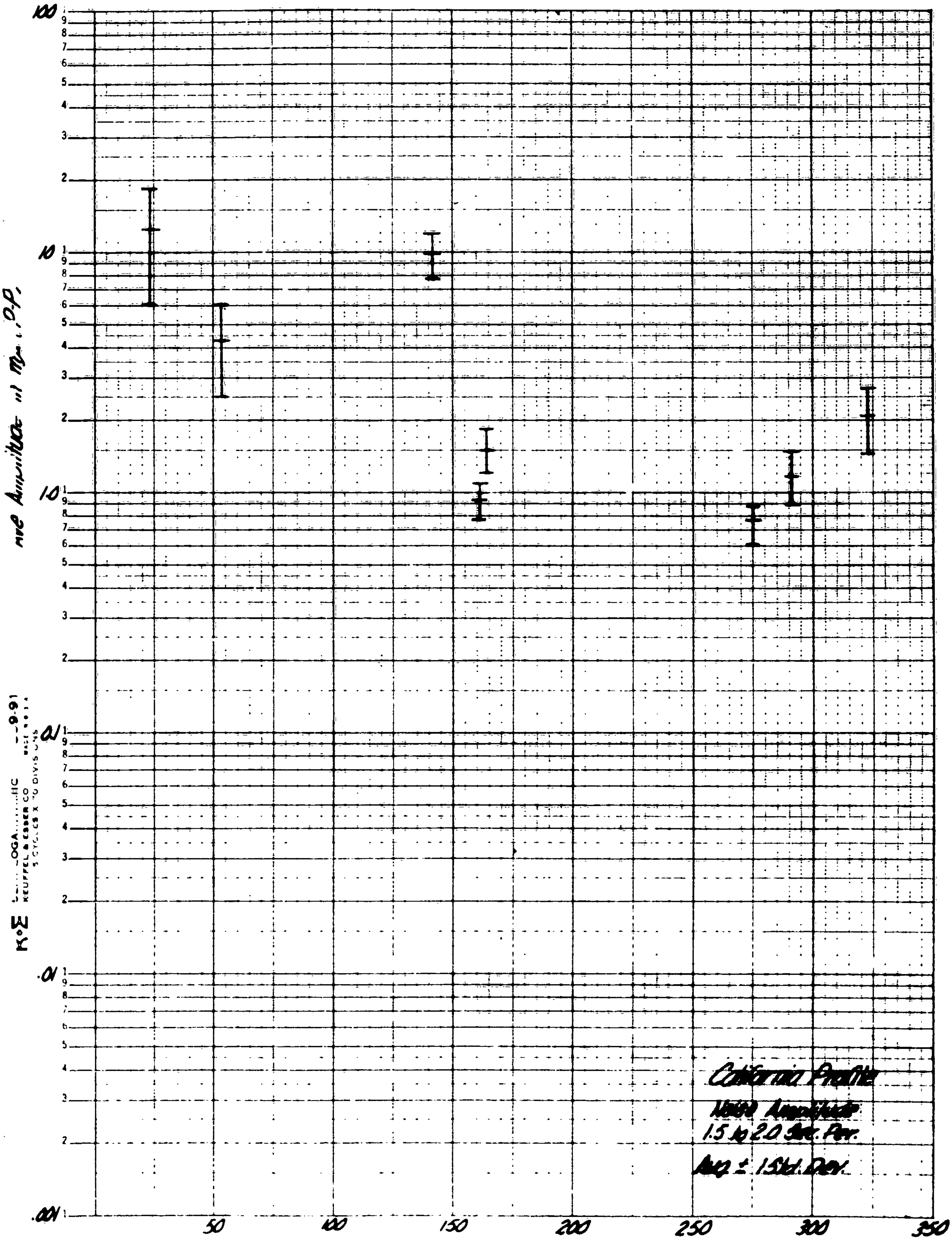

100
10
1.0
0.1
.01
.001
50
100
150
200
250
300
350
Distance From Coast in km.
California Profile
Noise Amplitude
1.5 to 2.0 Sec. Per.
Avg ± 1 Std. Dev.

Fig. 7.10

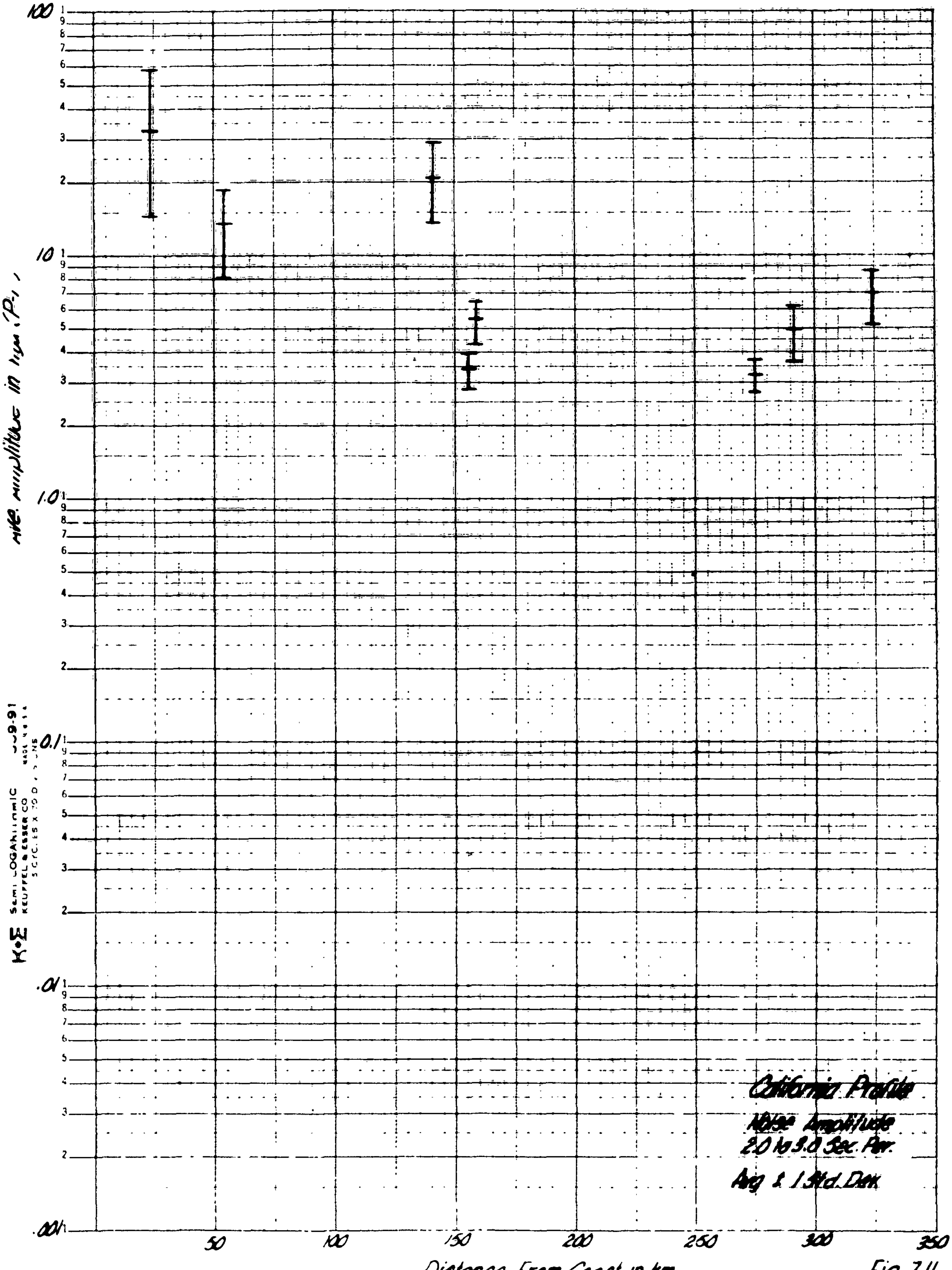

100
10
1.0
0.1
.01
.001
Ave. amplitude in μ (P.)
50
100
150
200
250
300
350
Distance From Coast in km.
California Profile
Noise Amplitude
2.0 to 3.0 Sec. Per.
Avg. & 1 Std. Dev.
K•E SEMI-LOGARITHMIC 359-91
KEUFFEL & ESSER CO.

Fig. 7.11

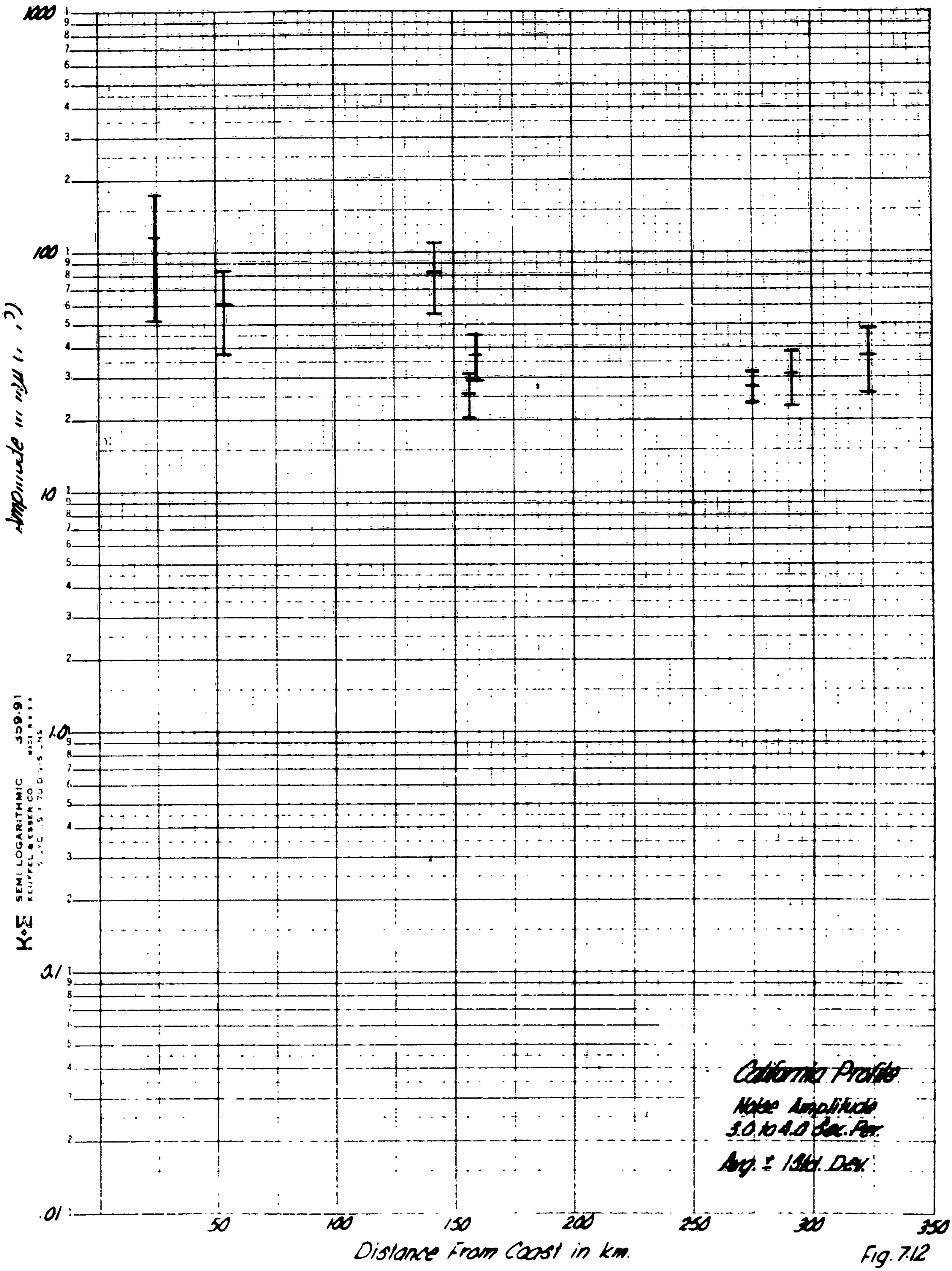

1000
100
10
1.0
0.1
.01
50
100
150
200
250
300
350
Distance From Coast in km.
California Profile
Noise Amplitude
3.0 to 4.0 Sec. Per.
Avg. ± 1 Std. Dev.
K+E 359-91
SEMI LOGARITHMIC
KEUFFEL & ESSER CO.

Fig. 7.12

8. Detail Noise Level of California Sites

Report No. VT/078-12 contains a preliminary discussion of noise level at one site. Because of the breakdown of noise into eleven short period bands of period, wind into arbitrarily chosen bands, signal levels into various periods and the difficulties of attaching numerical values to topography and geology, the problem of assembling the quantities of statistics is a formidable one. There are several unsolved problems.

The approach to this problem is to prepare a geologic and topographic map of each site, mark on it various values of the parameters and attempt to define relationships. This work is being continued. There are certain ways of quantizing geology and topography with respect to geology. This involves assigning a number proportional to rock density to each site. Topography can be quantized by methods similar to those used in gravity exploration methods to determine residual and second difference maps. Such techniques are being examined.

The various steps in the detail analysis are outlined in Figure 8.1. This block diagram has been used in earlier reports. It represents a somewhat idealized approach, which does however, emphasize the basic purpose and that is to determine how to design an array of seismometers at a particular site from an experimental aspect.

Previous reports contain various detail studies of particular sites. These will not be repeated, since they need synthesizing. Efforts currently being made toward better presentation should result in detail site studies that can be used.

8.1 Huasna River Slave Station

The following discussion includes only examples of some of the variations at one site, which was located at the western extremity of the California profile. Figure 8.2 is a plot of the distribution of noise amplitudes in various period bands. This plot is somewhat different than those at other sites. The asymmetry of the distribution for example, between 1.0 and 1.25 seconds indicates a fairly constant level of noise with a (p-p) value of about 1.5 mμ and occasional levels of noise to a maximum of about three times the base level. This is in contrast to noise at shorter periods which is more nearly normally distributed. The opposite case occurs at such sites

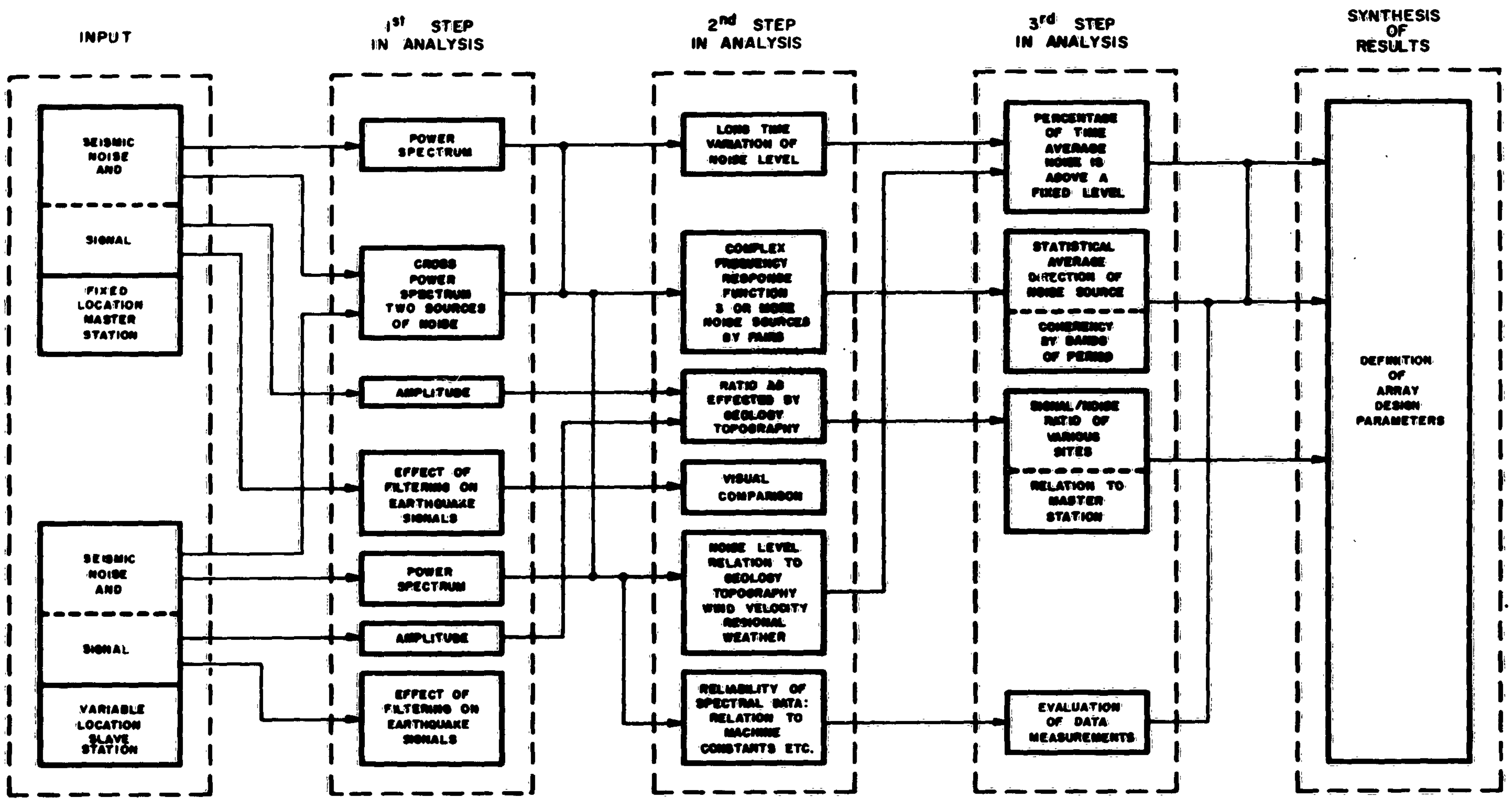

STEPS IN DATA ANALYSIS

FIGURE 8.1

H-10,430 Date 8-2-61
UNITED ELECTRODYNAMICS, INC.
PASADENA, CALIFORNIA

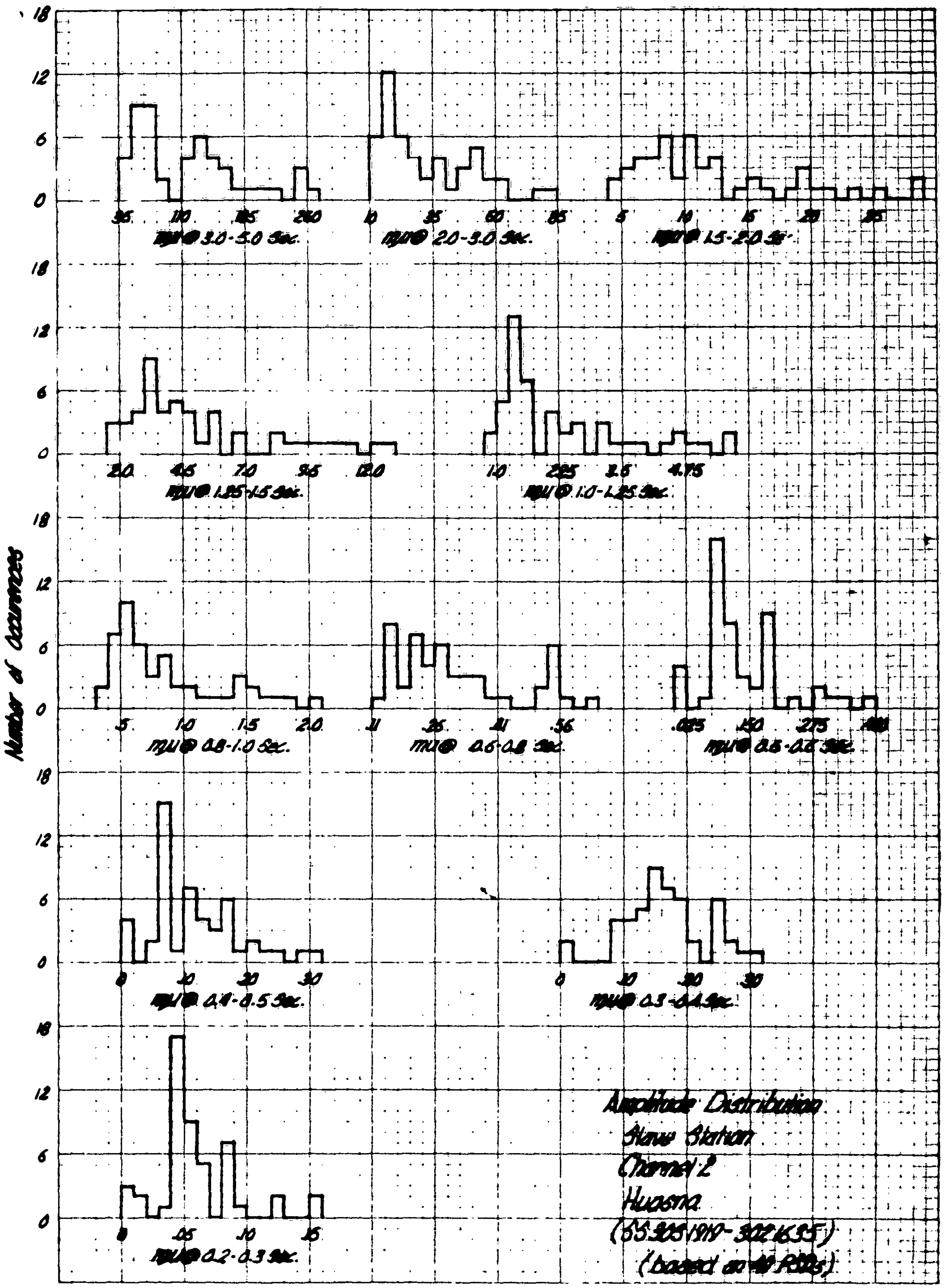

Average Amplitude in mμ p-p

Fig. 8.2

as Panamint where the longer period noise is more nearly normal and the short period noise is asymmetrically distributed.

Figure 8.3 is a comparison of noise amplitude as function of wind at Huasna River. The solid is the noise level curve for no effective wind (0-2.75 km/hr.). The dashed curve is for amplitude regardless of wind. An interesting feature of this curve is the apparent effect of increased wind velocity on noise level out to the longest periods measured (3.0-5.0 seconds.). Due to proximity to the coast (25 kms.) this is probably due to the fact that increased wind also increases the surf level generating a higher level of noise in the longer periods.

Figure 8.4 and 8.5 illustrate the variation of noise level at various locations within the Huasna River site area. Channel 2 in each case is in the center of the array; channel 4 is southeast; channel 5 is east. The marked difference in noise level of 0.5 to 0.6 second noise illustrates (Figure 8.4) one array design criterion. The contribution of the seismometer one-quarter mile east of the array, because of its high noise level between 0.5 and 0.6 seconds would probably have a negative effect on overall array performance.

Figure 8.5 shows that the seismometer location three-quarter miles southeast, has an overall slightly higher noise level, in particular at 2.0 seconds, and for periods less than 0.5 seconds.

It is this type of data that is being processed to obtain overall side performance results.

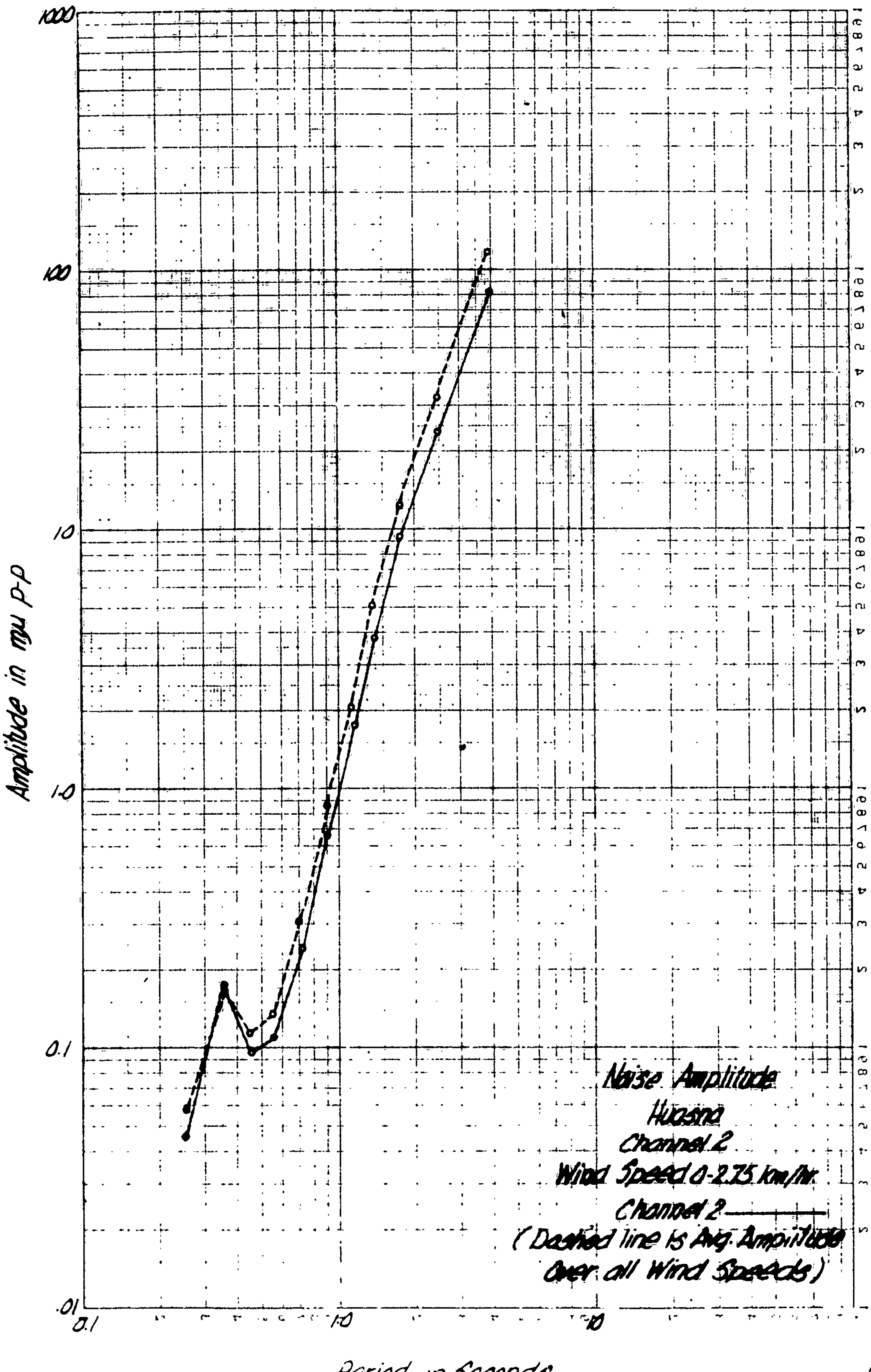
1000
100
10
1.0
0.1
.01
0.1
1.0
10
Amplitude in mμ p-p
Period in Seconds
Noise Amplitude
Huasna
Channel 2
Wind Speed 0-2.75 km/hr.
Channel 2
(Dashed line is Avg. Amplitude Over all Wind Speeds)

Fig. 8.3

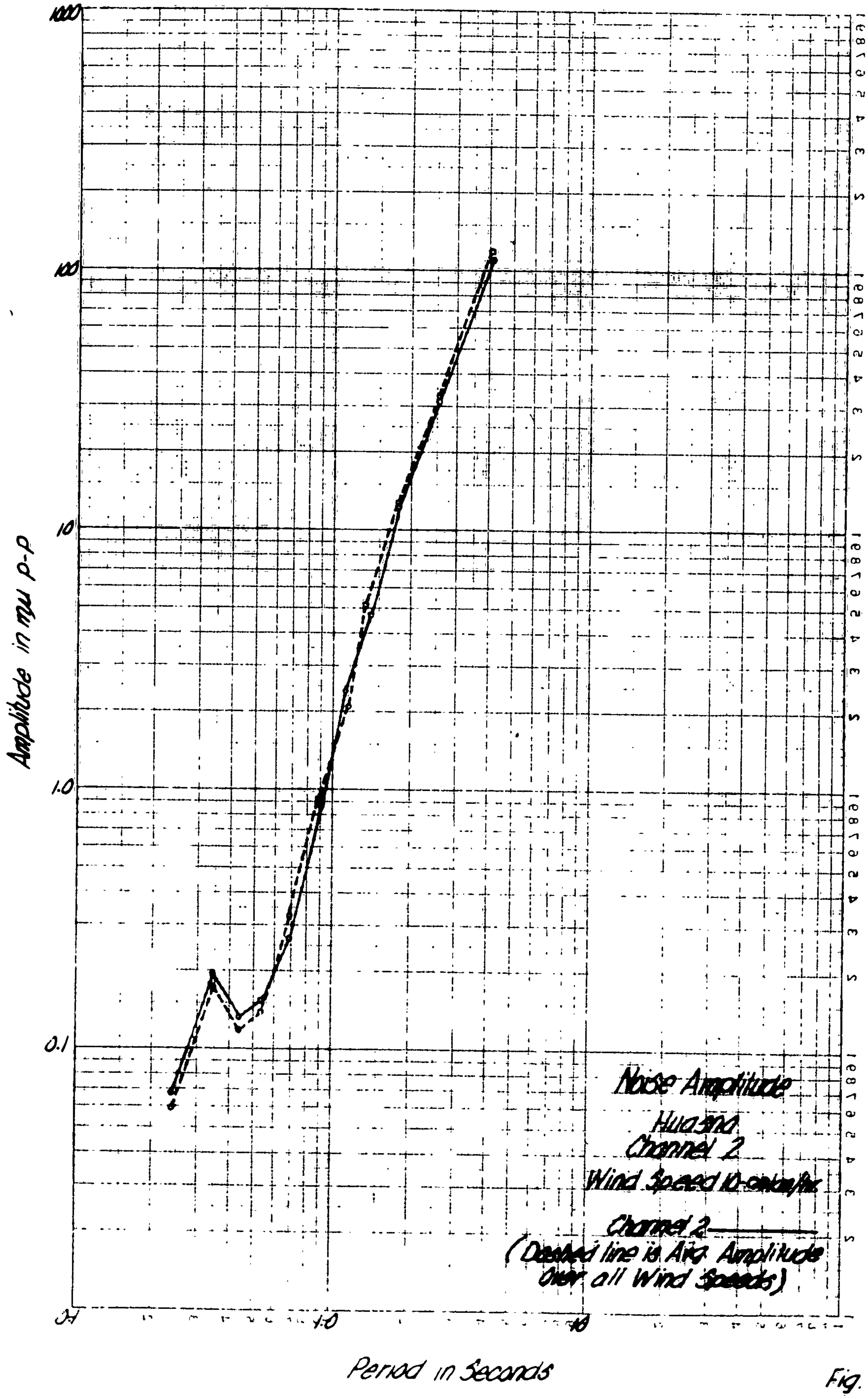

1000
100
10
1.0
0.1
Amplitude in mμ p-p
Noise Amplitude
Huasna
Channel 2
Wind Speed 10-
Channel 2
(Dashed line is Avg. Amplitude
Over all Wind Speeds)
1.0
10
Period in Seconds

Fig. 8.3a

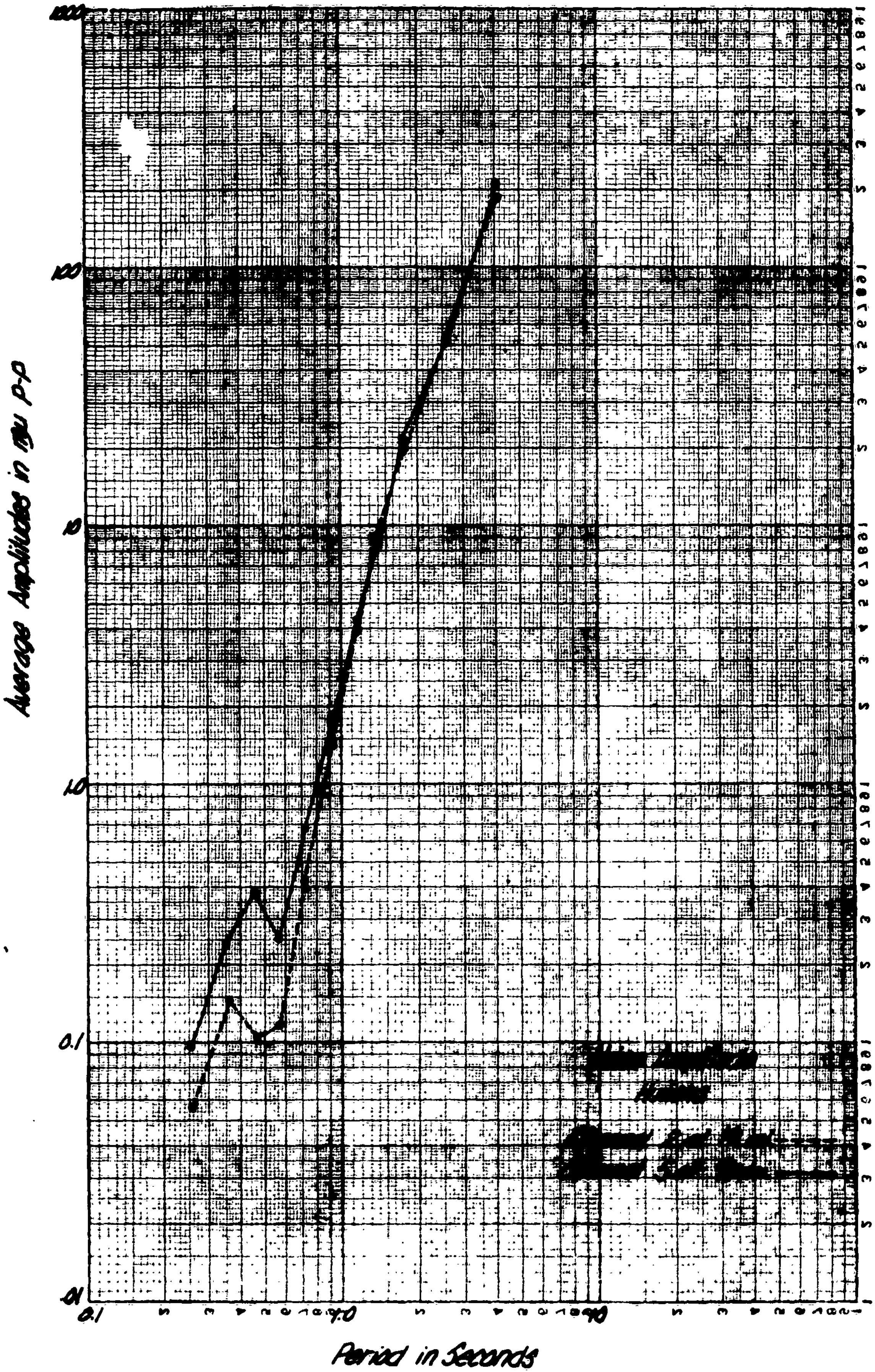

Average Amplitudes in mμ p-p
1000
100
10
1.0
0.1
.01
0.1
1.0
10
Period in Seconds

Fig. 8A

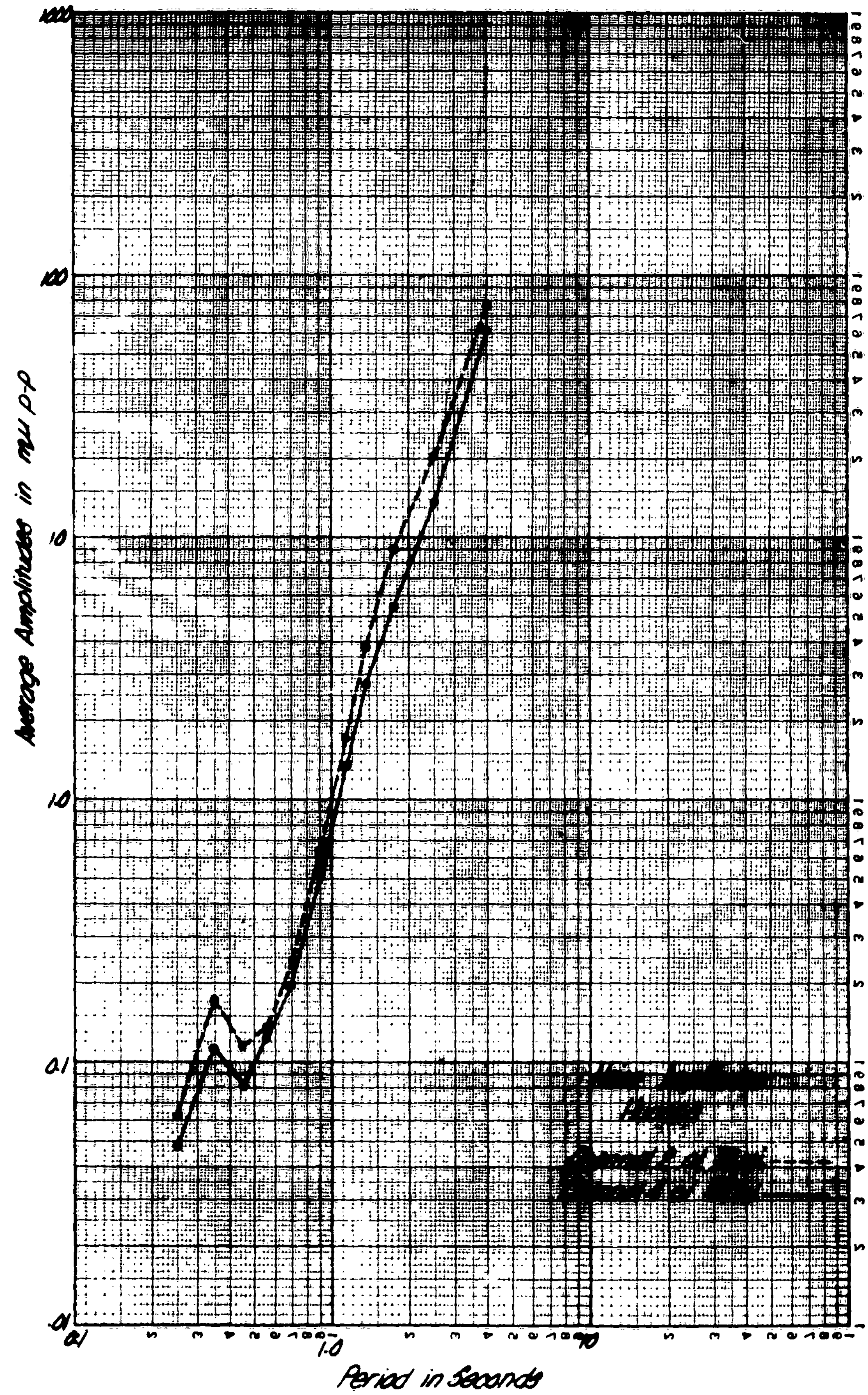

Average Amplitudes in mu p-p
1000
100
10
1.0
0.1
.01
.01
1.0
10
Period in Seconds

Fig. 8.5

9. Noise Levels Pacific Northwest Profile

Figure 9.1 is a plot of noise levels recorded at the Master Station at Toppenish Ridge and the Slave Station at Mabton. This chart is of the measured noise level of the 200 second samples taken each 5 hours. During this period the stations were 31 kms apart and had a rather similar noise level. The Slave Station had a slightly higher level of noise probably correlatable with geology. Both stations are on basalt, the Slave Station is in a conglomorate area from an old channel of the Columbia River. The noise level in the 0.8 to 1.0 second band has an estimated average of about 0.20 mμ average which is about the same level of noise in this period commonly observed in California.

Figures 9.2 and 9.3 are examples of the type of spectra obtained at the Paterson Site (the second Slave Station in Washington). Of particular interest is the relatively low level of noise between 0.7 and 1.4 cps. Should this pattern persist a pass band filter could be used to effectively reduce the noise and pass frequencies between 0.7 and 1.4. (Figure 9.4 is an example of the use of such a filter).

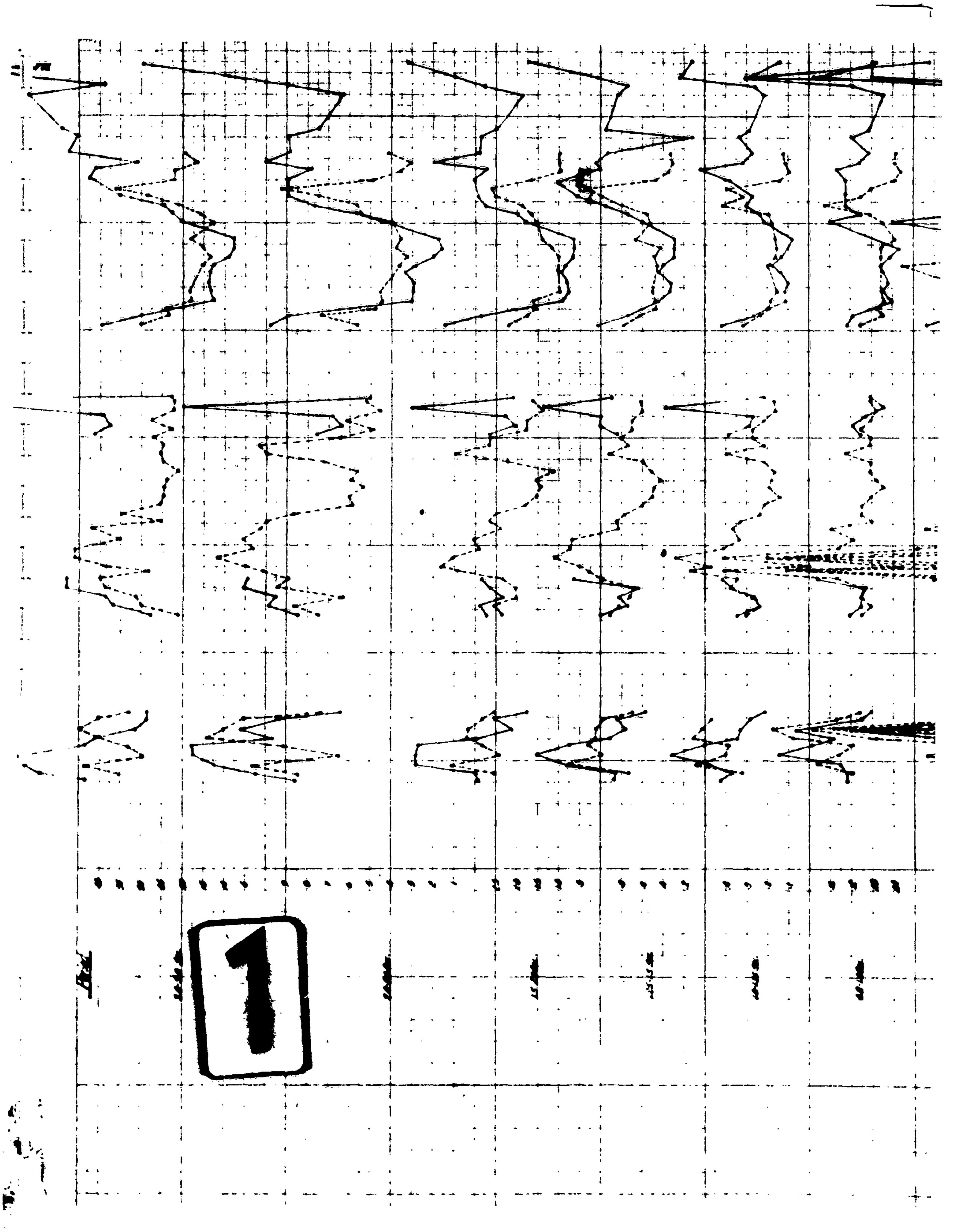
1

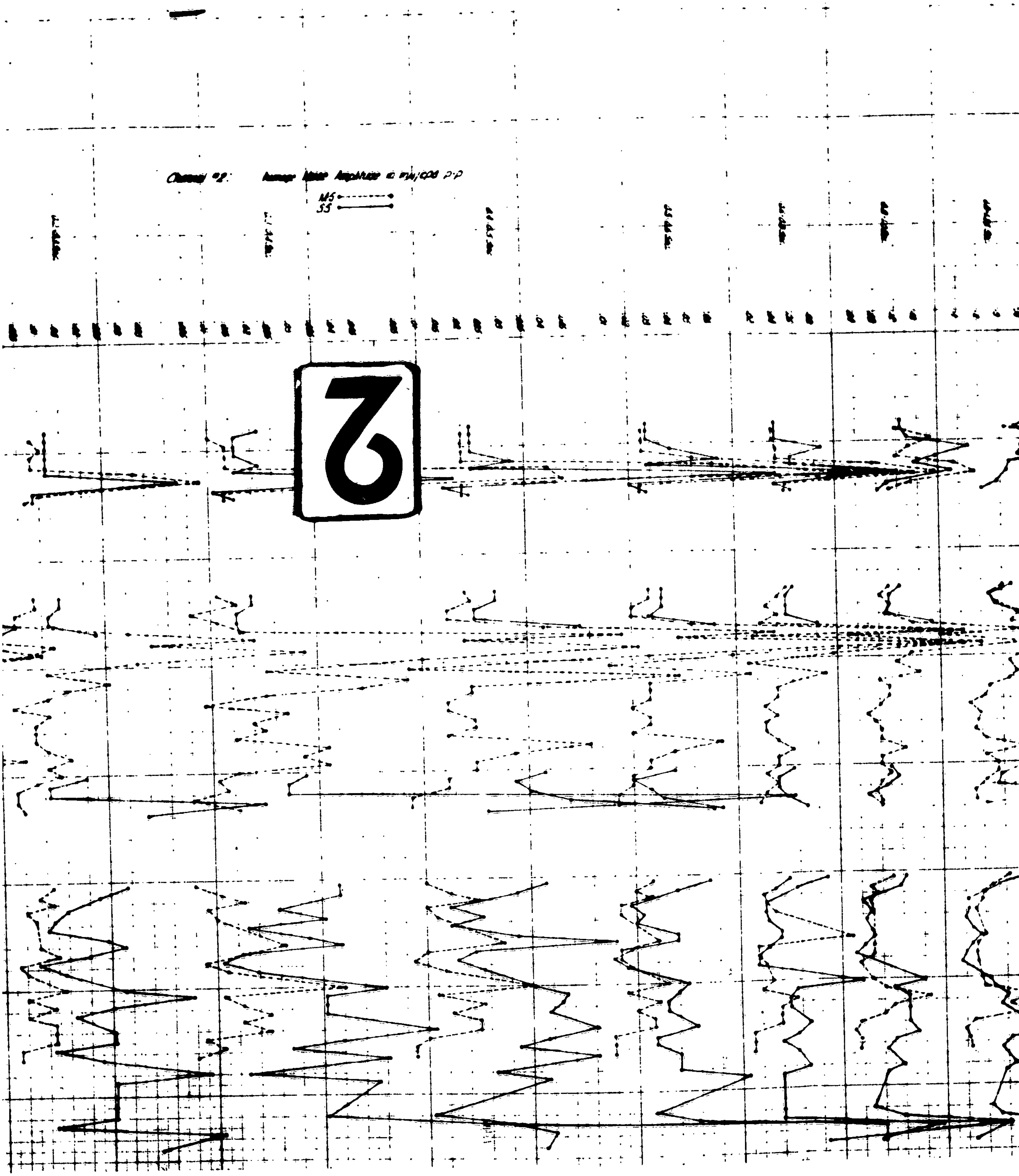
2
MS
SS

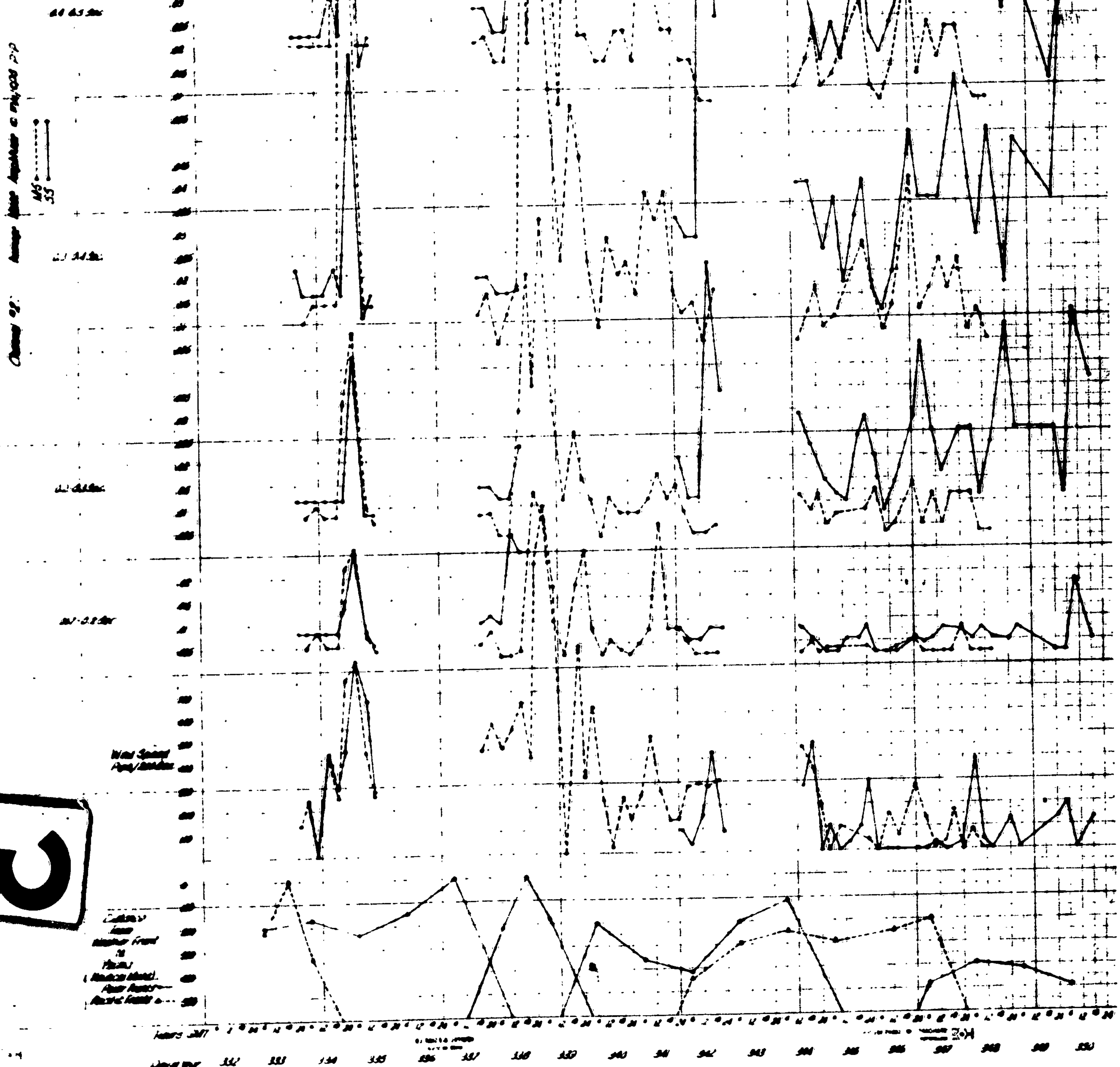

Fig. 91

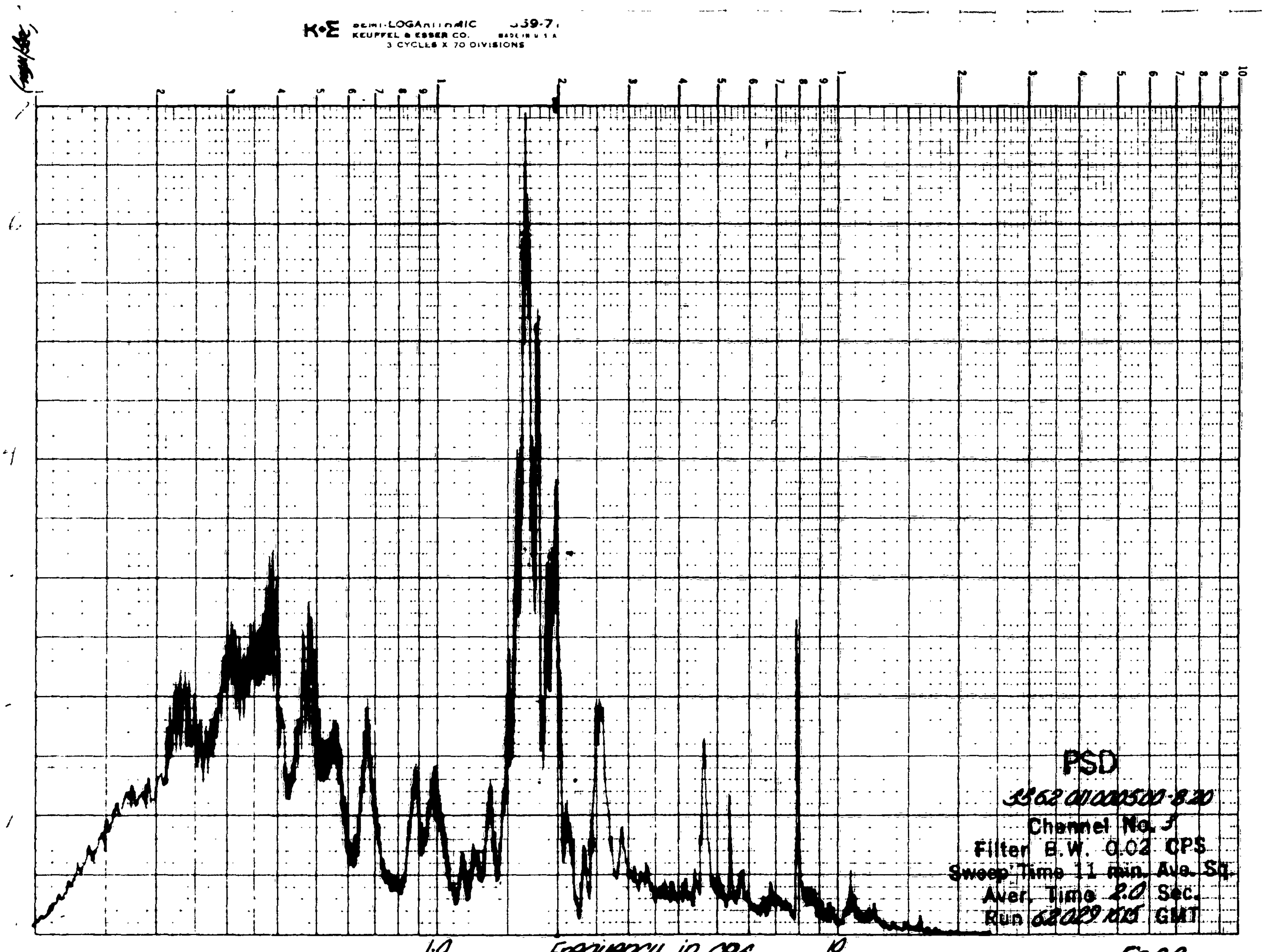
K•E SEMI-LOGARITHMIC 359-71
KEUFFEL & ESSER CO. MADE IN U.S.A.
3 CYCLES X 70 DIVISIONS
PSD
3362 001000500-8.20
Channel No. 5
Filter B.W. 0.02 CPS
Sweep Time 11 min. Ave. Sq.
Aver. Time 2.0 Sec.
Run 62029 1005 GMT
1.0
10
Frequency in CPS
Fig. 9.2

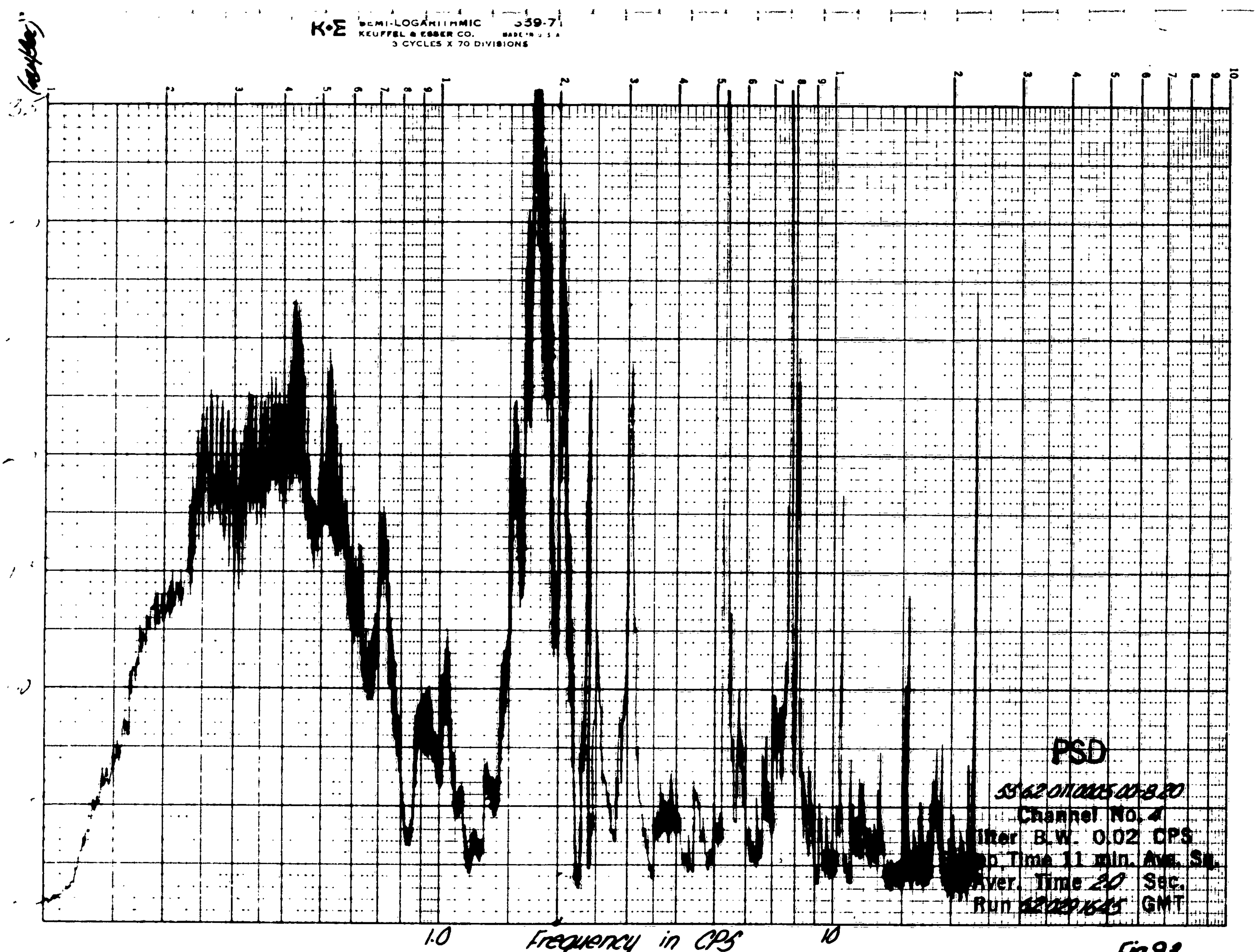
K•E SEMI-LOGARITHMIC 359-71
KEUFFEL & ESSER CO. MADE IN U.S.A.
3 CYCLES X 70 DIVISIONS
PSD
Channel No. 4
Filter B.W. 0.02 CPS
Rep Time 11 min. Ave. Sq.
Aver. Time 20 Sec.
GMT
1.0
Frequency in CPS
10

Fig.93

Paterson Slave Station

SS 62 011 00 07:00 - 07:30 GMT

Channel 4

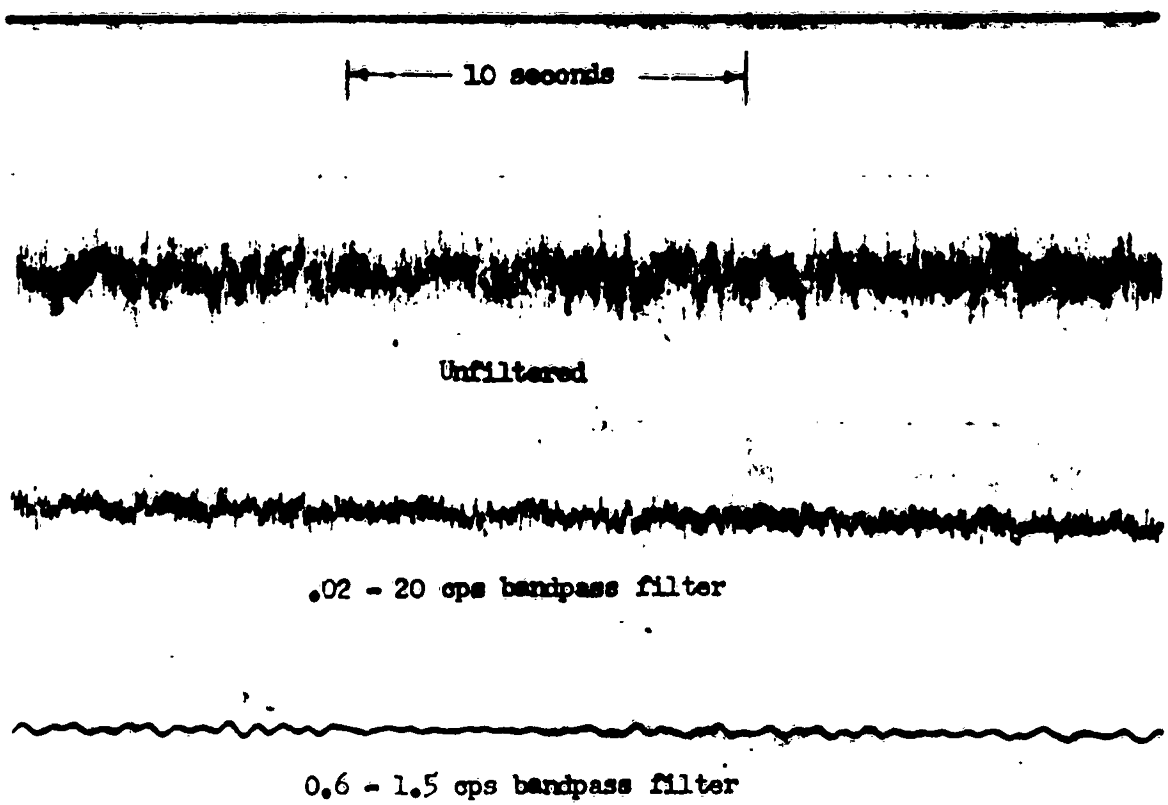

Example of Use of Band-Pass Filter
for Rejection of Large-Amplitude Noise
Below 0.6 cps and Above 1.5 cps
(See Fig. 9.3 for Spectrum)

Fig. 9.4

10. Projected Program

During the early part of 1962 the following work is scheduled:

(1) Occupy Slave Station sites as described in Section 2 at the rate of about one each calendar month. This would, if schedules are maintained, complete the Washington profile about 1 July.

(2) Work on the synthesis of site noise and signal information.

(3) Incorporate into the data results from the long period instrument.

(4) Use cross spectral analysis concepts and data to study noise source direction statistically.

(5) Develop as far as possible other uses for cross spectral concepts.

11. Financial Status

Total costs expended or obligated as of 31 December	521,100
Total funds allotted	503,731
Over-expended as of 31 December	17,369

12. Distribution:

Copies of this report are being distributed through proper channels as follows:

20 Copies	AFTAC/TD-1 Washington 25, D.C. Attn: Captain Walter Davis Project Officer
Transmittal letter only 1 Copy	Administrative Contracting Officer LAAPD/SBLCC Mr. George Ganz 1206 South Maple Street Los Angeles 15, California
1 Copy	Contracting Officer LMEMR/HSB Mr. R.E. Mueller AMC, WPAFB

BIBLIOGRAPHY

The Evolution of North America, P.B. King, Princeton University Press, 1959

Habitat of Oil-Geologic Environment of Cuyama Valley Oil Fields, California, Schwade, Carlson and O'Flynn, American Association of Petroleum Geologists 1958 pp 78-98

Geophysical Study of Subsurface Structure in Southern Owens Valley California, M.F. Kane and L.C. Pakiser, Geophysics Vol. XXVI, pp 12-26

A Stratigraphic Section in Yakima Basalt and the Ellensburg Formation in South Central Washington, J. Hoover Mackin, Washington Division of Mines and Geology, 1961

Operational and Maintenance Manual, Johnson-Matheson Vertical Seismometer Model 6480, p. 11

Electrical Noise, William R. Bonnett, McGraw-Hill 1960, pp 204-207

Statistical Theory of Communication, Y.W. Lee, Wiley 1960

Electron Tube Circuits, Samuel Seely, McGraw-Hill, 1958

An Introduction to the Theory of Random Signals and Noise, Davenport and Root, McGraw-Hill 1958

Methods and Techniques in Geophysics, S.K. Runcorn, Interscience Publishers 1960

Elementary Seismology, Charles F. Richter, W.H. Freeman 1958

Introduction to the Theory of Statistics, Alexander McFarlane Mood, McGraw-Hill 1950

Structural Geology of North America, A.J. Eardley, Harper 1951

APPENDIX I

1. United ElectroDynamics Proposal 7142 dated 28 April 1960, Field Study of Variation of Seismic Noise and Signals with Geologic and Geographic Environment.
2. United ElectroDynamics Cost Proposal 7142A dated 20 July 1960.
3. USAF Letter Contract AF 33(600)-42048 dated 22 August 1960.
4. USAF Contract AF 33(600)-42048 dated 16 November 1960.
5. Purchase Request No. EM-O-RD-7284.
6. Progress Report No. VT/078-1 through 20 November 1960.
7. Semi-annual Report No. VT/078-3 through 31 December 1960.
8. Monthly Report No. VT/078-4 through 20 January 1961.
9. Monthly Report No. VT/078-5 through 20 February 1961.
10. Monthly Report No. VT/078-6 through 20 March 1961.
11. Supplemental Agreement No. 2 Contract AF 33(600)-42048 dated 28 March 1961.
12. Monthly Report No. VT/078=7 through 25 April 1961.
13. Monthly Report VT/078-8 through 25 May 1961.
14. Monthly Report VT/078-9 through 25 June 1961.
15. Letter to R. E. Mueller/LMEMRA from R. J. Wegner dated 17 July 1961 - UBR 62-025 requesting contractural coverage to continue Project VT/078.
16. Semiannual Report No. VT/078-10 through 31 July 1961.
17. Monthly Report No. VT/078-11 through 31 August 1961.
18. Monthly Report No. VT/078-12 through 25 September 1961.

19. Special Report No. VT/078-13.

20. Contract No. AF 33(600)-42048 Supplementary Agreement No. 4, 10 October 1961.

21. Letter to Captain Walter Davis requesting approval of site principally in Washington State.

22. Monthly Report No. VT/078-14 through 25 October 1961.

23. Letter from Carl F. Romney to John R. Woolson, Subject: Approval of Next Area of Study Under VT/078.

24. Monthly Report No. VT/078-15 through 30 November 1961.